Aljoša Gračner

Assessing fouling communities in the Northern Adriatic trough photo-analysis of ARMS plates

UNIVERSIDADE DO ALGARVE
Faculdade de Ciências e Tecnologia

2020/2021

Aljoša Gračner

Assessing fouling communities in the Northern Adriatic trough photo-analysis of ARMS plates

Mestrado em Biologia Marinha

Main supervisor:

Borut Mavrič

Co-supervisor:

Ester Serrão

UNIVERSIDADE DO ALGARVE
Faculdade de Ciências e Tecnologia

2020/2021

Declaração de autoria de trabalho

Declaração de autoria de trabalho" followed by the following text "Declaro ser o(a) autor(a) deste trabalho, que é original e inédito. Autores e trabalhos consultados estão devidamente citados no texto e constam da listagem de referências incluída.

_____

1. ACKNOWLEDGEMENTS

Firstly, I would like to thank my main supervisor Borut Mavrič, PhD who gave me this remarkable opportunity to be involved in such an important project of the biodiversity research group at the Marine Biology Station in Piran, Slovenia. I am very grateful for his attentive guidance throughout all the fieldwork and research tasks. His assistance and advice for experimental design, statistical analysis of data and scientific writing, was very helpful and essential for achieving the desired goals and aims of this thesis. I really appreciate his effort of passing on important aspects of the scientific approach, and enabling me to participate on the adventurous fieldwork days in the Slovenian sea.

I would like to express my special thanks of gratitude to Ana Fortič, a young PhD student at the research station, for her generous help in taxonomic identification of biofouling organisms, and advice on the usage of the CPCe programme and associated tasks, as it was crucial for the proper execution of the study. Additionally, her previous work on experimental plates in the region provided important insights and observations of the fouling communities, which proved very useful for the thesis.

I am really thankful to Tristan for letting me steer the research vessel Sagitta and providing the crew with some nice burek and red wine on the fieldwork days. Being able to snorkel beside Tihomir Makovec and Borut, while they were inspecting the fouling community on the anchorage chains below the oceanographic Buoy Vida, during the ARMS retrieval, was truly an unforgettable experience.

2. ABSTRACT - Portuguese

Numa era caracterizada por impactos significativos de pressões antropogénicas nos ecossistemas marinhos costeiros, diversas comunidades de fundo duro estão a sofrer alterações severas sob a influência conjunta das alterações climáticas, degradação do habitat, poluição e introdução de espécies invasoras. Grandes proporções de comunidades de fundo duro estão localizadas em regiões costeiras pouco profundas e são constituídas por organismos predominantemente sésseis, o que as torna particularmente sensíveis, uma vez que não podem facilmente evitar perturbações.

A monitorização da biodiversidade marinha dessas comunidades é portanto crucial, uma vez que fornece provas para apoiar a gestão, conservação e investigação marinha, que ajudam a minimizar os nossos impactos, melhorar o seu estado ambiental e manter os seus serviços ecossistémicos essenciais. Apesar da sua importância, os habitats sub-mediterrânicos de fundo duro do Mar Mediterrâneo permaneceram significativamente não comunicados a este respeito, devido à sua difícil acessibilidade e à sua complexa e frágil natureza biogénica. O aspecto mais problemático das práticas de monitorização do fundo duro provém da grande variedade de diferentes métodos utilizados nesta investigação, resultando em comparações e integrações prejudicadas e difíceis dos resultados obtidos.

Nos últimos anos, as Estruturas Autónomas de Monitorização de Recifes (ARMS), concebidas para a amostragem da fauna enigmática dos habitats dos recifes de coral, provaram ser um dispositivo de amostragem eficiente e não destrutivo para tais comunidades que oferecem simultaneamente um elevado nível de padronização metodológica. A sua crescente relevância levou à fundação da Rede de Observação da Biodiversidade Marinha (MBON), que visa estabelecer locais de observação globais baseados em ARMS para fins principais de avaliação da biodiversidade da fauna bentónica e detecção de espécies não indígenas (NIS) através de foto-análise e métodos baseados na genómica.

Desde 2018, a Estação de Biologia Marinha Piran do Instituto Nacional de Biologia (MBP NIB) está envolvida no MBON. Como os tempos e períodos de implantação do ARMS variam, dependendo dos diferentes padrões de sucessão em áreas distintas, habitats bentónicos e questões científicas a serem abordadas, são necessárias implantações experimentais do ARMS antes de serem estabelecidos locais e protocolos de observação adequados. A este respeito, 11 unidades ARMS foram implantadas ao longo dos anos 2018-2021, servindo como testes em 3 locais distintos no Mar da Eslovénia, cada um representando um habitat bentónico notável na

região. O principal objectivo das unidades ARMS implantadas no local de amostragem de Piran, que representava um habitat bentónico dominado por rochas e o sítio da Bóia Vida, que se assemelhava a um habitat mais rico em sedimentos, era a avaliação da biodiversidade a longo prazo. Pelo contrário, o principal factor de interesse das unidades ARMS implantadas no local de amostragem do Porto de Koper era a detecção de NIS.

Com o objectivo de estabelecer uma análise fotográfica das placas ARMS como parte da monitorização da biodiversidade e do método de detecção NIS para o Mar da Eslovénia, a comunidade biofouling que se desenvolveu em 11 unidades ARMS implantadas em diferentes estações do ano dentro de vários períodos que vão de 3 a 13 meses, foi avaliada através da utilização de 3 métodos de foto-análise aprovados. Dois métodos foram baseados na estimativa da cobertura do organismo por uma sobreposição aleatória de pontos (100 & 300 pontos) com a ajuda de um software dedicado à anotação de imagens, sendo o outro um levantamento manual de taxa sob uma sobreposição de grelha 5x5. Foi feita uma comparação lado a lado dos diferentes conjuntos de dados, para determinar o melhor método de foto-análise para os fins desejados.

A estrutura e composição da comunidade derivada a partir de estimativas de taxas biofouling adquiridas por foto-análise de placas ARMS revelaram influências significativas do habitat circundante, estação de imersão, período de implantação e orientação da superfície das placas para a comunidade estabelecida.

A sobreposição aleatória de 300 pontos foi determinada como o método de foto-análise mais apropriado, uma vez que forneceu a informação mais precisa, precisa e estatisticamente robusta da composição da comunidade num período de tempo razoavelmente curto. A utilização da Contagem de Pontos de Coral com extensões Excel (CPCe), um software especial concebido para fins de anotação de imagens bentónicas, tornou a foto-análise pontual de placas um método muito simples e eficiente em termos de tempo, devido à grande quantidade de automatização que o programa oferece.

As faces das placas orientadas para baixo apresentavam uma cobertura colonizada significativamente maior, e comunidades taxonomicamente mais ricas em comparação com as de orientação superior. O principal factor responsável pela menor colonização das placas de orientação superior foi a maior sedimentação que suprimiu o assentamento e crescimento larvar. A influência da época de imersão na composição da comunidade pareceu ser uma consequência de poças larvares distintas, presentes na coluna de água no momento da implantação do ARMS.

Os propágulos já disponíveis na coluna de água podem iniciar directamente a colonização de placas ARMS recentemente implantadas, o que lhes confere uma vantagem pelo menos no processo de sucessão precoce de incrustações. Assim, salientamos fortemente a importância da implantação de ARMS para a monitorização repetida na mesma altura do ano, de preferência nos meses de Verão, a fim de minimizar a variabilidade deste factor de influência. O aumento da duração do período de implantação estava ligado a um maior desenvolvimento dos organismos incrustadores e a uma maior complexidade da comunidade, uma vez que havia mais tempo disponível para a fixação adicional de larvas, crescimento do organismo e outros processos sucessórios. Este padrão descrito resultou na validação de ARMS implantados durante cerca de 12 meses mais apropriados para avaliações da biodiversidade através de métodos de análise fotográfica, uma vez que era possível obter mais informação da comunidade analisada.

Em cada local de estudo, numerosos taxa biofouling foram exclusivos, com outros organismos presentes nos três locais, mas com quantidades diferentes. Isto ilustrou a presença de conjuntos de incrustação distintos em cada um dos três habitats bentónicos amostrados. Polychaetes, bryozoans e moluscos foram os grupos taxonómicos mais predominantes nos três locais, com contribuições significativas de algas em Piran, Porifera em Buoy Vida e Ascidiacea no local do estudo do Porto de Koper. Observou-se que os NIS se instalavam em placas ARMS independentemente da sua localização, indicando a sua relevância para efeitos de detecção de NIS. Como esperado, a maior quantidade de NIS foi detectada no local de amostragem do Porto de Koper, confirmando a área como um hotspot NIS e um local adequado do observatório ARMS para amostragem e avaliações NIS.

Com base nesta investigação, será proposto um melhoramento de um protocolo nacional de avaliação foto-analítica das unidades ARMS, que consideraria a análise exclusivamente de faces de placas orientadas exclusivamente para baixo, utilizando o método de sobreposição de 300 pontos para aumentar a eficiência, mas mantendo ainda a qualidade adequada dos resultados obtidos. A tese contribuiu para os aspectos solicitados no âmbito de estudos semelhantes, relativamente à amostragem ARMS e protocolos de foto-análise associados. Ao mesmo tempo, este trabalho fornece orientações importantes para experiências ARMS semelhantes no futuro, para facilitar e facilitar os estabelecimentos de novos locais de observação MBON na região e em todo o mundo.

Palavras-chave: Estruturas autónomas de monitorização de recifes, foto-análise, comunidades bentónicas, espécies não indígenas, Mar Adriático do Norte

3. ABSTRACT - English

In an era characterized by significant impacts of anthropogenic pressures on coastal marine ecosystems, diverse hard-bottom communities are undergoing severe changes under the jointly influence of climate change, habitat degradation, pollution and invasive species introduction. Monitoring marine biodiversity of such habitats is therefore crucial, as it provides evidence to support marine conservation policy and research, which can help to minimize our impacts, improve their environmental status and retain their essential ecosystem services.

Due to the lack of scientific literature and monitoring procedures of hard-bottom habitats in the northern Adriatic, the Marine Biology Station Piran of the National Institute of Biology (MBP NIB) became involved in the Marine Biodiversity Observation Network (MBON), which focuses on long-term biodiversity assessments and non-indigenous species (NIS) detection by the usage of Autonomous Reef Monitoring Structure (ARMS) sampling devices.

Since test trials of ARMS deployments are required before proper MBON observatory sites and protocols are established, 11 units were deployed at 3 locations, each representing a notable benthic habitat in the region, through the years 2018-2021. Aiming to establish photographic-based analysis of ARMS plates as a national monitoring programme for the Slovenian Sea, the biofouling community that developed on ARMS units deployed at different seasons of the year for various periods of 3-13 months was assessed through the use of 3 endorsed photo-analysis methods.

The derived community structure from cover estimates of biofouling taxa acquired by photo-analysis of ARMS plate-faces demonstrated significant influences of the surrounding habitat, immersion season, deployment period and plate-face orientation. The 300 random point-overlay was determined as the most appropriate photo-analysis method, as it provided the most accurate, precise and statistically robust information of the community structure in a reasonably short time, supported by the use of a special image annotation software CPCe. Bottom oriented plate-faces displayed significantly greater colonized coverage, and taxonomically richer community compared to those of top-orientation, mainly contributed by higher sedimentation and lesser light availability, which decrease the preference and progress of larvae settlement. The influence of immersion season on the community structure seemed a consequence of distinct larval pools, present in the water column at the time of ARMS deployment. Length of the deployment period was linked to more developed fouling organisms and greater community complexity, validating ARMS deployed for 12 months or so more appropriate for assessments

of biodiversity trough photo-analysis methods. At each study site, numerous biofouling taxa were exclusive, with others present in different amounts when compared among units from separate sites. Polychaetes, bryozoans and molluscs were the most prevalent taxonomic groups at all three sites, with significant contributions from Algae at Piran, Porifera at Buoy Vida and Ascidiacea at the Port of Koper study site. NIS were observed to settle on ARMS plates, with highest numbers of such taxa at the Port of Koper site, indicating their relevance for NIS detection purposes, especially at the respected site.

Based on this research an improvement of a national protocol for photo-analysis assessments of ARMS units will be proposed, which would consider the analysis of exclusively bottom oriented plate-faces using the 300-point overlay method to increase efficiency but still retaining the adequate quality of the obtained results. The thesis contributed to the requested aspects stressed within similar studies, regarding ARMS sampling and associated photo-analysis protocols. At the same time this work provides important guidelines for similar ARMS experiments in the future, to ease and facilitate the establishments of new MBON observatory sites in the region and around the globe.

Keywords: Autonomous Reef Monitoring Structures, photo-analysis, benthic fouling communities, non-indigenous species, Northern Adriatic Sea

4. INDICES

4.1. Table of Contents

4.2. Figures

4.3. Tables

5. LIST OF ABBREVIATIONS

- ARMS = Autonomous Reef Monitoring Structures
- ASSEMBLE+ = Association of European Marine Biological Laboratories Expanded
- CPCe = Coral Point Count with Excel extensions
- CRED = Coral Reef Division
- EU = European Union
- GES = Good Environmental Status
- MBON = Marine Biodiversity Observation Network
- MBP NIB = Marine Biology Station Piran of the National Institute of Biology
- MSFD = Marine Strategy Framework Directive
- NIS = Non-Indigenous Species
- NMDS = Non-parametric Multidimensional Scaling
- NOAA = National Oceanic and Atmospheric Administration
- SIMPER = Similarity Percentage

6. INTRODUCTION

6.1. Anthropocene and biodiversity

Without any doubt, the most unique feature of the planet Earth is the existence of life, with all its extraordinary biological diversity, and its ability to retain it (Cardinale et al., 2012). The Earths capability to harbour such diversity of species is mainly achieved due to periods of environmental stability (Rockstrom et al., 2009). Such thriving conditions are not always present, as roughly 5 periods of mass extinction events have occurred in the past (McElwain et al., 2007). Recently a new era has emerged, the Anthropocene, in which human activities are catastrophically altering the stability of our life-sustaining biosphere (Rockstrom et al., 2009). Our increasing population growth and resource overconsumption are the main drivers of environmental change (Halpern et al., 2008; Neeman et al., 2015). If this global exponential trend of biodiversity loss and habitat degradation continues, there is no doubt, that human actions will cause the 6th mass extinction (Barnosky et al., 2011).

Since biodiversity has a fundamental role in maintaining heathy ecosystem functions (Danovaro et al., 2016; Cahill et al., 2018) and nearly all its loss is driven by anthropogenic pressures (Halpern et al., 2008; Worm et al., 2006), it has become one of the main measure for assessing marine environmental status. Monitoring biodiversity is centered on measuring the community structure of an area and detecting changes in the composition, mainly driven by anthropogenic pressures or arrival of NIS (Borja et al., 2013). Most of the previous research on marine ecosystem health, focused on individual components of biodiversity, such as microbes, plankton, invertebrates, fish, etc. (Cochrane et al., 2016). This comes from the assumption that higher numbers of functional group types provide higher functional biodiversity organization and thus improve stability and resilience of an ecosystem (Borja et al., 2014). However, it has now become evident that proper understanding of the ecosystem requires the study of all biodiversity components, from the population genetic structure to food-webs and bio-physical parameters (Borja et al., 2014). Therefore, improving monitoring methods of marine biodiversity in nearshore ecosystems is a crucial step in understanding and conserving their healthy state (Danovaro et al., 2016; Cahill et al., 2018).

6.2. Coastal habitats

Among all marine habitats, those present in coastal areas, which harbour the most diverse ecosystems on Earth (Broderick, 2015), are the most affected (Lotze et al., 2006; Marbà et al.,

2012; Halpern et al., 2008; Neeman et al., 2015). Coastal areas are human settlement hot spots, since they provide essential resources and services for human civilization (Lotze et al., 2006). Almost a quarter (23%) of human population lives at the coast, with the highest density at the first 10km from the sea (Nicholls & Small, 2002). This leads to a concentration of human impacts at the closest proximity to coastal marine ecosystems (Neeman et al., 2015; Danovaro et al., 2016) supported by the finding of Broderick (2015) that health of marine ecosystems improves with distance from the coast. The combined synergistic risks of habitat alteration, pollution, eutrophication, overexploitation, non-indigenous species (NIS) introduction, combined with climate change and ocean acidification have placed coastal marine ecosystems into an alarming state (Halpern et al., 2008; Lotze et al., 2006; Danovaro et al., 2016), resulting in severe declines in biodiversity and shifts in species composition (Lotze et al., 2006). Because these ecosystems provide essential goods and services for human and marine life, they became the main scientific focus of conservation, restoration, and protection strategies in the recent years (Borja, 2014; Neeman et al., 2015).

6.3. Fouling organisms of hard bottom communities

Marine communities living on hard bottom habitats, also termed biofouling communities (usually for those on manmade substrata) or epibiota (predominantly for those on living substrata), represent some of the most productive and diverse communities on our planet (Caldwell et al., 2009). Despite exhibiting evolutionary heritage of functional biodiversity superior to that of tropical rainforests (Caldwell et al., 2009), such communities of numerous micro and macroscopic organisms of sessile, sedentary or motile, solitary and colonial form, have been greatly overlooked and have suffered from lack of public attention, mainly due to their small size and cryptic nature (Mather et al., 2013; Caldwell, 2009)

Biofouling communities living in hard bottom habitats are mostly represented by smaller invertebrates and algae, restricted to the hard substratum because of their sessile nature (Rees et al., 2009). Some of the most abundant colonial fauna, such as bryozoans and cnidarians are encrusting, and together with sponges and coralligenous algae form biogenic formations (Sheehan et al., 2013). This results in elevated structural complexity of the habitat, which provides nursery areas for larvae, additional substrate for organism settlement and cover from predators and currents (Pirtle et al., 2012). Most sessile species like ascidians and bivalves are suspension feeders, which recycle organic matter from the water column (Beaumont, 2009) and produce planktonic larvae that support higher trophic levels, contributing to benthic-pelagic

coupling (Sheehan et al., 2013). The high filtration efficiency of larger bivalves (*Ostrea edulis* & *Magallana gigas*) and individuals from the Ascidiacea family in particular, which can filter from 100-340 dm^3 of seawater daily, signifies their role as miniature water-cleaners, as they effectively remove bacteria, phyto- and zoo-plankton, marine snow, detritus and other organic matter, heavy metals and pollutants from the water column (Stachowitsch, 1998; Lipej et al., 2020). Therefore, artificial or natural surfaces harbouring a dense fouling community strain very large amounts of seawater in a short time, acting as natural eutrophication control of coastal habitats (Officer et al., 1982; Lipej et al., 2020). Serpulid polychaetes and other encrusting organisms form CaCO3 exoskeletons, and act as a CO2 sink (Peck et al, 2015). The resulting heterogenous habitats support communities that comprise most of the marine benthic biodiversity (Thorson, 1957; Rees, 2009). Due to the numerous functional groups and impressive internal trophic dynamics, these communities significantly contribute to benthic production and provide irreplaceable ecosystem services (Caldwell et al., 2009).

Large proportion of hard-bottom communities are located in shallow coastal regions and are therefore prone to the synergistic impacts of anthropogenic pressures and global climate change (Caldwell et al., 2009; Rees et al., 2009), listed in the previous chapter. Biofouling organisms are particularly affected, since many taxa are sessile and cannot avoid disturbances as their main modes of dispersal are by larvae or overgrowth (Solan et al., 2004). Their importance in the ecosystem functioning and high sensitivity to environmental changes by the cause of impaired movement, makes them a good target for monitoring and assessments of environmental status (Carugati et al., 2015; Beisiegel et al., 2017).

6.4. Importance of monitoring

The alarming state of coastal ecosystems and its inhabitants attracted much focus on biological monitoring research of such communities, as it contributes to the understanding of the general ecological functioning of these ecosystems (Barrio Froján et al., 2016), provides assessments of the environmental status and helps to detect changes in community structure, that support marine policy and conservation (Rees et al., 2009).

Hard bottom subtidal zone ecosystems, located in numerous coastal areas in the Mediterranean, remained significantly unreported, compared to other benthic marine habitats (Cahill et al., 2018; Pearman et al., 2016). Lack of knowledge about biodiversity patterns and dynamics is mainly due to the fact that monitoring these habitats is exceptionally difficult and complicated (Cahill et al., 2018; David et al., 2019), since they are three-dimensionally complex and hard to

access (Beisiegel et al., 2017). Sampling methodology used to implement expensive technological equipment (is situ benthic chambers), as well as time-consuming scientific diving (observational surveys) and was in many cases destructive and disturbing to the community (dredging, grabbing) (Beisiegel et al., 2017; Cahill et al., 2018). Despite their huge cost and effort, such methods overlooked a considerable amount of benthic biodiversity (Pearman et al., 2016; Carvalho et al., 2019). In addition, the morphological identification of the sampled organisms proved to be demanding even for specialized expertise (Cahill et al., 2016), since many species are hard to taxonomically identify (cryptic species) or are in their juvenile stage, thus lacking morphological characteristics, needed for precise identification (Danovaro et al., 2016).

Overcoming the problematics of benthic hard bottom monitoring explained above, the use of artificial substrates proved to be a promising approach (Obst et al. 2020, David et al., 2019). The first artificial sampling units used to monitor biofouling communities were settlement plates (e.g., benthic/experimental plates/tiles) (Sutherland et al., 1977; Glasby et al., 1999, 2001), which proved to be a fairly standardized, sensitive and non-invasive sampling method for the job (Glasby, 2000). Their ease of use and presence of limited space, with high species turnover made them particularly valuable (Dean & Hurd, 1980), especially for NIS detection purposes and biodiversity monitoring of such communities (Marraffini et al., 2017).

The plates were extensively used in temperate and tropical latitudes, with some studies undertaken even in the Antarctic (Bowden et al., 2006). The major drawback of these studies was their variation in size and materials of the benthic plates used, as well as different processing and analysis methods. This resulted in biased interpretations of otherwise globally-comparable results (David et al., 2019).

An important milestone in marine monitoring and assessment strategies was the implementation of Marine Strategy Framework Directive (MSFD; 2008/56/EC) by the European Union (EU), with an aim to achieve a good environmental status (GES) in all European seas by 2020 (David et al., 2019). The status is achieved by assessment of a variety of descriptors of which biodiversity and presence of NIS are of paramount importance (Danovaro et al., 2016). Since previous methods of marine monitoring used site-specific and few-species approach with unstandardized methods obtaining non-comparable data (Pearman et al., 2020; Danovaro et al., 2016), the MSFD severely promoted the shift to functional, whole-sea ecosystem-based approach (Borja et al., 2013). Promoted by the MSFD demands and technological advancements, new standardized, scalable, and precise monitoring methods are under intense

development and testing under different EU projects. The main technological advancements predominantly include rapid and innovative molecular approaches and autonomous sampling systems with high sensitivity (She et al., 2016).

6.5. Photographic analysis methods

The revolutionary technological advancements in the last decades made camera technologies more suitable for examining marine communities, than ever before (Bicknell et al., 2016). Improvements in image quality, reduced costs, exponential data storage capabilities and computerized annotation software development (Hustache et al., 2015) made possible for photographic methods to deliver highly repeatable and standardized information which is easily stored and accessed for analysis of marine benthic assemblages (Bicknell et al., 2016; Hustache et al., 2015). The most used image-based sampling methods were based on autonomous underwater vehicles (AUVs), remotely operated vehicles (ROVs), towed video recordings and underwater still photography (Waddington et al., 2010).

On the contrary to other methods, still photography provides rapid, non-destructive, and cost-effective means of sampling (Waddington et al., 2010). Since information from images must be converted into quantitative data, many annotation programs, such as Coral Point Count with Excel extension (CPCe) software, have been developed to ease the process (Hustache et al., 2015). Obtained images or photo-quadrats of defined size, allow quantitative assessments of the underlying community, like organism surface coverage, species composition and abundance of different benthic groups, at relatively fine taxonomic resolution (Beisiegel et al., 2017; Waddington et al., 2010). These permanent records of species composition of satisfactory detail can be applied for monitoring purposes of benthic assemblages (Waddington et al., 2010), and go in concordance with the term ‘A picture is worth a thousand worms’ by Solan et al., (2003). The fact that software and image based algorithms are exponentially advancing and improving, like machine-learning and artificial intelligence, the use of such analysis methodologies seems to be a step in the right direction (Beyan & Browman, 2020).

6.6. ARMS development and standards

To further standardize the sampling of benthic habitats, the Coral Reef Division (CRED) of the United States' National Oceanic and Atmospheric Administration (NOAA) developed Autonomous Reef Monitoring Structures (ARMS) (www.oceanarms.org; 2020), designed particularly to sample cryptic flora and fauna of the coral reefs, where minimal disturbances are

of paramount importance as such habitats are very fragile and are even considered as endangered. Due to their effectiveness and ease of use, ARMS quickly became the leading edge of artificial sampling devices for benthic monitoring purposes (Cahill et al., 2018; Leray & Knowlton, 2015; Pearman et al., 2016; Pearman et al., 2018). The structures consist of 9 gray PVC settlement plates that are stacked in an alternating series. This simple, but effective design creates layers that are open or obstructed by the currents. Plates also receive different light levels, exposure to predators (top plate most exposed) and currents (David et al., 2019). The ARMS design therefore effectively mimics the complex three-dimensional structure of the adjacent benthic habitats (Danovaro et al., 2016). The structures can be manufactured according to the same specifications globally, achieving standardization with ease (David et al., 2019).

During their usual 0.5-3 year deployment periods, the ARMS are colonized by bacteria, algae, sessile and mobile benthic fauna (Obst et al., 2020). Throughout the deployment, colonization and succession patterns are under the influence of environmental conditions, present in the surrounding habitat. This makes ARMS a proper tool for marine monitoring of coastal areas, and if re-deployed in the same location, even suitable for assessing long-term changes in biodiversity (Danovaro et al., 2016). Newly deployed surfaces of ARMS plates present bare substrate, greatly suitable for the adjacent flora and fauna as well as NIS colonization (Obst et al., 2020).

After their retrieval, the ARMS are dismantled and are processed with respect to the standardized methods of molecular metabarcoding and macroscopic photo-analysis (Danovaro et al., 2016; Obst et al., 2020). Each plate face is photographed with high detail and resolution, before being scraped, homogenized, and analysed by molecular metabarcoding techniques (Danovaro et al., 2016). The use of plate photo-analysis, focusing on morphology in combination with molecular methods, which focus on molecular markers, produce complementary results of abundance and species richness on each ARMS respectively (Danovaro et al., 2016).

ARMS became well-established in the last 10 years (Obst et al., 2020) and are considered as the most promising new systems for marine biodiversity monitoring (Cahill et al., 2018; Leray & Knowlton, 2015; Pearman et al., 2016; Pearman et al., 2018; Danovaro et al., 2016). They were initially used to monitor coral reef habitats (Zimmerman & Martin, 2004) in different tropical regions, such as Red Sea (Carvalho et al., 2019: Pearman et al., 2016, 2019) and French Polynesia (Ransome et al., 2017). However, due to their simplicity and reproducibility, their use expanded to other hard bottom habitats on the Atlantic coast of US (Leray & Knowlton,

2015) and also in the European waters (David et al., 2019; Pennesi & Danovaro, 2017; Pearman et al., 2020). ARMS are now deployed globally (www.oceanarms.org, 2021), allowing researchers to investigate biodiversity patterns and species dispersal on a pan-regional scale (Pearman et al., 2020) and comparisons of benthic communities between marine biogeographic realms, provinces and ecoregions (David et al., 2019; Spalding et al., 2007).

6.7. A method in development

Despite the use of standardized sampling units and homogenous protocols of molecular and morphological identifications, the ARMS methodology still has some limitations to consider (Ransome et al., 2017; David et al., 2019). The PVC plates may not be as perfect in mimicking the natural substrata, as are other materials (clay, limestone, etc.), but the power of global comparability, by far exceeds the bias in this aspect (David et al., 2019). Although metabarcoding is such an advanced, rapid, and precise species identification tool, it comes with certain limitations (Pearman et al., 2020; Ransome et al., 2017). Danovaro et al., (2016) addressed the issues of metabarcoding in detail, mainly questioning variability in sequencing protocols (primers, preservatives) and accuracy and availability of the results obtained. The overall time and cost for metabarcoding analysis still are high (David et al., 2019). Alternative morphological-based identifications also have flaws, mainly from mis-identification and lower resolution of present organisms (Obst et al., 2020).

The number of ARMS articles focusing on metabarcoding methods (Pearman et al., 2018; Pennesi & Danovaro. 2017; Ransome et al., 2017), compared to photo-analysis (David et al., 2019), made the morphological methods seem slightly inferior to the more technologically advanced ones. The study of David et al., (2019) severely increased the potential of photographic-based approach. Their results showed that community structure, obtained from photo-analysis of ARMS plates, could discriminate ARMS sites at very small spatial scales (tens of kilometres; within an ecoregion), despite using broad taxonomic categories. They therefore validated the use of photo-analysis as a fast and efficient screening tool for biodiversity monitoring in concordance to the MSFD demands, since biodiversity descriptor of the MSFD does not explicitly require that all species are taxonomically identified (Danovaro et al., 2016).

6.8. Marine biodiversity observation network

Despite above listed drawbacks, the future for ARMS research looks bright as projects like the Marine Biodiversity Observation Network (MBON) significantly contribute to the relevance of the sampling method and support synergistic development and fine-tuning of associated molecular and image-based analysis approaches (Obst et al., 2020). The ARMS-MBON project, supported by the ASSEMBLE+ (Association of European Marine Biological Laboratories Expanded) programme, aims to establish a network of ARMS-based observatory sites in EU and arctic waters, to assess the status and changes of benthic hard-bottom communities in near-coast environments. Since its trial phase launch in 2018, the project already resulted in 134 ARMS units, from 20 observatories, deployed in 14 European countries, sampling all major European continental seas as well as Greenland and Antarctica (Obst et al., 2020). So far, huge improvements in complementing image-based and molecular methods have been achieved, trough comparative studies. The project also improved the ARMS-based NIS detection potential and contributed to a growing open-access database that allows continuous enrichment (Obst et al., 2020). Limitations of the methods stated above, therefore steadily decline as genetic and image reference libraries continue to grow and identification methods exponentially improve (Obst et al., 2020).

6.9. Gulf of Trieste

Gulf of Trieste, where this study took place, is a shallow, semi-enclosed embayment, which represents the northernmost part of both the Mediterranean as well as the Adriatic Sea (Pitacco et al., 2014). The gulf contains the entire Slovenian coastal sea, which is located in its southern part (Lipej et al., 2012). The area has been characterized by severe resource depletion since the Roman times (Lotze et al., 2006). The approximate 2500-year-old history of anthropogenic impacts resulted in severe degradation of this coastal sea, which is possibly the most exploited basin of the Mediterranean (Barausse et al., 2009; Lotze et al., 2006). The shallow and enclosed region is influenced by nutrient enrichment, habitat degradation (Cozzi et al., 2020; Spagnolo et al., 2017), fishing pressures (Barausse et al., 2011), mariculture (Crocetta, 2011; Spagnolo et al., 2017) and intense shipping traffic (Spagnolo et al., 2017), which are synergistically contributing to the degradation of the biological community (Barausse et al., 2011). Fluctuating patterns of eutrophication and oligotrophication have been discussed in the region as well, and have caused loss of benthic fauna in the past (Cozzi et al., 2020; Mozetič et al., 2010).

Recently, the shore and some coastal habitats have been modified by urbanisation, construction of infrastructure and massive tourism pressure, particularly present in the Gulf of Piran (Orlando-Bonaca et al., 2012). The latter, along with NIS introduction, are the major concerns for marine biodiversity in the region, as they disrupt the delicate equilibriums of native biota, affect species richness and the stability of ecosystems (Spagnolo et al., 2017; Gofas & Zenetos, 2003). Northern Adriatic is characterized by the presence of numerous ports such as Trieste Harbour and Port of Koper, which contribute to intense shipping traffic in the region (Spagnolo et al., 2017). Combined with mariculture (fish & mussel farms), these activities represent the main sources of NIS introduction (Occhipinti-Ambrogi et al., 2011). To illustrate the issue, a large amount of NIS (n = 52) have been found just within the Slovenian during the recent years (Orlando-Bonaca et al., 2020). There is an urge to deploy early warning systems for such species close to their introduction hot spots, to help minimize their spread and impact (Reiss et al., 2014).

6.10. Work so far and contributions

According to the ARMS official website (https://www.oceanarms.org/deployments/search, 2021), 90 sampling units have been deployed in the Mediterranean so far. Most were deployed in the North-Western part of the Mediterranean at the coasts of Gulf of Lion (33) and Ligurian Sea (30) as well as the coasts of the Tyrrhenian (9) and Adriatic (18) seas. Despite the seemingly large number of ARMS deployed, scientific literature derived from them is not so extensive, as the studies are usually of greater geographic range and target different subsets of associated communities and methodologies. For example, Pennesi & Danovaro (2017) focused on assessments of microphytobenthic communities colonizing ARMS in the Adriatic. Papers from Cahill et al., (2018) and David et al., (2019) analysed biofouling communities from similar locations in the Mediterranean, but focused on different methodologies of molecular methods and photo-analysis, respectively. Lastly, some ARMS were deployed in the Gulf of Lion and Adriatic for the pan-regional metabarcoding study by Pearman et al., (2020).

Aiming to mitigate the effects of anthropogenic disturbances mentioned above, many studies of environmental condition assessments have been undertaken in the Northern Adriatic (Cozzi et al., 2020). Previous work focused primarily on phytoplankton (Mozetič et al., 2010; Cozzi et al., 2020), fish stocks (Barausse et al., 2011), microphytobenthos (Giani et al., 2012) and soft-bottom habitats (Mancinelli et al., 1998), with hard-bottom communities getting less attention in this aspect.

The study from Nerlović et al., (2018) discussed the biofouling community structure derived from experimental plates, focusing on NIS detection and effects of mariculture. Additionally, Fava et al., (2016), addressed some dynamics within communities inhabiting coralligenous outcrops in the adjacent waters. Previous benthic hard-bottom monitoring using experimental tiles in Slovenian waters required manual observations of settlement tiles in the laboratory, resulting in time consuming and destructive tasks, with no or very limited data on the quantity of the organisms (e.g. Vrišer, 1986; 1978). Only recently, a benthic plate study by Fortič et al., (2021) focused exclusively on sessile hard-bottom communities in the Bay of Piran (Slovenian Sea) and provided crucial foundations on temporal changes, seasonal occurrence, effects of tile placement season and NIS detection.

Further, the scientific literature focusing on different photo-analysis method comparison is very scarce and focuses on imagery of megafauna derived from ROVs (Drummond & Connell, 2005; Durden et al., 2016; Moore et al., 2019) and not on smaller sessile invertebrates present on experimental settlement plates, without even considering the organism annotation software (Drummond & Connell, 2005; Moore et al., 2019), such as CPCe in their analysis. These image annotation software programmes are rapidly developing and seem to offer many benefits, some of which will affect the usefulness and application of different annotation methods (Moore et al., 2019). In this regard, comparing and evaluating different photo-analysis methods is to be very useful for future studies of such sorts and represents an important aspect of discussion (Durden et al., 2016; Moore et al., 2019).

6.11. Focus of the thesis

With regards to the scientific focus of the recent years, it is crucial to contribute to the field of benthic monitoring and NIS early warning system development to mind the missing gap in scientific literature for benthic communities in the Northern Adriatic Sea. In this instance the Marine Biology Station Piran (MBSP) is involved in the ARMS-MBON project since its debut in 2018, with hopes to establish long term ARMS-based biodiversity and NIS detection observatory sites within the Slovenian Sea.

Before ARMS observatory sites are applicable for long-term monitoring research, optimal deployment periods and immersion times for the study area must be assessed (Obst et al., 2020). Benthic communities from distinct benthic habitats possess different colonisation pressures, resulting in unique composition patterns of settled species on ARMS plates. This comes from the fact that once submerged, the plates are colonized by the adjacent benthic fauna and flora

through the process known as succession (Lindeyer & Gittenberger, 2011). This process, described as directional change in a community structure over time (MacMahon, 1979) is influenced by the unique life-history characteristics of particular species in the specific habitat and environmental factors present (temperature, salinity, light, etc.) (Lindeyer & Gittenberger, 2011). Since these factors, that govern communities larval supply and growth, tend to differ strongly among seasons (Dziubińska & Janas, 2007), immersion season and deployment periods of ARMS are important aspects to consider as they immensely contribute to the developed hard-bottom community structure on the plates, especially in temperate regions (Qvarfordt et al., 2006; Lindeyer & Gittenberger, 2011; Obst et al., 2020).

Governed by the succession pace, density of the associated biofouling community greatly contributes to the usefulness of result obtained. If ARMS are deployed for too long, the resulting species density significantly decreases the resolution of molecular and photographic analysis (Obst et al., 2020). This effect is particularly severe for photo-analysis, since these organisms like to stack up on top of each other, forming consecutive layers. Seasonality may produce overcrowding with a few species, increasing the chance of missing a rare organisms, with consequences for NIS detection and biodiversity estimation (Obst et al., 2020). On the other hand, ARMS of shorter deployments may not carry sufficient diversity of organisms to be representative of any sense. The combined effects of undesired species density contribute to impaired and biased community assessments. Therefore, immersion periods should be fine-tuned for each ARMS observatory respecting the specific variable of interest and region-specific succession dynamics.

Photo-analysis methods, particularly point overlay annotation, proved to be a very accurate and rapid methods of obtaining estimates of sessile marine invertebrate cover estimates (Drummond & Connell, 2005), which are essential for assessments of community structure (Moore et al., 2019). As the scientific literature focusing on the usage of photo-analysis of ARMS plates as the main method for benthic community assessments is scarce and should be examined in detail (David et al., 2019), this thesis considers a comparison of results derived by three different annotation methods (100, 300 point overlay & 5x5 grid survey), frequently used in similar assessments. By incorporating a dedicated annotation software (CPCe) for both point overlay methods apart from the manual input based 5x5 grid survey, we aim to illustrate and promote the significant usefulness of such programmes (Durden et al., 2016) for obtaining community structure, trough cover estimates, in ARMS and benthic plate-based studies.

As no long-term ARMS-MBON observatories have been established in the northern Adriatic so far, this work investigates what immersion seasons and deployment periods of ARMS are required to achieve optimal community structure for biodiversity monitoring and NIS detection trough plate photo-analysis. ARMS used in this work represent the first trials of such deployments in the Slovenian Sea, with the main interest in developing the most optimal protocol for future observatories in the area. Therefore, our main research question is what length of ARMS deployments in distinct benthic habitats are most optimal for monitoring benthic communities through photo-analysis. Further, we aim to assign the most suitable photo-analysis method for obtaining the biofouling community structure trough cover estimates. Additionally, this thesis will introduce important aspects of ARMS photo-analysis of using finer taxonomic categories within a region and analysis of all 17 plate-faces for obtaining community structure and comparisons of such as was recommended by David et al. (2019) and provide important guidelines for photo-analysis annotation methods, recommended by Moore et al. (2019) for assessments of community structure and NIS detection purposes, proposed by Obst et al., (2020).

The following thesis focuses on developing optimal ARMS deployment protocols, providing guidelines for future experiments and development of photo-analysis methodology, hoping to promote establishments of other observatory sites in the Northern Adriatic. We aim to help in establishing these methods as one of the standards for marine biological monitoring and NIS surveys in relevant hard substrate and biogenic habitats, capable of building up time-series of standardized data, as recommended by ARMS-MBON (Obst et al., 2020). The aspects considered in the thesis will therefore provide crucial methodological foundations for photo-analysis and deployment protocols of ARMS plates throughout the whole ARMS-MBON, therefore being very useful for countless future studies and assessments of sessile hard bottom communities around the globe (Obst et al., 2020).

7. MATERIALS AND METHODS

7.1. Study area

The three studied sites are located in the Slovenian Sea, which is a part of the Gulf of Trieste, the northernmost part of the Adriatic Sea and consequently the whole Mediterranean Sea. It is characterized by the lowest temperatures in the Mediterranean, which can fall below 10°C in the winter months (Boicourt et al., 1999). Hydrodynamic conditions display seasonal patterns of thermal stratification of the water column in the summer months, due to surface heating and freshwater inflow (Boicourt et al., 1999). This state changes in the autumn, as cooling processes and strong wind regime establish vertical homogeneity of the water column during the winter period (Mozetič et al., 1998). The gulf is relatively shallow, with an average depth of about 20 m (Lipej et al., 2012). It reaches its maximum spot of 33 m near the Bay of Piran, the largest bay within the Gulf (Pittaco et al., 2014).

The surface sediments of the coastal zone, which is a few 10 m wide and coincides with the 5 m isobath, consist of silt and sandy silt with rocky substratum of Eocene Flysch, with alternating solid sandstone and soft marl (Ogorelec et al., 1991). Sediments of the two main bays of Koper and Piran are mainly composed of silty clay, while a gradual increase in grain size is present towards the open part of the Gulf, where the sand fraction, consisting of about 80% of biogenic detritus, prevails (Ogorelec et al., 1991). The adjacent rivers contribute to freshwater inflow and sediment resuspension, but sedimentation rates within the smaller bays remain high (3-5 mm yr-1) (Ogorelec et al., 1991).

The area was underlined by oligotrophication over the last decades (Mozetič et al., 2010) and is influenced by many anthropogenic stressors like tourism, overfishing, mariculture, pollution and busy ship traffic (France & Mozetič, 2006; Mozetič et al., 2008). Recently, the shore and some coastal habitats have been modified by urbanisation, construction of infrastructure and mass tourism pressure, particularly present in the Gulf of Piran (Orlando-Bonaca et al., 2012).

7.2. Monitored sites

11 ARMS units were deployed at 3 distinct locations (study sites), each representing a distinct marine benthic habitat of interest for future monitoring applications for the Slovenian and adjacent waters of the northern Adriatic (ARMS deployment information shown in **Table 1**, locations shown in **Fig. 1**). Two study sites: Piran (PIR, orange) and Buoy Vida (VID, blue),

correspond to fundamental benthic habitats, which are frequently found in the marine region and are characterized by a rich epifauna. At the corresponding research sites, 1 or 2 ARMS units were deployed at the same time (same deployment), but for different deployment periods ranging from 3 – 13 months. The one remaining site, Port of Koper (PK, purple), is located within the industrial port, where ARMS were deployed one at a time in a subsequent manner, for the same period of 4 months. All 3 ARMS sampling sites represent localities that are easily accessible, so the structures can be regularly re-deployed and retrieved, with minimal costs and effort.

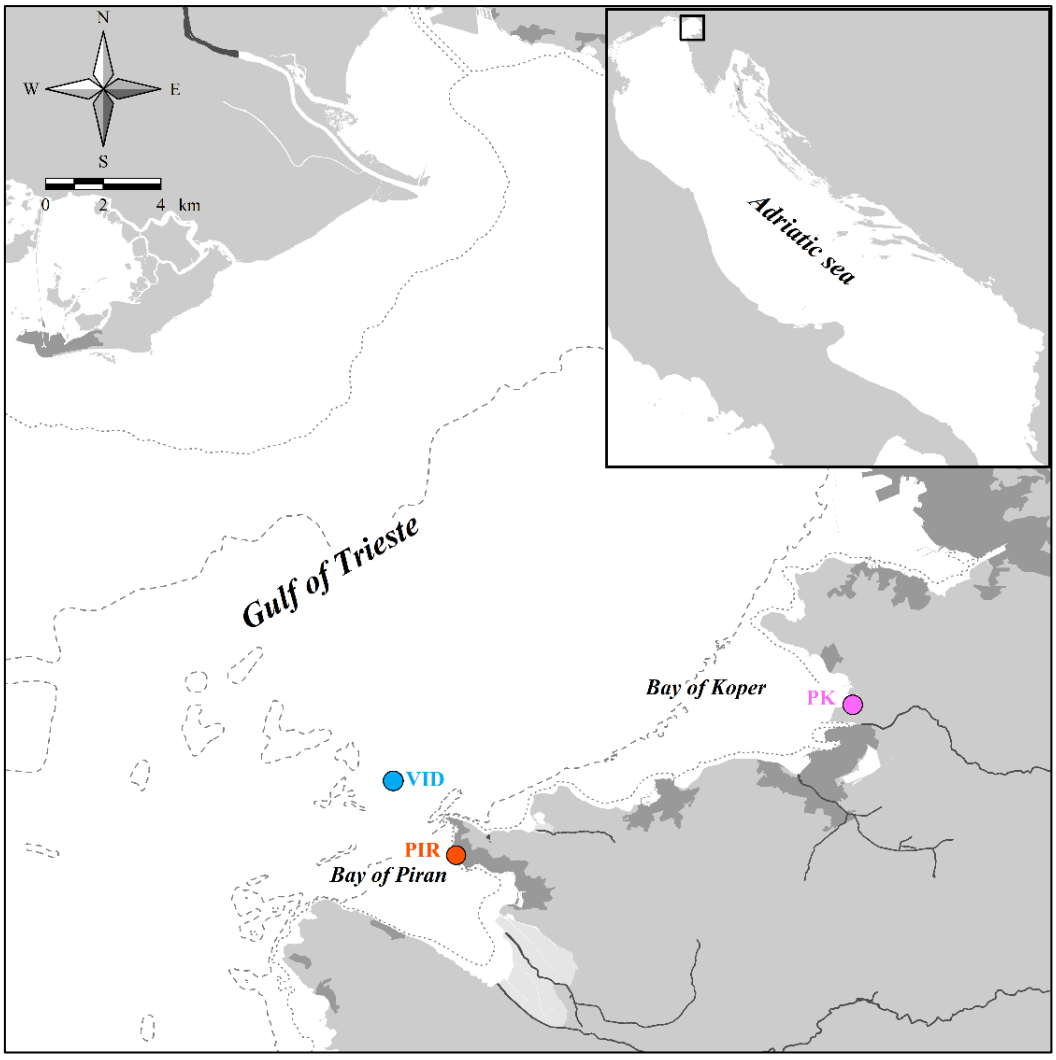

Figure 1: Map of the Gulf of Trieste study area, indicating 3 distinct study sites (Piran = orange, Buoy Vida = blue, Port of Koper = purple) within the Slovenian sea, where ARMS units were deployed.

Table 1: Precise information of 11 distinct ARMS sampling units, deployed at 3 study sites within the Slovenian sea for the means of the study during the years 2018 - 2021. Seq. = sequence, Dep. Seq. = deployment sequence & Dep. Per. = deployment period estimate (in months).

Seq.	Study site	Coordinates	Depth (m)	Deployed	Retrieved	Dep. Seq.	Dep. Per. (Mo.)	ARMS id
1	Piran	45.5188 - 13.5673	9	15.08.2018	15.02.2019	1	6	PIR_1_6M
2					18.11.2018		3	PIR_1_3M
3				2.07.2019	27.01.2020	2	6	PIR_2_6M
4					10.06.2020		11	PIR_2_11M
5	Buoy Vida	45.5487 - 13.5507	22	11.07.2019	31.01.2020	1	6	VID_1_6M
6					11.06.2020		11	VID_1_11M
7				11.06.2020	28.07.2021	2	13	VID_2_13M
8	Port of Koper	45.564856 - 13.743586	3.5	22.06.2020	20.10.2020	1	4	PK_1_4M
9				20.10.2020	23.02.2021	2	4	PK_2_4M
10				23.02.2021	22.06.2021	3	4	PK_3_4M
11				22.06.2021	27.10.2021	4	4	PK_4_4M

7.2.1. Piran study site

The 4 ARMS sampling units of the Piran site (**Fig. 1**, PIR) were deployed in a near-shore lower infra-littoral zone in the Bay of Piran, mounted on a concrete structure at approx. 9 m of depth (GPS position: 45.5188, 13.5673). The surrounding area is characterized by transition from a rock dominated hard bottom habitat into a muddy to sandy seabed, with addition of biogenic (*Pinna nobilis* shells and other remains of calcified exoskeletons, etc.) and artificial (concrete, pipeline system, remains of fishing nets, tires, etc.) elements, that together with native rocks and stones, host benthic epifauna and flora of rich biodiversity (Lipej at al., 2016). In the vicinity of the ARMS deployment location, metal constructions carrying benthic experimental tiles were present, due to the previous research by Fortič et al., (2021), addressing temporal changes of the biofouling community in the area.

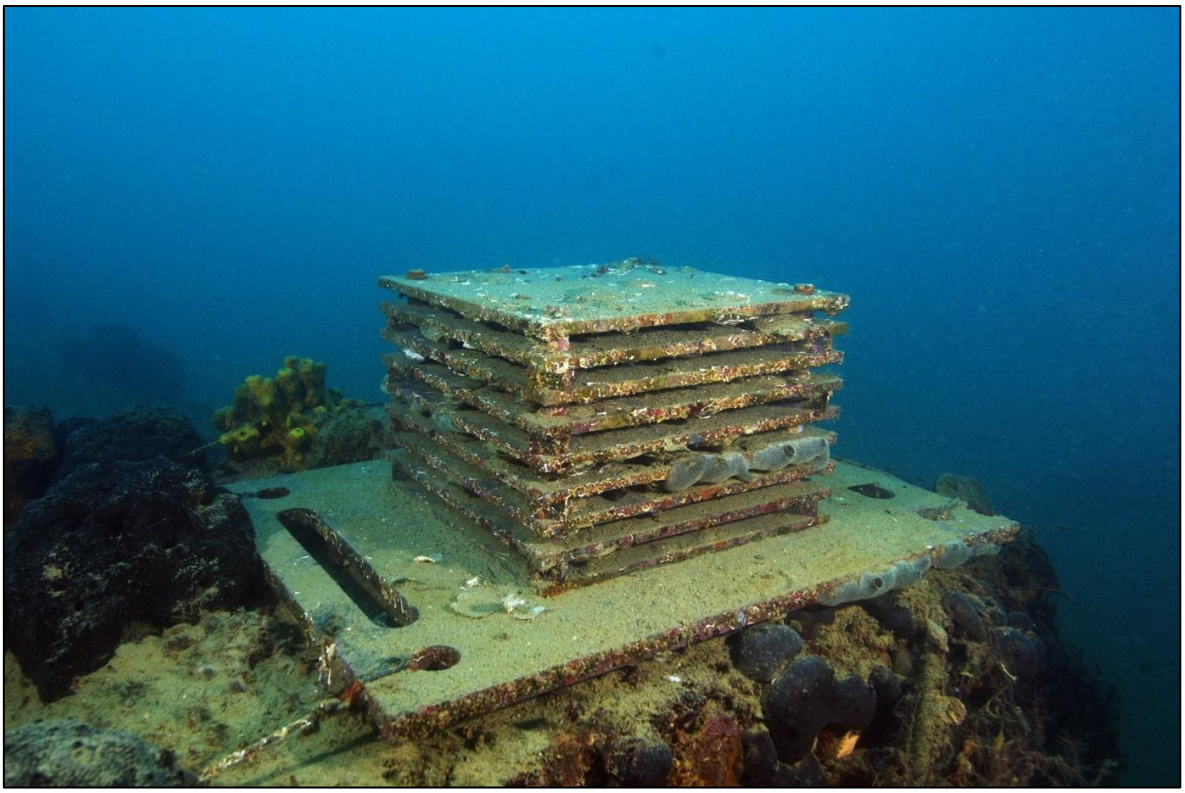

Figure 2: A photograph of the ARMS unit and the surrounding flora and fauna that was present on rocky surfaces at its vicinity at the Piran study site, just before its retrieval. Photograph by Borut Mavrič, PhD.

7.2.2. Buoy Vida study site

The following 3 ARMS units were deployed in a an off-shore circalittoral zone near the oceanographic buoy Vida at approx. 22 m of depth (GPS position: 45.54875, 13.5507) (**Fig. 1**, VID) The area is characterised by the presence of a sandy to muddy seabed, heavily enriched by organic detritus (additionally coming from the community of *Mytillus galloprovinicialis* developed on the anchoring chains) which is densely populated by epibenthic invertebrates, dominated by the ophiurid *Ophiotrix quinquemaculata*, echinoderm *Psammechinus microtuberculatus*, sponges of the genus *Axinella, Ulosa, Suberites, Tethya, Haliclona, Dysidea, Tedania, Ircinia,* etc., tunicates *Phallusia mamillata*, species of the genus *Microcosmus*, etc. Due to the anchorage system of the oceanographic buoy Vida and wave dynamics at the surface there is some locally increased resuspension at the bottom.

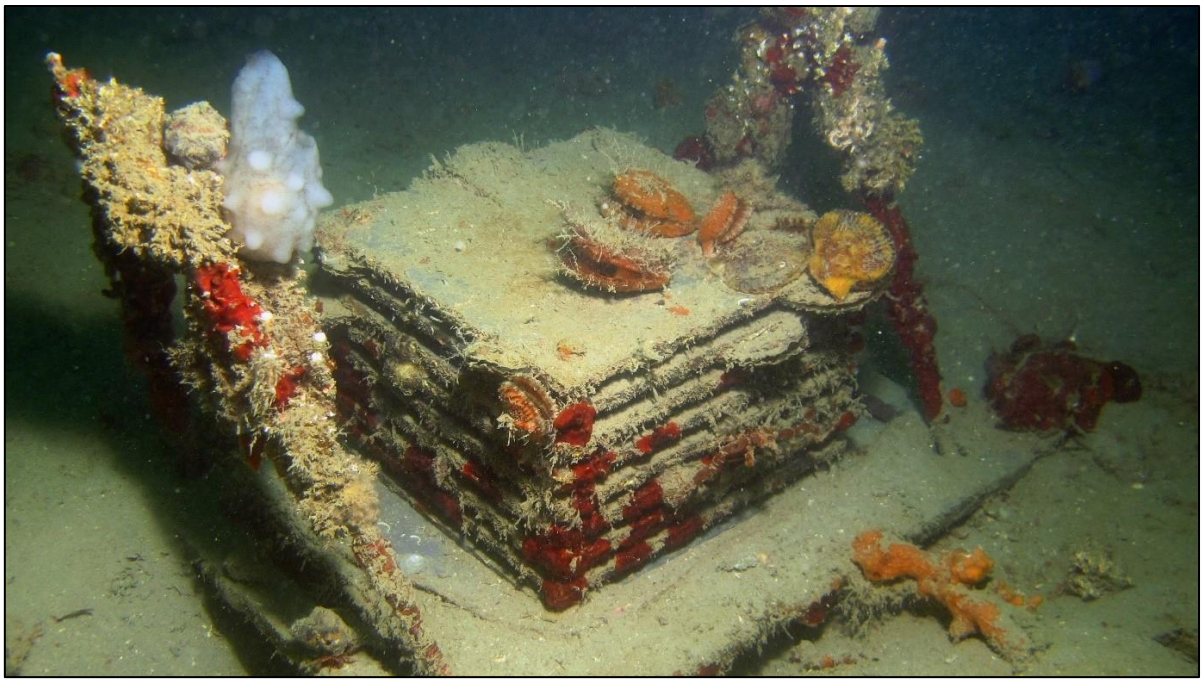

Figure 3: A photograph of the ARMS unit and the surrounding fauna that was present on sandy seabed at its vicinity at the Buoy Vida study site, just before its retrieval. Photograph by Borut Mavrič, PhD.

7.2.3. Port of Koper study site

The remaining 4 ARMS, deployed within the industrial Port of Koper (**Fig. 1**, PK), were attached between the concrete pillars of the pier II (GPS position: 45.564856, 13.743586) with synthetic ropes, securely positioned in the water column, at approx. 3.5 m depth, during the whole deployment period. The surrounding infralittoral habitat is characterized by limited-light availability, freshwater inflow from River Rižana, high sedimentation and resuspension due to ship manoeuvres and port activities and presence of numerous artificial hard surfaces (concrete pillars, metal pylons, ship hulls, barrier buoys, ropes, etc.). The bottom below is muddy and ranges between 5-15 m of depth. Remains of organic detritus, coming from above fouling community and occasional artificial hard particles from port activities are present within the water column. The shade-loving fouling community, colonizing the artificial hard substrates in the area, mainly consists of filter feeding bivalves (*Ostrea* sp. & *Mytilus* sp.) and polychaete tube-worms (Sabella sp., Serpula sp.), cnidarian polyps (*Aurelia aurita)*, tunicates (e.g. genus *Pyura*, *Microcosmus, Ascidia* and *Ascidiella*) and sponges (*e.g. genus Clathrina* sp., *Haliclona, Dysidea, Oscarella*). Presence of macroalgae on the concrete pillars is very limited due to the scarce light availability (Lipej et al., 2020).

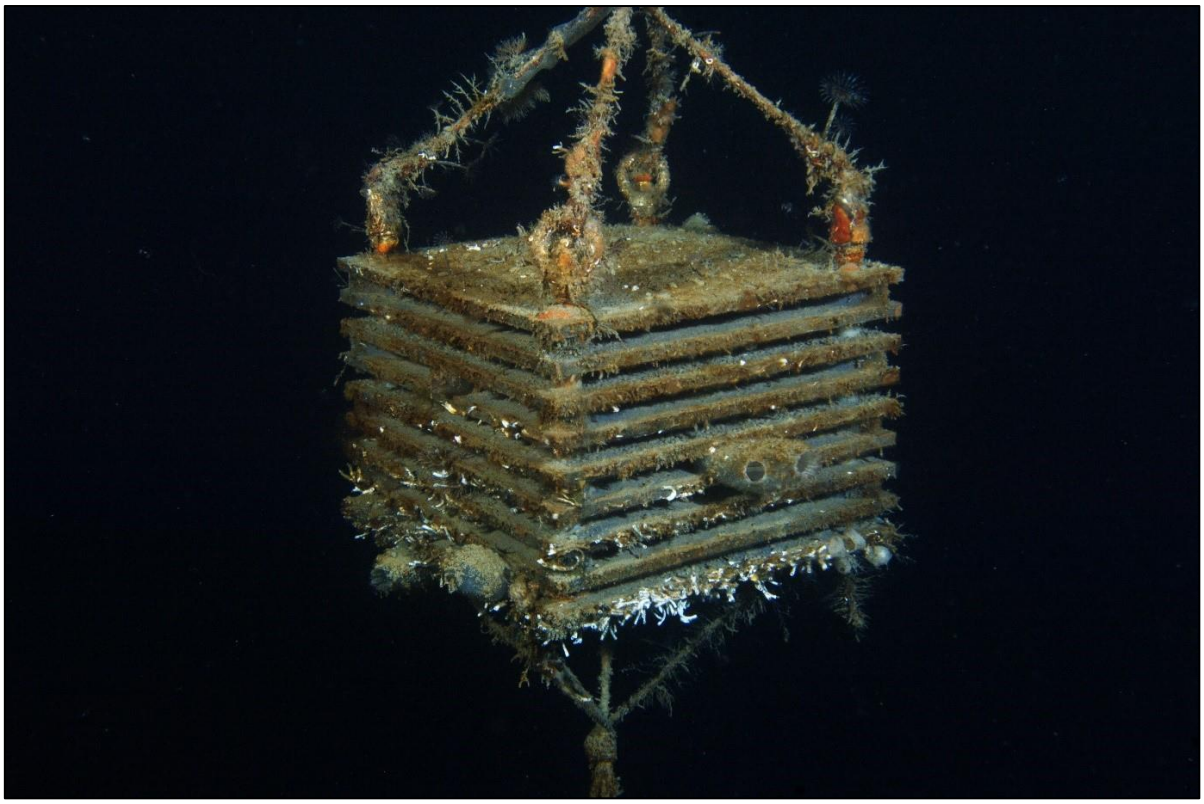

Figure 4: A photograph of the ARMS unit, deployed below the pier and within the water column at the Port of Koper study site, just before its retrieval. Photograph by Borut Mavrič, PhD.

7.3. Sampling procedure

7.3.1. Deployment

Prior to each sampling, the ARMS units were constructed at the diving facility of MBSP or aboard the research vessel Sagitta, with respect to the standard protocol (https://www.oceanarms.org/protocols/deployment, 2021). The assembly consists of stacking 9 standardized (22.5 cm × 22.5 cm) PVC plates in an alternating series, with plastic spacers in between, mounted on a base plate of larger dimensions (35 cm × 45 cm). The fully assembled ARMS units were then transported by a research vessel (VID & PK) or by foot (PIR), depending on their deployment site. After reaching the desired location, the structures were immersed into the ocean with the help of two SCUBA divers. Units deployed at Piran and Buoy Vida site, were attached to the seafloor, where divers carefully installed the ARMS on a horizontal plane, most suitable (representative) of the monitored habitat. The base plate was attached to the hard-bottom substrate with plastic ropes, to secure the structure in place (**Fig. 2 & 3**). At the Port of Koper site, the ARMS unit was not mounted to the seabed, but was attached to the concrete

pillars of the pier by ropes, from the top and bottom side (**Fig. 4**). This deployment design achieved a fixed position of ARMS in the water column, thus adding an additional colonizable plate face (1B), to the usual 17.

7.3.2. Retrieval, disassembly and processing

Retrieval process of the colonized ARMS at the end of their deployment period is somewhat more demanding. After locating the deployment site, SCUBA divers carefully enclosed the structure in a plastic container (crate), securing biofouling organisms before any major disturbance. The ropes were cut to detach the base plate from the seafloor/pier. The fully-enclosed structure was then flipped upside-down, with the upward-facing base plate secured to the crate by rubber ropes. Divers then slowly ascend to the surface, carefully holding the crate at each side. The enclosed ARMS unit was then carefully transported to the wet-lab inside the research station, where air bubblers were installed inside the retrieval crate, to aerate the fouling organisms of the colonized plates.

ARMS units were then carefully disassembled the same day as they were retrieved, while still being submerged in the retrieval crate filled with seawater. Before the plates were individually transferred into white trays, filled with filtered seawater, they were sensibly shaken inside the crate, to remove the excessive sediment, that accumulated on the plate surface. Plate identifiers, containing the information about the ARMS unit: location, deployment date, retrieval date, plate sequence (1, 2, 3 …) and orientation (T & B), were also attached to the tray.

Each plate was then thoroughly photographed with a Nikon D2X digital camera and flash in a consequent and standardized manner. Firstly, a photograph of the whole plate with the identifier was taken, followed by 4 close-up photographs of the plate in the clockwise-manner and lastly detailed macro-photos of individual specimens found on the plate surface. After all plate-faces were thoroughly photographed, some organisms of questionable identification were collected and stored in 70% EtOH for morphological examinations.

7.3.3. Photo-analysis

The first step in photo-analysis, was transferring photos to a computer where files of digital photographs were renamed and labelled with respect to the requirements provided by the ARMS-MBON handbook protocol (Obst et al., 2020). The organized photographs were then transferred to the Adobe Lightroom v. 6.0 photo-editing software, where colour correction, brightness, clarity, shadow intensity and other basic parameters were adjusted. Photographs

containing the whole surface of the plates were cropped in a 1x1 (square format) manner, with still some space at the edges (shown in **Fig. 5**), so the full morphology of organisms on the edges was still visible. Close-up photographs of individual organisms were transferred to an excel spreadsheet, where organism categories to the lowest taxonomical level possible (taxonomic categories) were assigned to morphologically similar organisms, serving as an identification reference catalogue.

When all the taxonomic categories from the reference catalogue were defined by the help of my main supervisor Borut Mavrič, PhD and young researcher assistant Ana Fortič, BSc, a specified code file for the photo-analysis software - Coral Point Count with Excel extensions (CPCe, v4.1, 2020) programme (Kohler et al., 2006), was made with the aid of Microsoft Notepad. The corrected 1x1 photos of plates, containing the whole plate surface, were individually loaded into the CPCe software, where borders of the region of interest (solely the surface of the 22.5 cm × 22.5 cm plates) were manually selected (**Fig. 5**, yellow lines). Finally, based on the photo-analysis method of choice, 3 different types of data point distributions were chosen as follows:

- **100 point overlay method:** Stratified 10 x 10 grid (10 rows & 10 columns) with 1 randomly assigned point within each cell, resulting in 100 points overlaid per plate (Not shown).
- **300 point overlay method:** Stratified 10 x 10 grid (10 rows & 10 columns) with 3 randomly assigned points within each cell, resulting in 300 points overlaid per plate (**Fig. 5**, left).
- **5 x 5 grid survey method:** Uniform 6 x 6 point grid overlay, resulting in 25 equal cells to be surveyed per plate surface (**Fig. 5**, right).

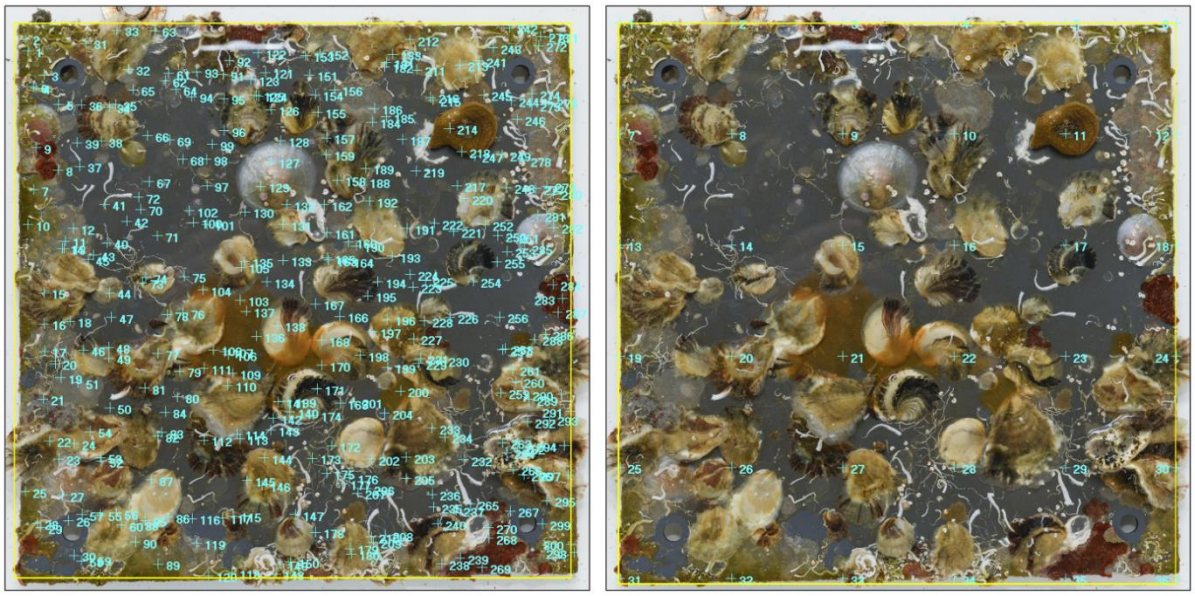

Figure 5: Screenshots of 2 different point distributions for the random 300 point overlay (left) and 5x5 grid survey (right) photo-analysis method, taken from the CPCe programme. Overlaid points (light blue) are scattered accordingly within the manually selected region borders (yellow).

The 3 distinct methods of organism surveys required 2 different approaches of image analysis (annotation). For both 100 and 300 point overlay methods, organisms underlying each assigned point were annotated by the appropriate taxonomic category from our before-hand specified code-file, accessible within the CPCe programme, and were exported directly in the form of a Microsoft Excel spreadsheet. This point-overlay annotation approach counts the frequency of each overlaid taxon for each plate-face and has been proven as an efficient sampling method to obtain estimates of coverage for sessile organisms (Drummond & Connell, 2005; Moore et al., 2019). In this study, cover estimates derived from point-overlay were used as an approximation for relative abundance of the taxa. Points which overlaid empty surfaces, biofilm or sediment were considered as uncolonized (empty). In the case of overgrowth, where more than one organism was present at one overlaid point, more taxonomic categories were assigned for the respected point.

On the contrary, the 5x5 grid survey method required a more demanding visual survey approach, where all taxonomic categories present at each of the 25 individual cells per plate-face were manually labelled within the before-made Microsoft Excel spreadsheet. As each image was divided up into equal areas (cells) and the presence of any taxonomic categories recorded within each of the grid cells, the occurrence of each taxon in a cell represented 4% to

the total coverage. A taxon lying under more than one cell (even if only a small fraction) was annotated for each of those cells.

7.4. Data analysis

The main focus of the analysis was to explore the biofouling community structure, which is defined as ecologist's term for indicating what organisms are present in a given environment, in what numbers, and how they relate to each other (Adey & Loveland, 2007). In this regard, organisms of the ARMS associated macroscopic biofouling community were sorted into individual taxonomic categories, to the lowest taxonomical or morphological level possible and were arranged into broader taxonomic groups. This resulted in some organisms defined to the species, genus or even broader taxonomic categories based on their visually apparent morphology. The photo analysis methods used, provided information of the frequency of occurrence under a certain area/points, that serves as an equivalent for taxa coverage estimation. This obtained coverage estimates could later be compared, as they were expressed as percentages of the total plate surface or the total colonized area.

After annotating all the overlaid points within the CPCe programme, automatically generated Microsoft Excel (v. 365, 2021) datasheets, containing data from both 100 and 300 point overlay methods, were exported and adjoined to the manually filled Excel datasheet from the 5x5 grid survey method, for further data analysis. Basic statistical parameters, tables and most graphical representations (box-plots, bar charts and 5x5 diagrams) were done with the Excel programme. For obtaining the more demanding statistical parameters (Mann-Whitney-U test, one-way ANOVA, Similarity Percentage, etc.) and plots (non-parametric multiple dimension scaling), PAST statistical software v. 3.26 was used (Hammer et al., 2001).

7.4.1. Comparison of methods

To compare and evaluate the 3 distinct photo-analysis methods of interest the community structure of the fouling assemblages from 3 ARMS units from the Piran study site were annotated by 100 and 300 point overlay as well as 5x5 grid survey. The derived datasets were compared side by side in the aspects of the numbers of taxonomic categories detected per plate and individual unit (box-plots), the proportions of the broader taxonomic groups (stacked column charts) and distances of the plate-face community structures (NMDS). Additionally, a graphical diagram was constructed from the 5x5 grid survey, to show the taxonomic density of the colonized organisms on ARMS plate surface.

7.4.2. Community structure

To assess the structure of the developed biofouling community at each study site, all plate-faces from each individual ARMS were analysed by a 300 point overlay photo-analysis method. For a particular study site, a list of taxonomic categories was created, with information at what proportions each such was present at ARMS units, plate-faces and total overlaid points. Community structure was displayed trough stacked column charts of the broader taxonomic groups. The total community structure from all ARMS from a study site combined was firstly compared to those of distinct orientations, later among all individual ARMS units and finally regarding both the AMRS unit and also plate orientation. Most frequently detected taxa were underlined for the total units at the site and also distinct orientation.

By tracking the number of points under which an organism was present (colonized) or not (empty) from the total 300 overlaid, stacked column chart were made for each site regarding the orientation and both combined, to illustrate the amount of colonized surfaces of ARMS plates (stacked column charts). Additionally, the amount of colonized proportions per plate-faces was compared among ARMS units from the same site (box-plots).

Lastly, distances of the plate-face community structures (NMDS) and frequency of occurrence dissimilarity values among the developed communities (SIMPER) were presented for all individual ARMS units at the site, regarding the plate-face orientation.

7.4.3. Comparison of sites

To compare the colonization patterns and community structure between the 3 different ARMS sampling sites and to display the effects of the various submersion seasons and deployment periods, the data from all 11 ARMS units obtained by the 300 point overlay method were used. The total derived data were compared side by side for each individual ARMS unit in the aspects of the numbers of taxonomic categories detected per plate-face of the individual unit (box-plots) and colonized proportions of plates. Both were displayed next to the data obtained solely from bottom oriented plate-faces.

To show the differences in community structure, proportions of the broader taxonomic groups (stacked column charts) and distances of the plate-face community structures (NMDS) were shown in the same manner (Total vs Bottom). Additionally, SIMPER tests were made to illustrate the percentages of the dissimilarities of the frequency of occurrence of taxonomic categories among the developed communities (SIMPER).

8. RESULTS

8.1. Comparison of different photo-analysis methods

The 3 datasets, each obtained by a different photo-analysis method (100 point, 300 point & 5x5 grid) of colonized plates from the 4 ARMS units, deployed at the Piran site (PIR_1_3M, PIR_1_6M, PIR_2_6M, PIR_2_11M), were used to evaluate the most appropriate method for the community structure analysis. For the comparison, organisms of the ARMS associated macroscopic biofouling community were sorted into 36 individual taxonomic categories (list not shown), arranged into 8 broader taxonomic groups (Cirripedia, Cnidaria, Porifera, Algae, Ascidiacea, Mollusca, Polychaeta & Bryozoa).

Our first interest was to investigate the differences based on the number of taxonomic categories detected per each plate from all 4 ARMS units altogether (shown in **Fig. 6**) and from the individual ARMS units (shown in **Fig. 7**), by the photo-analysis method of choice.

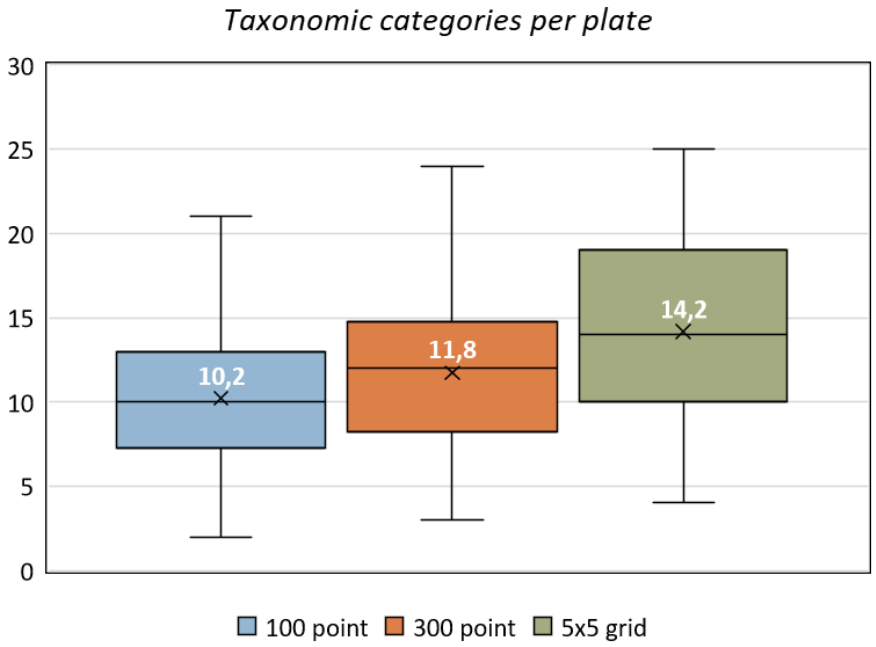

Figure 6: Box plot chart representing the numbers of taxonomic categories, detected per ARMS plate, obtained with 3 different photo-analysis methods. Sample means are indicated with an X, with their values shown in white.

The 3 boxplots of **Fig. 6**, show that 5x5 grid method detected the most taxonomic categories (mean = 14.2, max. = 25), followed by 300 point (mean = 11.8, max. = 24) and 100 point (mean = 10.2, max. = 21) method. The data was tested by a Mann-Whitney-U test ($p < 0.05$) and one-

way ANOVA (F = 11.26, p = 2.3E-05), to confirm that the numbers of detected taxonomic categories and their mean values are indeed statistically different depending on the photo-analysis method used.

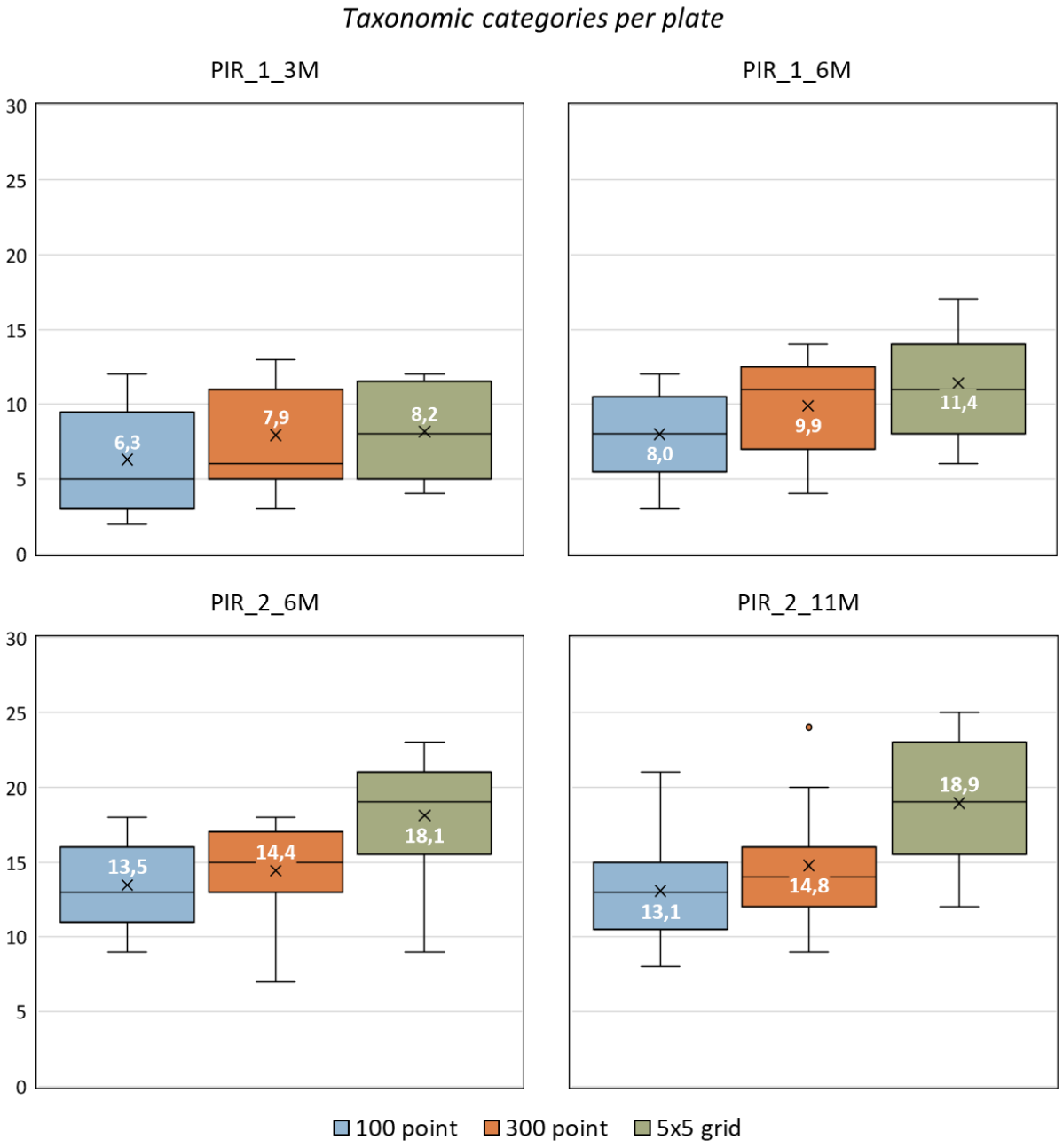

Figure 7: Box plots representing the number of taxonomic categories, detected per plate on each of the 4 ARMS units, using 3 different photo analysis methods. Sample means are indicated with an X, with their values shown in white.

The same trend regarding the numbers of taxonomic categories can be seen in **Fig. 7** where the same data used in **Fig. 6**, are presented for each of the 4 individual ARMS units at the Piran

site. According to the one-way ANOVA test, the mean values obtained by different photo-analysis methods at 3 ARMS: PIR_1_6M (F = 5.6, p = 6.5E-03), PIR_2_6M (F = 9.2, p = 4.2E-04) and PIR_2_11M (F = 11.7, p = 7.5E-05) were significantly different, but not at the PIR_1_3M (F = 1.5, p = 0.24) unit. The 5x5 grid method once more provided the highest mean numbers of categories detected per plate at all 4 ARMS units, with most significance at PIR_2_6M (mean = 18.1, max. = 23) and PIR_2_11M (mean = 18.9, max. = 25), followed by the 300 point and 100 point method, accordingly. Regarding the max. number of categories, the same trend is observed, except at the PIR_1_3M unit, where the 300 point method (max. = 13) detected more categories than the 5x5 grid (max. = 12).

Concerning the total numbers of taxonomic categories detected on each ARMS unit (taxonomic diversity), the 5x5 grid method exhibited the highest amounts on PIR_1_6M (n = 25) and PIR_2_11M (n = 31) from all three methods. The amount was tied at the PIR_2_6M unit (n = 30), however on the PIR_1_3M unit, the 300 point method detected most taxa (n = 20), with the other two both detecting only 18.

Secondly, we investigated how the 3 different photo-analysis methods illustrate the structure of the biofouling community. Contributions (proportions; %) of the 8 broader taxonomic groups from the 4 ARMS units altogether, grouped by the annotation method, are presented in the 3 stacked column charts, below (**Fig. 8**).

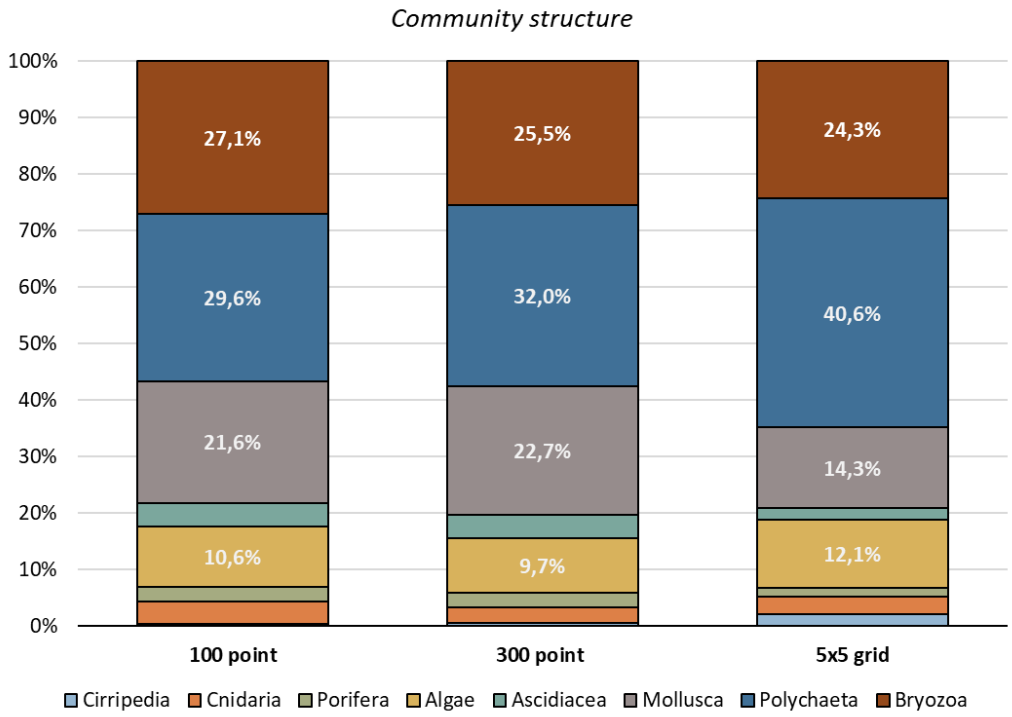

Figure 8: Stacked column charts representing the structure of the biofouling community, using the relative proportions of broader taxonomic groups from 4 ARMS units, obtained with 3 different photo-analysis methods. Proportion values (> 5%) are shown in white.

As can be seen from the pie charts from **Fig. 8**, the relative proportions of groups within the biofouling community do not seem to differ significantly among methods. Proportions of the same groups, derived from the 100 & 300 point overlay methods are almost identical (min. difference = 0.1%, max. difference = 2.5%) whereas the percentages for some groups of the 5x5 grid method (min. difference = 0.3%, max. difference = 11.1%) seem to differ more significantly, especially for the more abundant Polychaeta (difference = 11.1%) and Mollusca (difference = 8.5%) groups. Overall, the coverage contributions of the broader taxonomic groups to the whole community follow accordingly, regardless of the method used.

To statistically compare the detection potential between 100 and 300 point methods, a Mann-Whitney-U test was carried out among the detection frequency data from all plates of 4 ARMS units from the Piran site, for each of the 36 categories and 8 taxonomic groups, individually (Table not shown). Frequencies for the 300 point method were standardized (x / 3) for appropriate comparison. From all 36 taxonomic categories, frequencies of only 6 (17%) were not significantly different ($p > 0.05$). Same comparison was done for the 8 taxonomic groups,

where frequencies from 4 groups (50 %) were not considered to be significantly different ($p > 0.05$).

As both point overlay methods provide information whether the plate surface at the overlaid point is colonized by an organism (colonized) or not (empty), we tested weather the percentages of such points differ among 100 and 300 point datasets, using the Mann-Whitney-U statistical test (data not shown). Data from all plates from the 4 ARMS were used, and frequencies for the 300 point method were standardized (x / 3) for the comparison. The test showed that there were no significant differences ($p > 0.05$) for colonized or empty proportions between the two methods.

As 5x5 grid method could not be directly compared to the two point overlay ones in the sense of detection potential and colonized/empty proportions, the method did however provide information about the density of taxonomic categories at each of the 25 squares during the survey of individual plate. Therefore, a graphical diagram (**Fig. 9**), using mean values of taxonomic categories for each of the 25 squares from all plates of the 4 distinct ARMS units (PIR_1_3M = blue, PIR_1_6M = orange, PIR_2_6M = green, PIR_2_11M = yellow) was constructed. For a better display of organism distribution on the surface of the plates, mean density values of squares at each ARMS unit were divided into quartiles and were coloured accordingly with darker tones as the taxonomic density increased (min. – Q1 = light tone, Q1 – Q3 = darker tone, Q3 – max. = darkest tone).

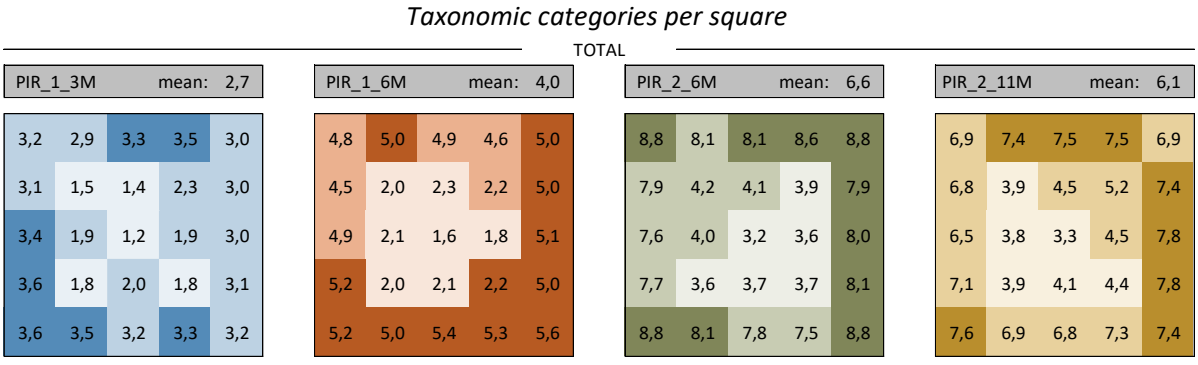

Figure 9: Graphical diagram of average numbers of taxonomic categories present on each square used for the 5x5 grid method from all plates together (Total) for 4 ARMS units separately. Darker tones indicate higher density of taxonomic categories detected.

Looking at the graphical diagrams from **Fig. 9**, a significant pattern of higher taxonomic density at the edges of the plates can be observed at each ARMS deployment. Mean density values

from the squares near the edges have roughly twice the number of taxa than those from the central region of the plates.

Further, a graphical diagram (**Fig. 10**, below) was constructed by the same principles as the previous one (**Fig. 9**), using mean values of taxonomic categories for each of the 25 squares from all plates of the 4 distinct ARMS units (PIR_1_3M = blue, PIR_1_6M = orange, PIR_2_6M = green, PIR_2_11M = sandy) grouped by the plate face orientation (T, B, 9T), to better illustrate the influence of plate orientation on the final organism distribution.

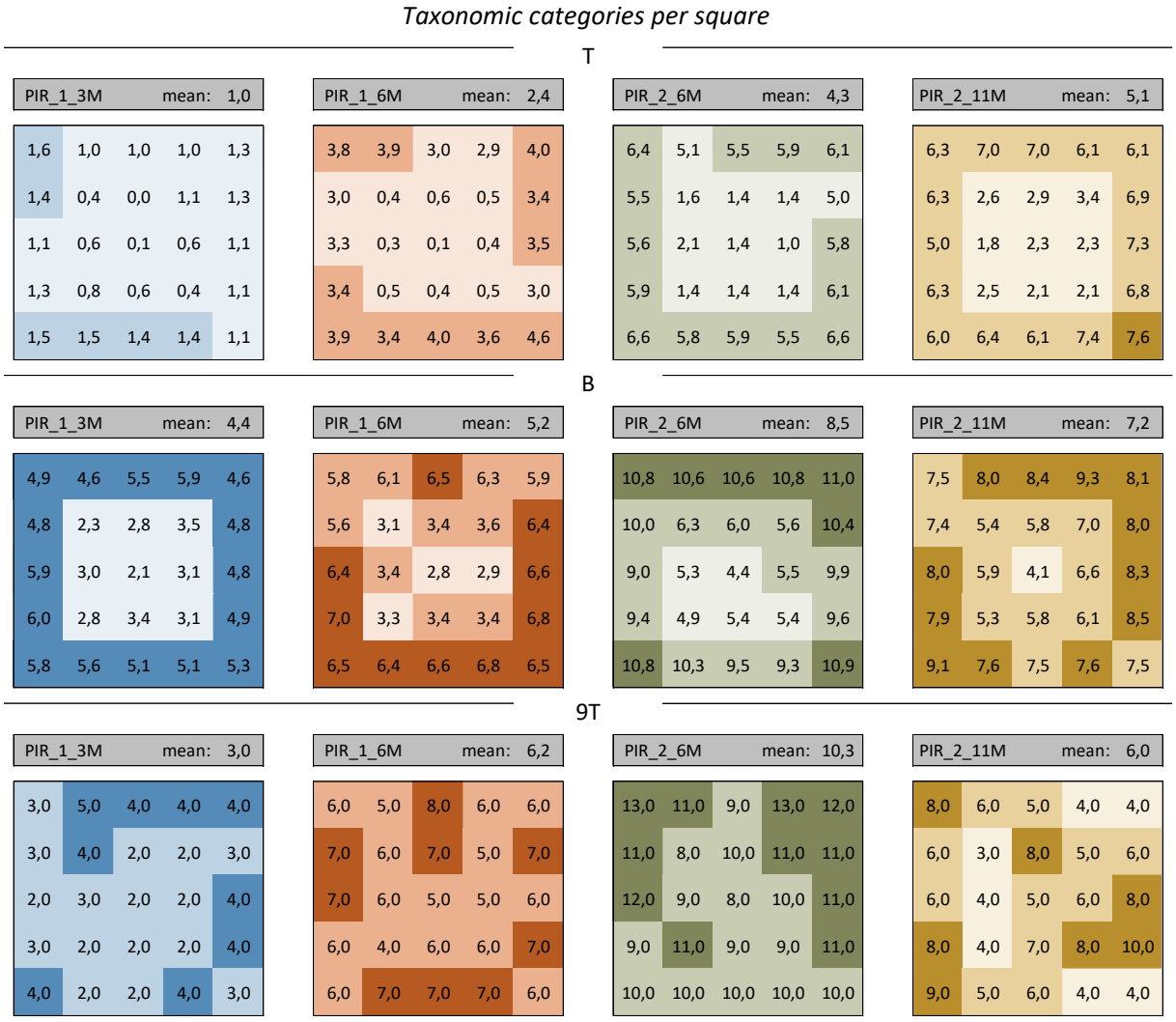

Figure 10: Graphical diagram of average numbers of taxonomic categories present on each square used for the 5x5 grid method for 4 ARMS units, with respect to the plate orientation (1st row = T, 2nd row = B, 3rd row = 9T). Darker tones indicate a higher density of taxonomic categories detected.

The first apparent trend seen from **Fig. 10** is that top oriented plates (T) display the lowest overall mean density values, compared to bottom (B) and topmost (9T) plates. A one-way ANOVA test showed that mean density values were statistically different based on plate orientation at each of the 4 ARMS units (PIR_1_3M (F = 83.0, p = 2.0E-19), PIR_1_6M (F = 49.7, p = 2.7E-14), PIR_2_6M (F = 58.5, p = 8.3E-16) and PIR_2_11M (F = 9.4, p = 2.4E-04)). Interestingly, PIR_1_3M (mean = 4.4) and PIR_2_11M (mean = 7.2) both had the highest mean values on B oriented plates, whereas PIR_1_6M (mean = 6.2) and PIR_2_6M (mean = 10.3) units on the 9T plates. As in **Fig. 9**, significant patterns of higher taxonomic density at the edges of the plates can be observed on T and B plates on all 4 ARMS, however 9T plates failed to illustrate such a pattern.

Lastly, 2 dimensional (2D) non-parametric multiple dimension scaling (NMDS) plots (**Fig. 11**) were generated from the coverage estimates of taxonomic categories dataset, to illustrate the community structure displayed by each photo-analysis method from the 4 ARMS units. Each dot on the plot represents one of the 17 plates from the respected ARMS, labelled by colour (blue, brown, green, sandy). 95% concentration ellipses were outlined, to better visualize the overlap among groups.

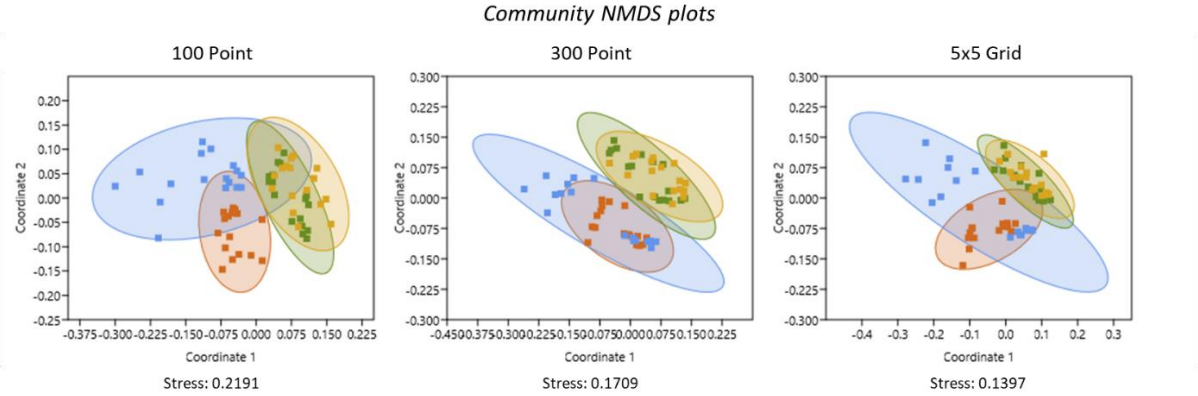

Figure 11: 2D NMDS plots based on Bray-Curtis similarity index of the biofouling community obtained by 3 distinct photo-analysis methods. Dots are grouped by the ARMS unit (PIR_1_3M = blue, PIR_1_6M = brown, PIR_2_6M = green, PIR_2_11M = sandy).

The point scatter and shapes of the 95% ellipses of **Fig. 11** indicate that that the 100 point method provides the most scattered and overlapped pattern, hence the high 2D stress value of 0.22. On the contrary, plots from 300 point and 5x5 grid method have better stress values (300 point = 0.17, 5x5 grid = 0.14) and also express a more similar distribution pattern of points and ellipses, when compared with one another, suggesting that these methods produce a more similar approximation of the biofouling community structure.

8.2. Structure of the biofouling community

For obtaining data of the fouling community structure intended for comparisons among ARMS at each of the 3 study sites and the between sites, solely the 300 point overlay method was used, as it seemed the most optimal photo-analysis method for the job, illustrated in the previous chapter.

8.2.1. ARMS units from the Piran site

Using the 300 point overlay method on 68 (17 x 4) plate faces from 4 ARMS units deployed at the Piran (PIR) study site (PIR_1_3M, PIR_1_6M, PIR_2_6M, PIR_2_11M), 10366 points (50.8% of all overlaid) were annotated with 33 taxonomic categories (taxonomic categories) from 8 groups (shown in **Table 2**). From the 33 total categories, 12 were identified to the species level (species name in concordance with the WoRMS, 2021), 6 to the genus level (sp.) with others assigned with a less precise identification (indet.) or a morphological category (e.g. coralligenous algae, Porifera yellow veins, etc.). Most taxonomic categories were detected on PIR_2_11M unit (n = 27), followed by PIR_2_6M (n = 26), PIR_1_6M (n = 23) and lastly PIR_1_3M (n = 19), indicating a trend of more taxonomic categories present on units deployed for a longer period.

Table 2: List of 33 taxonomic categories and their 8 groups, used for the annotation of the organisms on plates of ARMS units from the PIR site. Values (%) indicate the percentage of ARMS units, plates and points on which the respected taxonomic category was detected. Most frequent categories (> 2% of points) are shown in **bold**.

Taxonomic category	Units (%)	Plates (%)	Points (%)
Cirripedia (n = 2)			
Balanidae *indet.*	50.0	17.6	0.3
Balanus trigonus Darwin, 1854	50.0	13.2	0.3
Cnidaria (n = 1)			
Hydrozoa *indet.*	**50.0**	**35.3**	**2.7**
Porifera (n = 4)			
Crambe crambe (Schmidt, 1862)	50.0	11.8	0.4
Porifera flat brown	**75.0**	**23.5**	**1.9**
Porifera *indet.*	50.0	8.8	0.2
Porifera yellow veins	25.0	2.9	0.1
Algae (n = 4)			
Coralligenous algae	**100.0**	**67.6**	**7.6**
Flat red algae	100.0	30.9	1.3

Red macroalgae	75.0	41.2	0.7
Algal turf	50.0	10.3	0.2
Ascidiacea (n = 2)			
Ascidia sp.	25.0	1.5	0.1
Didemnidae	**25.0**	**25.0**	**4.1**
Mollusca (n = 5)			
Anomidae	**100.0**	**82.4**	**6.3**
Bivalvia *indet.*	25.0	1.5	0.0
Mimachlamys varia (Linnaeus, 1758)	100.0	10.3	0.2
***Ostrea edulis* Linnaeus, 1758**	**75.0**	**54.4**	**16.1**
Anadara transversa (Say, 1822)	50.0	5.9	0.1
Polychaeta (n = 4)			
***Salmacina* sp. - *Filograna* sp.**	**100.0**	**60.3**	**4.1**
Serpulidae *indet.*	**100.0**	**97.1**	**14.7**
***Spirobranchus triqueter* (Linnaeus, 1758)**	**100.0**	**76.5**	**7.5**
***Spirorbis* sp.**	**100.0**	**92.6**	**5.7**
Bryozoa (n = 11)			
***Aetea* sp.**	**100.0**	**42.6**	**2.1**
Encrusting bryozoan *indet.*	**100.0**	**52.9**	**2.3**
Schizobrachiella sanguinea (Norman, 1868)	50.0	33.8	1.8
Schizoporella dunkeri (Reuss, 1848)	100.0	42.6	1.0
***Schizoporella errata* (Waters, 1878)**	**100.0**	**41.2**	**3.2**
Calpensia nobilis (Esper, 1796)	50.0	11.8	0.7
Cellepora sp.	50.0	5.9	0.0
Patinella radiata (Audouin, 1826)	100.0	14.7	0.3
***Terwasipora complanata* (Norman, 1864)**	**100.0**	**72.1**	**13.4**
Tubulipora sp.	75.0	19.1	0.3
Encrusting small orange	75.0	19.1	0.3

To display the structure of the biofouling community that developed on 4 ARMS deployed at the PIR site, stacked column charts (**Fig. 12**) for all the 4 units combined (Total) and grouped by the orientation of the plate-face (Top = T, Bottom = B, Topmost = 9T), were made to illustrate the structure of the overall developed community (Total) and that of plates of different orientation with proportions of 8 taxonomic groups.

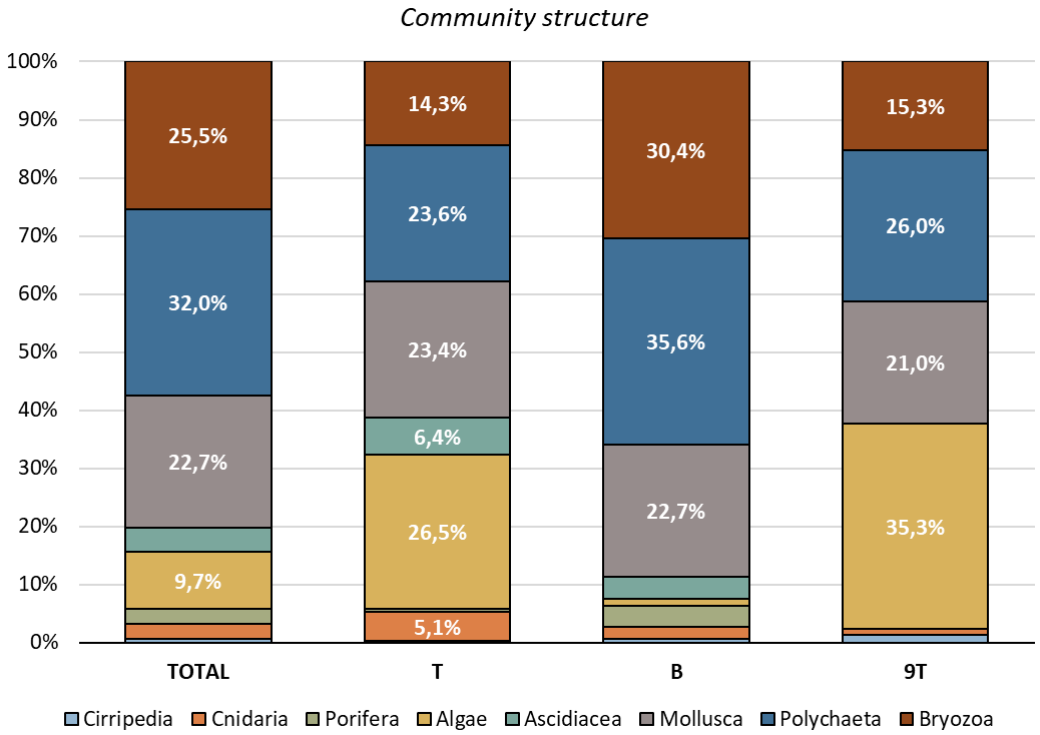

Figure 12: Stacked column chart representing relative proportions of plate coverage of 8 broader taxonomic groups, from all the 4 ARMS at the PIR site combined (Total) and based on the plate orientation (T, B, 9T). Proportion values (> 5%) are shown in white.

Concerning the community from all 4 units combined (**Fig. 12,** Total) taxa from the Polychaeta group were present at most points (32.0%), followed by Bryozoa (25.5%), Mollusca (22.7%) and Algae (9.7%). On the contrary, organisms belonging to the Ascidiacea (4.2%), Cnidaria (2.7%), Porifera (2.6%) and lastly Cirripedia (0.6%) groups, were detected at the least amount of points. The overall dominant taxonomic categories, present under the majority of overlaid points were *O. edulis* (16.1%), Serpulidae *indet.* (14.7%), *T. complanata* (13.4%), coralligenous algae (7.6%) and *S. triqueter* (7.5%).

It is evident from **Fig. 12** that taxonomic groups were present in different proportions on plate faces of contrasting orientations. Starting at the top oriented plates (**Fig. 12**, T), the percentage cover of 8 taxonomic groups seem to be most evenly distributed. The 3 most frequent groups: Algae (26.5%), Polychaeta (23.6%) and Mollusca (23.4%) expressed very similar proportions. Top oriented plates also have the most Ascidiacea (6.4%) and Cnidaria (5.1%), but least bryozoan (14.3%) taxa. The most dominant categories on T plates were by far coralligenous algae (20.4% of all points annotated), followed by Anomidae (13.7%), *S. triqueter* (10.1%), *O. edulis* (9.3%) and Serpulidae *indet.* (7.7%).

Bottom oriented plates (**Fig. 12**, B) displayed a considerable proportion of colonized space occupied by polychaetes (35.6%), bryozoans (30.4%) and molluscs (22.7%), with other 5 groups: Ascidiacea (3.9%), Porifera (3.6%), Cnidaria (2.1%), Algae (1.3%) and Cirripedia (0.6%), having less than 15% altogether. The 5 most dominant taxonomic categories of bottom oriented plates were: *O. edulis* (18.0% of all points annotated), Serpulidae *indet.* (17.6%) and *T. complanata* (16.2%), followed by Spirorbidae (6.3%) and *S. triqueter* (5.9%).

Proportions of taxonomic groups, colonizing the topmost plate (**Fig. 12**, 9T) were very similar and in the same order to those of top (T) oriented plates. Proportions of Algae (35.3%) were the highest of all orientations and were followed by polychaetes (26.0%), molluscs (21.0%) and bryozoans (15.3%), with other 2 groups being hardly detectable (Cirripedia = 1.2%, Cnidaria = 1.1%). Concerning the dominant categories, coralligenous algae occurred on almost a third (29.4%) of all points annotated, followed by *O. edulis* (19.3%), *S. triqueter* (13.4%), Serpulidae *indet.* (9.8%) and *T. complanata* (6.2%).

Further, by tracking the number of points under which an organism was present (colonized) or not (empty) from the total 300 overlaid, a stacked column chart (**Fig. 13**, below), was made to illustrate the amount of plate surface covered by sessile biofouling taxa, regarding the orientation of the plates (T, B, 9T) from the 4 ARMS units from the Piran site.

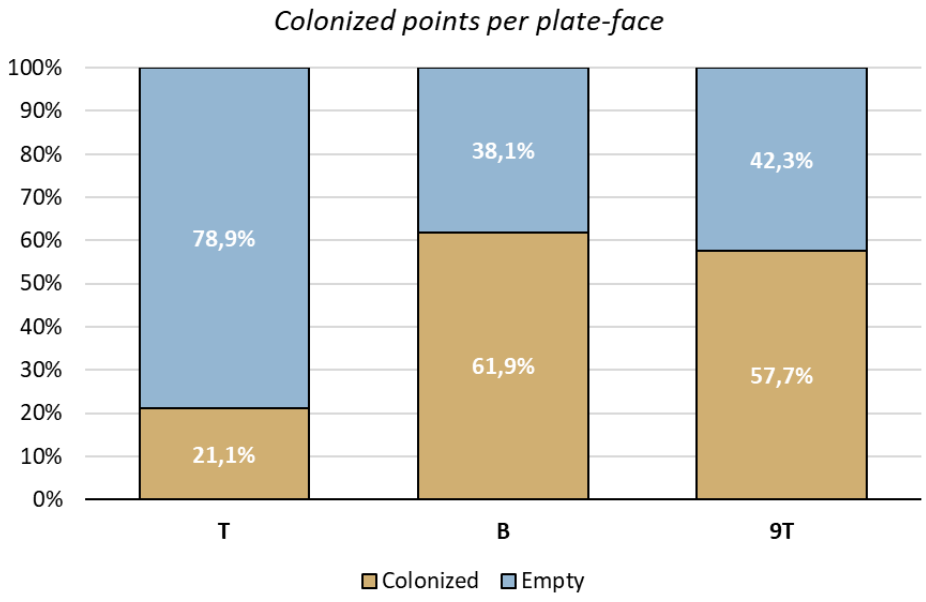

Figure 13: Stacked column charts representing colonized (sandy) and empty (blue) proportions of points on ARMS plates from the Piran location, regarding their orientation (T, B, 9T). Percentage values (> 5%) are shown in white.

Column charts from **Fig. 13** clearly show that T oriented plates express a lower number of colonized coverage on the surface (21.1%), than B (61.9%) and 9T (57.7%) plates. Mann-Whitney-U pairwise test of the colonized/empty point data used for **Fig. 13**, confirmed that T plates have significantly lower proportions of colonized surfaces than B ($p = 3.9E-10$) and 9T ($p = 0.03$) and that colonized proportions between B and 9T oriented plates do not differ significantly ($p = 0.98$).

To graphically represent the distances of the biofouling community structure on plate faces of different orientations (T, B, 9T), a 2D NMDS plot (**Fig. 14**) was constructed from all plates of the 4 ARMS units from the Piran site. Each dot on the plot (**Fig. 14**, left) represents the community structure of a plate-face, which are labelled by colour, depending on their orientation (T = teal, B = red, 9T = sandy) . In addition to the point-only plot (**Fig. 14** left), 95% concentration ellipses were outlined, to better visualize the overlap among T and B groups, with the absence of 9T plates (**Fig. 14**, right).

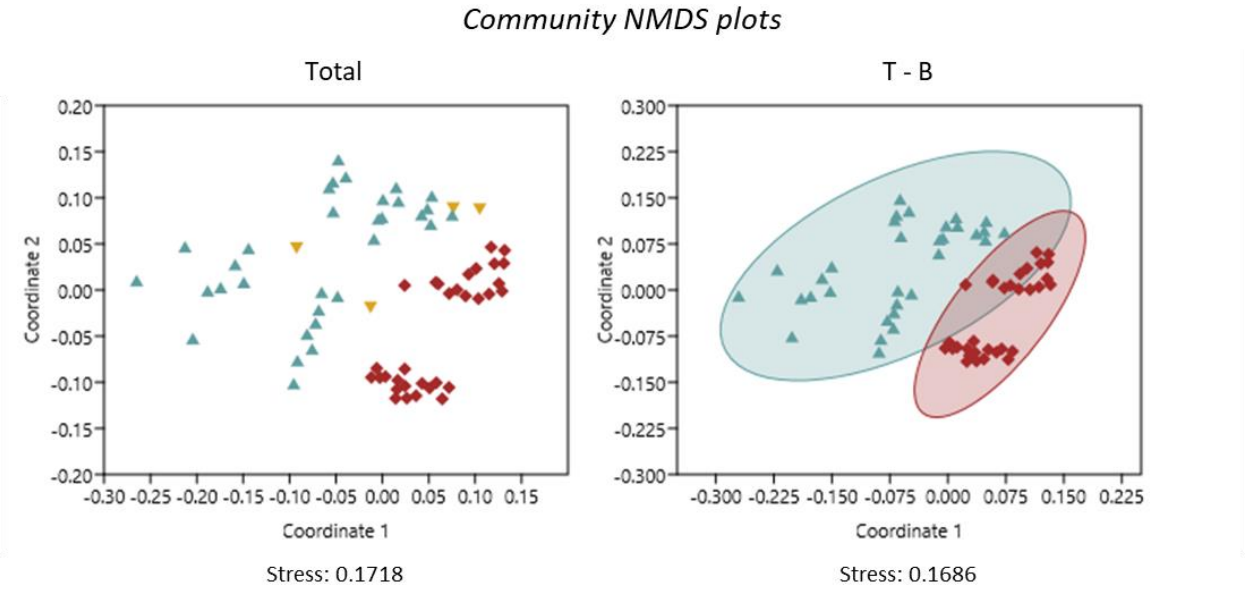

Figure 14: 2D NMDS plots based on Bray-Curtis similarity index from 300 point overlay data of the biofouling community. Symbols are grouped by the orientation of the respected plate (T = teal, B = red, 9T = sandy).

The 2D NMDS plots (stress = 0.17) of **Fig. 14** (above), suggest to a distinction between T and B plate communities of ARMS units deployed at the PIR study site. The scatter pattern of B plates appears to be much tighter, than that of T plates, hence the significantly bigger 95% ellipse of T group compared to that of B, seen on the left plot of **Fig. 14**. Additionally, a considerable overlap among the ellipses of T and B groups can also be seen. Distribution of the

4 sandy-coloured points (**Fig. 14**, left), belonging to topmost (9T) plates, indicates that their developed community resembles more to that on the T oriented plates. An additional SIMPER analysis revealed an overall high 87.6% dissimilarity among the groups (T, B & 9T), mainly contributed by the *O. edulis* (15.5%), Serpulidae *indet.* (15.2%) and *T. complanata* (14.0%) taxonomic categories. Dissimilarities between T - 9T (71.6%) and B - 9T (71.4%) were high as well, with highest contributions from coralligenous algae (T vs 9T = 23.3%, B vs 9T = 17.9%) and *O. edulis* (T vs 9T = 16.6%, B vs 9T = 15.9%). SIMPER analysis between T and B groups reported a very high 80.3% dissimilarity between the developed communities, mainly contributed by the Serpulidae *indet.* (16.5%), *O. edulis* (15.3%) and *T. complanata* (14.7%).

To illustrate how length of the deployment period influences the amount of plate surface that is colonized, a box plot (**Fig. 15**) was made with data of colonized proportions of points from all 4 ARMS units at the PIR site individually.

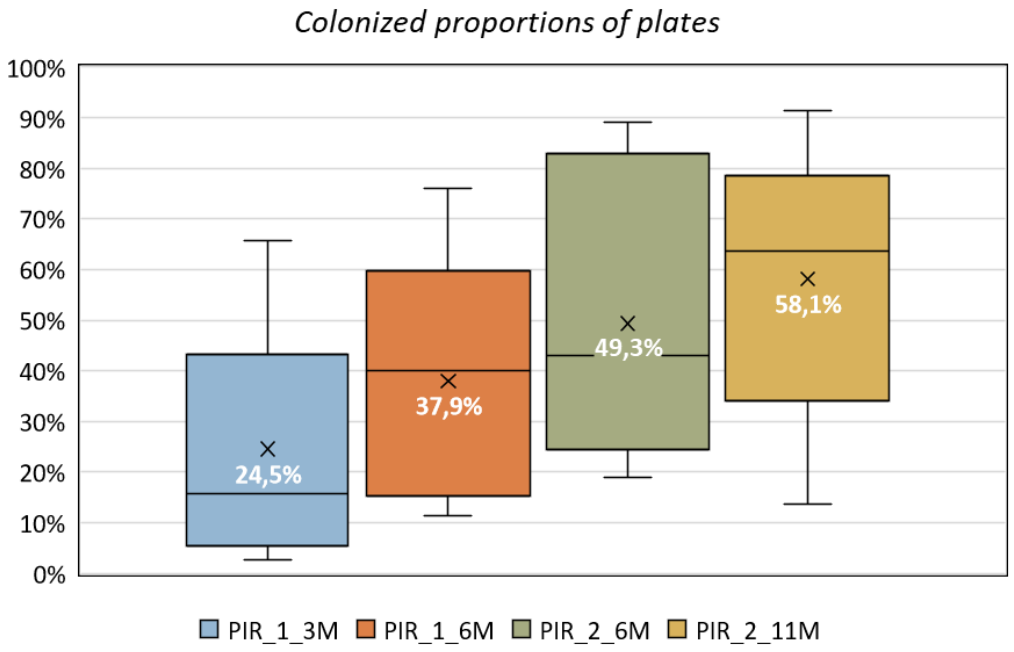

Figure 15: Box plots representing percentages of colonized points from plates for each of the 4 ARMS units, deployed at the PIR site. Sample means are indicated with an X, with their values shown in white.

Results of the one-way ANOVA test (F = 6.1, p = 9.7E-04) show that mean values of colonized proportions of points are statistically different among all 4 ARMS units. Plates on the PIR_1_3M unit, which was deployed for the shortest period (3 months), displayed the lowest proportions of colonized surfaces (mean = 24.5%), whereas the PIR_2_11M, that was deployed

for the longest period (11 months), displayed the largest colonized proportions (mean = 58.1%). Both ARMS, that were deployed for 6 months (PIR_1_6M and PIR_2_6M) had their mean colonized proportions somewhere in between the previously mentioned units, with PIR_2_6M having a higher value (mean = 49.3%) than the PIR_1_6M (mean = 37.9%). When looking at the median lines from the graph, the difference in colonized proportions between PIR_1_3M and PIR_2_11M become even more apparent, with the ones from PIR_1_6M and PIR_2_6M more similar. The reach (min.- max.) was overall high, but was by far the highest for the PIR_2_11M unit (min. = 13.7%, max. = 91.3%).

Due to the influence of the plate orientation (T, B, 9T) on the number of colonized points on plates, shown in **Fig. 13**, the below chart (**Fig. 16**) was constructed, in addition to the **Fig. 15** (above). As previously, amounts of points overlying an organism from the 300 total were transformed into percentages and are shown grouped firstly by ARMS unit and by plate orientation within.

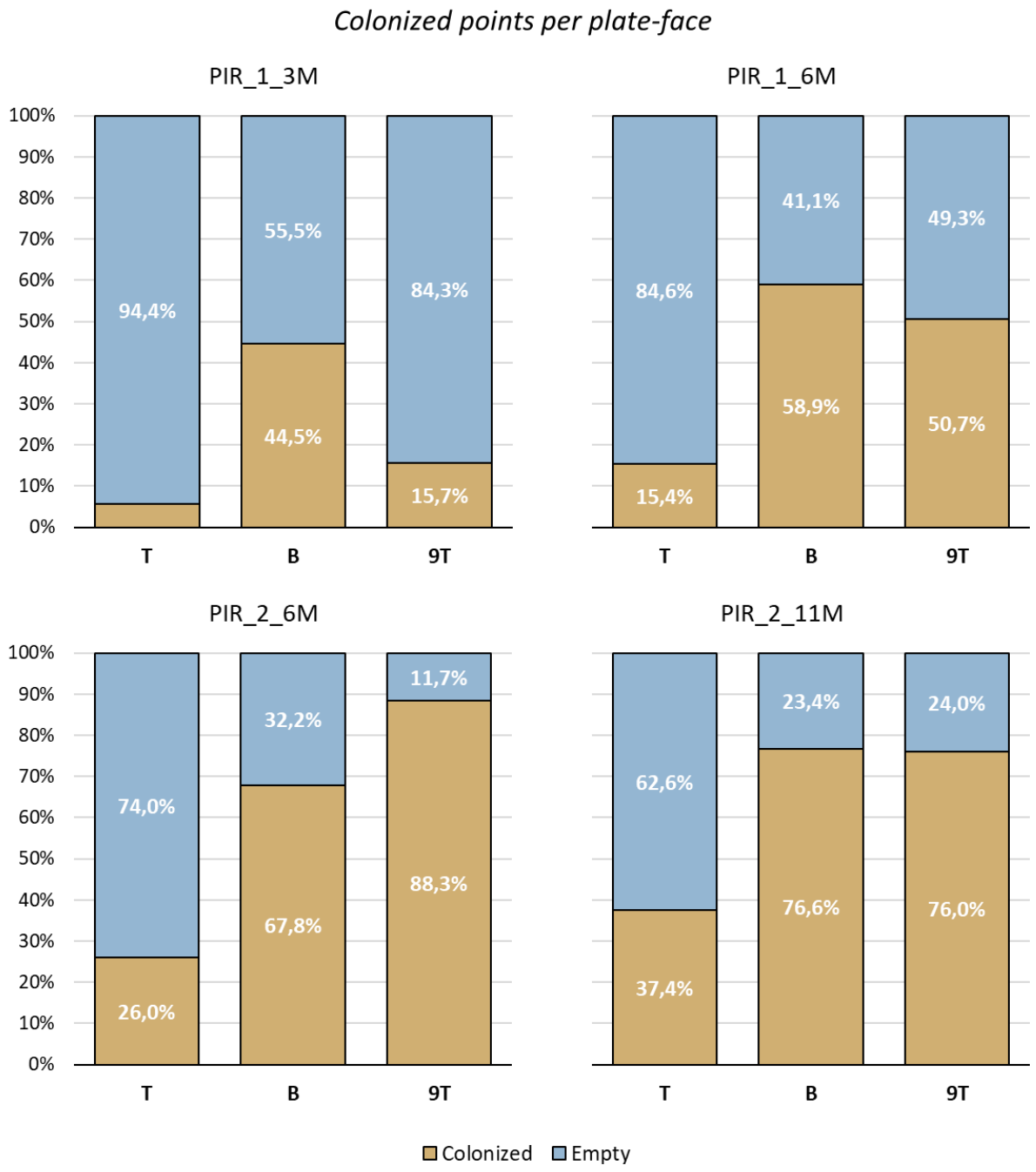

Figure 16: Stacked column charts representing colonized (sandy) and empty (blue) proportions of points on each from the 4 ARMS units from the PIR site, regarding their orientation (T, B, 9T). Percentage values (> 10%) are shown in white.

Fig. 16 (above) clearly shows the apparent differences in plate surface colonization among differently oriented plates and deployment periods. The trend of lower proportions of colonized points on T oriented plates, compared to B and 9T, is present at each ARMS unit from the PIR study site. The differences of colonized proportions among T and B plates were significant at each of the 4 unit, tested with a Mann-Whitney-U test (PIR_1_3M: p = 9.2E-04, PIR_1_6M: p

= 9.4E-04, PIR_2_6M: p = 9.3E-04, PIR_2_11M: p = 9.4E-04). The unit with the lowest deployment period of 3 months (PIR_1_3M), had the lowest proportions of colonized points at all orientations (T = 5.6%, B = 44.5%, 9T = 15.7%). On the contrary, the longest deployed unit, PIR_2_11M, had largest colonized proportions for both T and B plates (T = 37.4%, B = 76.0%). Therefore, B plates from PIR_1_3M had approx. 8 times more points assigned as colonized compared to T plates, whereas on the PIR_2_11M unit, the same factor dropped to approx. 2 times.

The relative proportions of 8 broader taxonomic groups, that make up the sessile biofouling community, derived by the use of a 300 point overlay method is presented in **Fig. 17** (below), for each individual ARMS unit deployed at the Piran site.

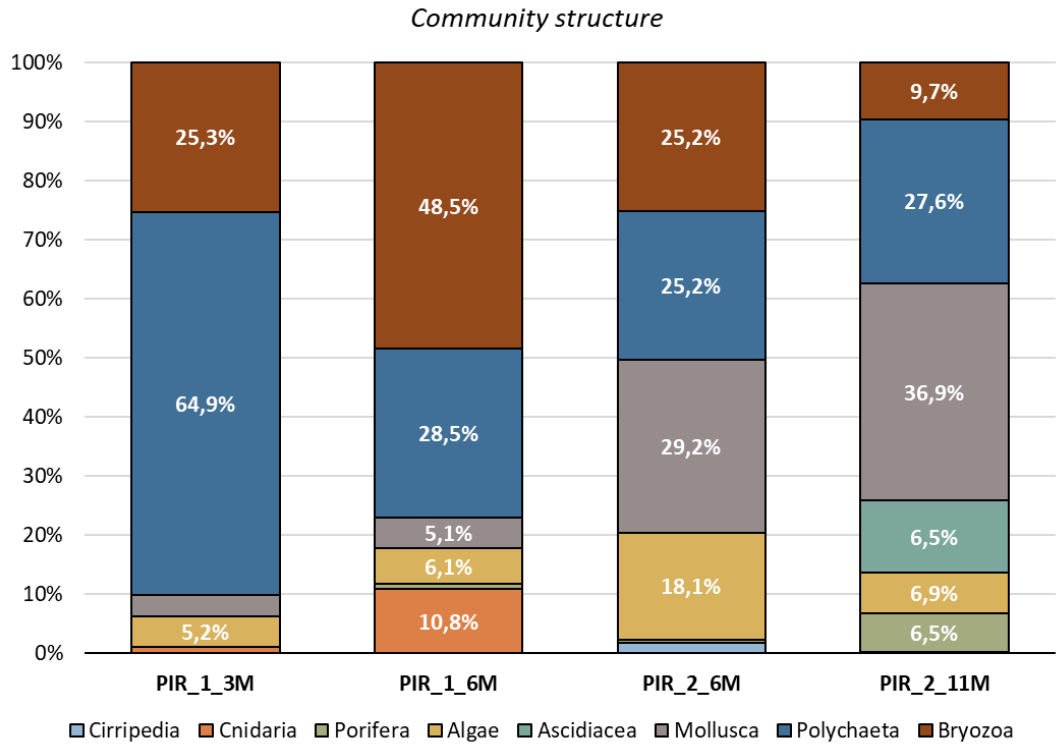

Figure 17: Stacked column charts representing the relative proportions of plate coverage of 8 broader taxonomic groups, based on 300 point overlay method from each of the 4 ARMS at the PIR site. Proportion values (> 5%) are shown in white.

Relative proportions contributed by the same taxonomic groups tend to differ significantly among different ARMS deployments (PIR_1 - PIR_2) and units. Polychaetes exclusively dominated the plate coverage at the PIR_1_3M unit, with a 64.9% contribution to the total community. They were less frequent on other units, but occupied fairly similar shares (PIR_1_6M = 28.5%, PIR_2_6M = 25.2%, PIR_2_11M = 27.6%). Bryozoans occurred as most

frequent on PIR_1_6M (48.5%), with lower but similar proportions on PIR_1_3M (25.3%), PIR_2_6M (25.2%) and were least frequent on PIR_2_11M (9.7%). Proportions of molluscs was high on units from the second deployment PIR_2_11M (36.9%) and PIR_2_6M (29.2%), but were scarce on units from the first deployment (PIR_1_6M = 5.1%, PIR_1_3M = 3.7%). Algae were frequent on PIR_2_6M unit (18.1%), but were mostly present in smaller proportions on other ARMS (PIR_2_11M = 6.9%, PIR_1_6M = 6.1%, PIR_1_3M = 5.2%). On PIR_2_11M, Ascidiacea (12.2%) and Porifera (6.5%) groups occurred almost exclusively, whereas on PIR_1_6M, the same went for Cirripedia taxa (10.8%), as they were scarcely present on other units.

Dominant taxonomic categories, the ones which appeared under most of total overlaid points, for every individual ARMS unit were: Serpulidae *indet.* (49.3%), *T. complanata* (9.0%) and *Salmacina sp. - Filograna sp.* (8.2%) for PIR_1_3M; *T. complanata* (42.8%), Serpulidae *indet.* (16.7%) and Hydrozoa *indet.* (10.8%) for PIR_1_6M; *O. edulis* (25.3%), coralligenous algae (14.6%) and *S. triqueter* (8.9%) for PIR_2_6M; and lastly *O. edulis* (24.9%), *S. triqueter* (12.2%) and Didemnidae (11.9%) for the PIR_2_11M unit.

To display the differences in community structure based on plate-face orientation (T, B, 9T), each of the 4 bar charts from ARMS units from **Fig. 16** have been divided in such regard and are presented in **Fig. 18**, below.

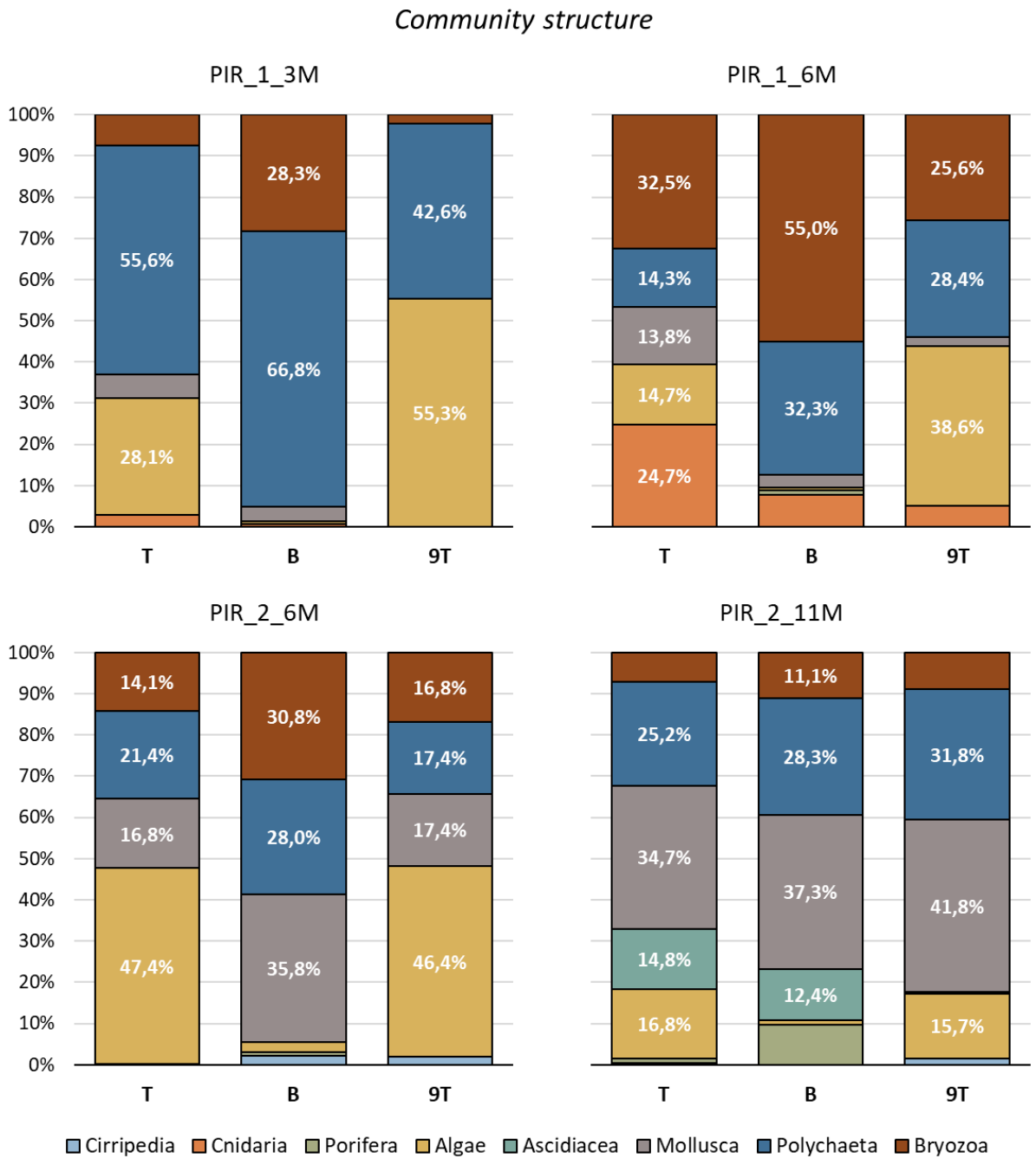

Figure 18: Stacked column charts representing the relative proportions of plate coverage of 8 broader taxonomic groups, based on 300 point overlay method from each of the 4 ARMS at the PIR site, regarding plate orientation (T, B, 9T). Proportion values (> 10%) are shown in white.

Seemingly, the proportional structure of the 8 taxonomic groups shown, differs in regard to the plate orientation. The most occurrent pattern displayed in **Fig. 18** is present for the Algae group, as they took up significant proportions of points on T (max. = 47.4%, min =14.7%) and specially on 9T (max. = 55.3%, min =15.7%), while at the same time, they were almost absent on B

oriented plates. Both polychaete and bryozoan groups show a slight tendency to occur more frequently on B plates (based on proportions shown in **Fig. 18**). As shown in **Fig. 12**, the bar charts of T and 9T plates, exhibit more coherent proportions of the same taxonomic groups than those of B orientation. On PIR_2_11M unit, the one on which the Ascidiacea and Porifera groups were almost exclusively relevant, they occurred only on T (Ascidiacea = 14.8%) and B (Ascidiacea = 12.4%) plates, whereas Porifera (9.7%) occurred almost solely on B oriented plates.

Lastly, to graphically represent the distances of the biofouling communities among ARMS units, a 2D NMDS plot (**Fig. 19**) was constructed using T and B plate data of the 4 ARMS units from the Piran site to illustrate the influence of deployment time, immersion period and plate orientation to the final obtained structure of the communities from the 4 ARMS units. Each dot on the plot represents a community from one of the plates which are labelled by colour, to distinguish individual ARMS units (**Fig. 19**, left) and shade (**Fig. 19**, right), to distinguish plate orientation. At each plot, 95% concentration ellipses were outlined, to better visualize the overlap among groups.

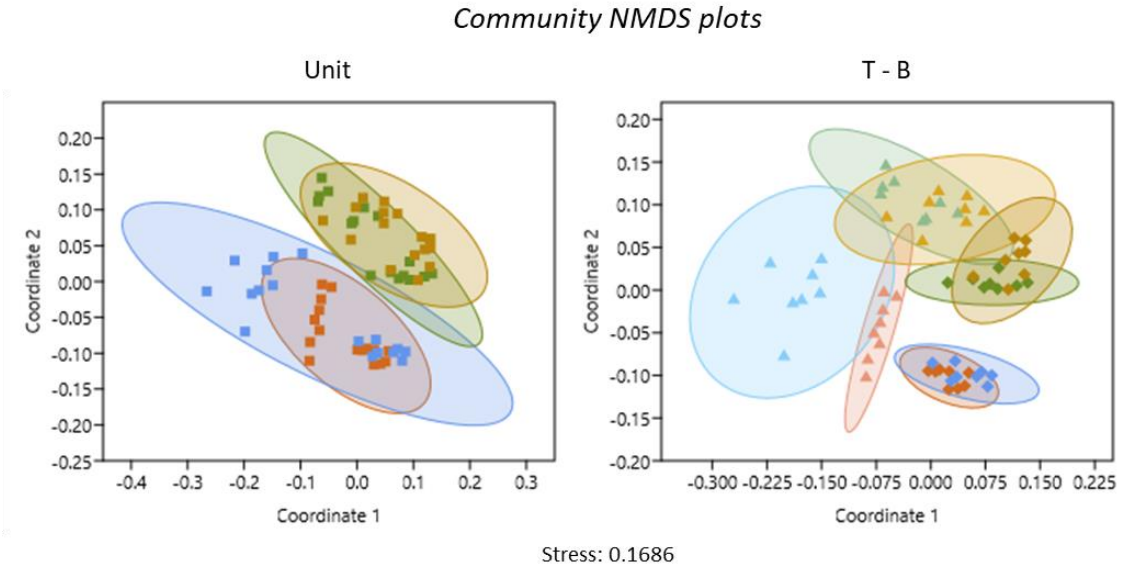

Figure 19: 2D NMDS plots based on Bray-Curtis similarity index from 300 point overlay data of the biofouling community from 4 ARMS units at the PIR site from T and B oriented plates. Symbols are grouped by the ARMS unit (PIR_1_3M = blue, PIR_1_6M = brown, PIR_2_6M = green, PIR_2_11M = sandy) and plate orientation (T = light tone, B = dark tone).

The 2D NMDS scatter plot with 95% conc. ellipses, where points are grouped by the ARMS unit (**Fig. 19**, Left), indicates a very apparent overlap among communities on ARMS units from the same deployment (PIR_1 = blue & brown; PIR_2 = green & sandy), while any significant overlap regarding the deployment period (3, 6 or 11 months) is not present. A SIMPER analysis between PIR_1 and PIR_2 showed a large dissimilarity of 81.5% among those two groups, mainly contributed by *O. edulis* (16.9%), *T. complanata* (12.1%) and Serpulidae *indet.* (10.9%). Differences between ARMS units within each deployment were tested with SIMPER as well. The test showed that ARMS units from the 1st deployment (PIR_1_3M & PIR_1_6M) display an overall 75.4% dissimilarity between units, contributed mostly by *T. complanata* (32.6%), Serpulidae *indet.* (20.3%) and Hydrozoa *indet.* (11.6%). ARMS units from the 2nd deployment (PIR_2_6M & PIR_2_11M), showed a slightly lower, but still high overall dissimilarity of 62.3%, for which *O. edulis* (20.7%), *Didemnidae* sp. (10.9%), and coralligenous algae (9.8%) had the highest contributions of all taxonomic categories. ARMS units that showed the highest SIMPER dissimilarity (84.9%) between their biofouling communities were PIR_1_3M and PIR_2_13M, contributed mostly by *O. edulis* (19.0%), Serpulidae *indet.* (12.7%) and Anomidae (11.1%)

Looking at the NMDS plots where plate orientations are considered (**Fig. 19**, right side), B plates (darker tone) display a significantly tighter scatter (points closer together, smaller 95% ellipses), than T (lighter tones), for all 4 ARMS units. Points representing B plates (darker tone) show a considerable overlap with those of the other ARMS unit of the same deployment (within PIR_1 and PIR_2 groups), whereas the distances between these two deployments remain clear, with minimal overlap. T plates (lighter tone) show a slight overlap with same oriented plates regardless of the deployment and its period. Additionally, points indicating B plates from the different ARMS units from the same deployments are much closer to each other, compared to T plates of the same ARMS unit.

According to the results of the Bray-Curtis based SIMPER test, the PIR_1_3M unit, that had the shortest deployment period (3 months), displayed the highest dissimilarity value among T & B oriented plates (84.9%), for which Serpulidae *indet.* (49.4%), *T. complanata* (10.8%) and *Salmacina sp. - Filograna sp.* (10.1%) were most accountable. On the contrary, plates from the PIR_2_11M unit, that had the longest deployment period (11 months), showed the lowest dissimilarity (59.1%) between differently oriented plates, contributed mostly by *O. edulis* (26.9%), Didemnidae (8.3%), and Porifera flat brown (8.2%) categories.

8.2.2. ARMS units from the Buoy Vida site

Using the 300 point overlay method on 51 (17 x 3) plate faces from 3 ARMS units deployed at the Buoy Vida (VID) study site (VID_1_6M, VID_1_11M, VID_2_13M), 5049 points (33.0% of all overlaid) were annotated using 34 taxonomic categories (taxonomic categories) from 7 groups (shown in **Table 3**). From the 34 total categories, 14 were identified to the species level (species name in concordance with the WoRMS, 2021), 6 to the genus level (sp.) with others assigned with a less precise identification (indet.) or a morphological category. Most taxonomic categories were detected on VID_1_6M unit (n = 29), followed by VID_1_11M & VID_2_13M which both had 27 of categories detected. On all 3 ARMS units from the site, the *Pyura* sp. category, the only representative of the Ascidiacea group was detected at only 1 point, the respected group has not been used in the following figures (only 6 taxonomic groups used), as it represents a neglectable proportion of the community.

Table 3: List of 34 taxonomic categories and their 7 groups, used for the annotation of the organisms on plates of ARMS units from the VID site. Values (%) indicate the percentage of ARMS units, plates and points on which the respected taxonomic category was detected. Most frequent categories are shown in **bold** (> 2% of points).

Taxonomic category	Units (%)	Plates (%)	Points (%)
Cnidaria (n = 2)			
Aurelia aurita (Linnaeus, 1758) polyp	66.7	15.7	0.4
Hydrozoa *indet.*	**100.0**	**39.2**	**3.5**
Porifera (n = 5)			
Crambe crambe (Schmidt, 1862)	66.7	5.9	0.4
Porifera *indet.*	100.0	19.6	0.6
Porifera light brown	**100.0**	**54.9**	**5.2**
Porifera spiked	33.3	7.8	0.3
Porifera yellow veins	**100.0**	**45.1**	**4.8**
Algae (n = 3)			
Coralligenous algae	66.7	19.6	0.6
Flat red algae	33.3	3.9	0.0
Red macroalgae	100.0	35.3	1.8
Ascidiacea (n = 1)			
Pyura sp.	33.3	2.0	0.0
Mollusca (n = 6)			
Anomidae	**100.0**	**74.5**	**3.9**
Bivalvia *indet.*	33.3	3.9	0.0
Hiatella arctica (Linnaeus, 1767)	100.0	7.8	0.1

Mimachlamys varia (Linnaeus, 1758)	100.0	29.4	1.4
***Ostrea edulis* Linnaeus, 1758**	**100.0**	**47.1**	**5.4**
Pododesmus patelliformis (Linnaeus, 1761)	100.0	15.7	0.3
Polychaeta (n = 4)			
***Salmacina* sp. - *Filograna* sp.**	**100.0**	**39.2**	**17.7**
Serpulidae *indet.*	**100.0**	**74.5**	**12.6**
***Spirobranchus triqueter* (Linnaeus, 1758)**	**100.0**	**74.5**	**18.4**
Spirorbis sp.	100.0	25.5	0.4
Bryozoa (n = 13)			
Aetea sp.	66.7	19.6	0.6
Bryozoa arborescent white	33.3	5.9	0.2
Encrusting bryozoan *indet.*	**100.0**	**56.9**	**6.1**
Celleporaria brunnea (Hincks, 1884)	33.3	3.9	0.0
***Schizobrachiella sanguinea* (Norman, 1868)**	**100.0**	**66.7**	**8.0**
Schizoporella dunkeri (Reuss, 1848)	100.0	41.2	1.4
Schizoporella errata (Waters, 1878)	33.3	2.0	0.0
Schizoporella unicornis (Johnston in Wood, 1844)	100.0	29.4	1.1
Cellepora sp.	100.0	13.7	0.2
***Tubulipora* sp.**	**100.0**	**39.2**	**3.1**
Escharoides coccinea (Abildgaard, 1806)	100.0	11.8	0.4
Encrusting bright orange	66.7	17.6	0.9
Fenestrulina malusii (Audouin, 1826)	100.0	9.8	0.3

To display the structure of the biofouling community that developed on 3 ARMS deployed at the Buoy Vida site, stacked column charts (**Fig. 20**) for all the 4 units combined (Total) and grouped by the orientation of the plate face (T, B, 9T) were made to illustrate the structure of the overall developed community and that of plates of different orientation with proportions from 6 broader taxonomic groups.

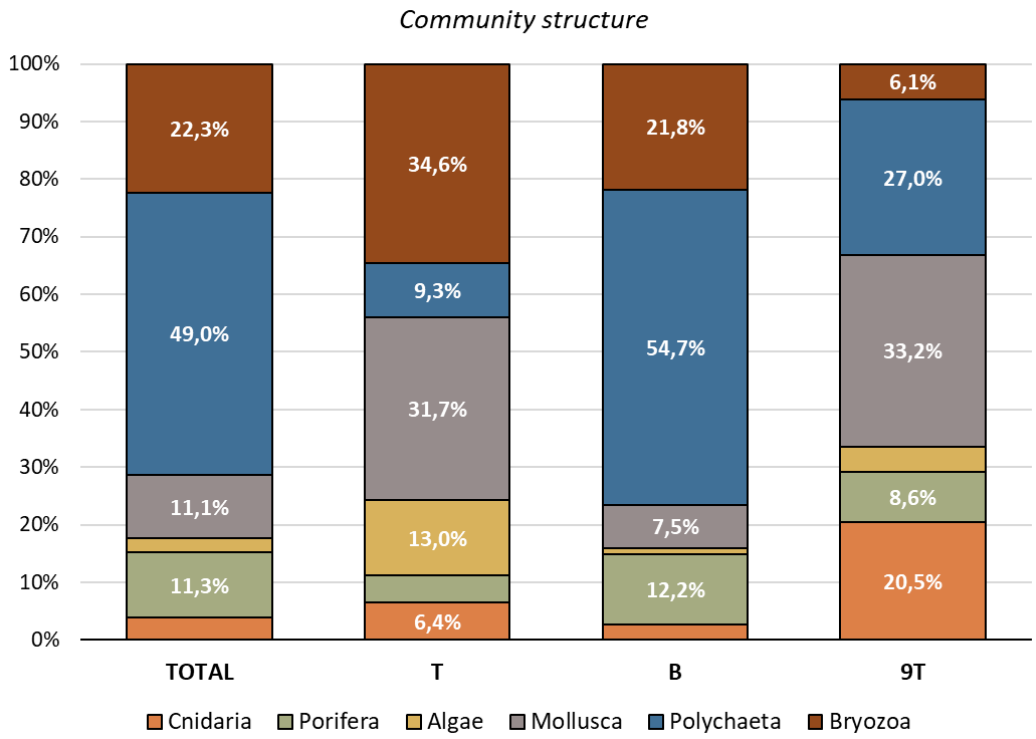

Figure 20: Stacked column chart representing the relative proportions of plate coverage of 8 broader taxonomic groups, from all the 3 ARMS at the Buoy Vida site combined (Total) and based on the plate orientation (T, B, 9T). Proportion values (> 5%) are shown in white.

Concerning the community from all 43 units combined (**Fig. 20**, Total) taxa from the Polychaeta group were present at most points (49.0%), contributing to almost a half of the total community, followed by Bryozoa (22.3%), Porifera (11.3%) and Mollusca (11.1%). Taxa belonging to the Cnidaria (3.9%) and Algae (2.4%), groups, were detected at the least number of points. The overall dominant taxonomic categories, present under the majority of total overlaid points were *S. triqueter* (18.4%), *Salmacina sp. - Filograna sp.* (17.7%), Serpulidae *indet.* (12.6%), *S. sanguinea* (8.0%) and Encrusting bryozoan *indet.* (6.1%)

It is evident from **Fig. 20** that taxonomic groups were present in different proportions on plate faces of contrasting orientations (T, B, 9T). Starting at the top oriented plates (**Fig. 20**, T), the percentage cover of 6 taxonomic groups seem to be fairly evenly distributed. The 2 most frequent groups: Bryozoa (34.6%) and Mollusca (31.7%) both represent around a third of the total community. Top oriented plates also have the most Algae (13.0%) and the lowest proportions of polychaete (9.3%) taxa by far. The most dominant categories on T plates were *S. sanguinea* (31.3% of all points annotated), followed by Anomidae (26.1%), Red macroalgae

(9.1%), Hydrozoa *indet.* (6.4%), with *O. edulis*, Serpulidae *indet.* and *S. triqueter* all occupying 4.6% of points.

Bottom oriented plates (**Fig. 20**, B) displayed similar proportions and in the same order as those of the total ARMS units combined. A considerable proportion of colonized space, highest from all orientations, was occupied by polychaetes (54.7%) followed by bryozoans (21.8%) and Porifera (12.2%). The remaining 3 groups: Mollusca (7.5%), Cnidaria (2.7%) and Algae (1.1%) occupied less than 15% altogether. The 5 most dominant taxonomic categories of bottom oriented plates were: *Salmacina sp. - Filograna sp.* (20.7% of all points annotated), S. triqueter (20.4%), Serpulidae *indet.* (13.3%) Encrusting bryozoan *indet.* (6.9%) and lastly, Porifera light brown (5.8%).

Topmost plates (**Fig. 20**, 9T) were mostly colonized by bivalves (33.2%) and polychaetes (27.0%), followed by the highest proportions colonized by cnidarians (20.5%) from all orientations, with Porifera (8.6%), Bryozoa (6.1%) and Algae (4.5%) taxa occupying lesser proportions of plates. Concerning the dominant categories, Hydrozoa *indet.* occurred on 20.5% of all points annotated, followed by *M. varia* (18.0%), Serpulidae *indet.* (16.0%), *O. edulis* (14.8%) and *S. triqueter* (10.7%).

Additionally, by tracking the number of points under which an organism was present (colonized) or not (empty) from the total 300 overlaid, a stacked column chart (**Fig. 21**, below), was made to illustrate the amount of plate surface covered by sessile biofouling taxa, regarding the plate-face orientation (T, B, 9T) from the 3 ARMS units from the Buoy Vida study site.

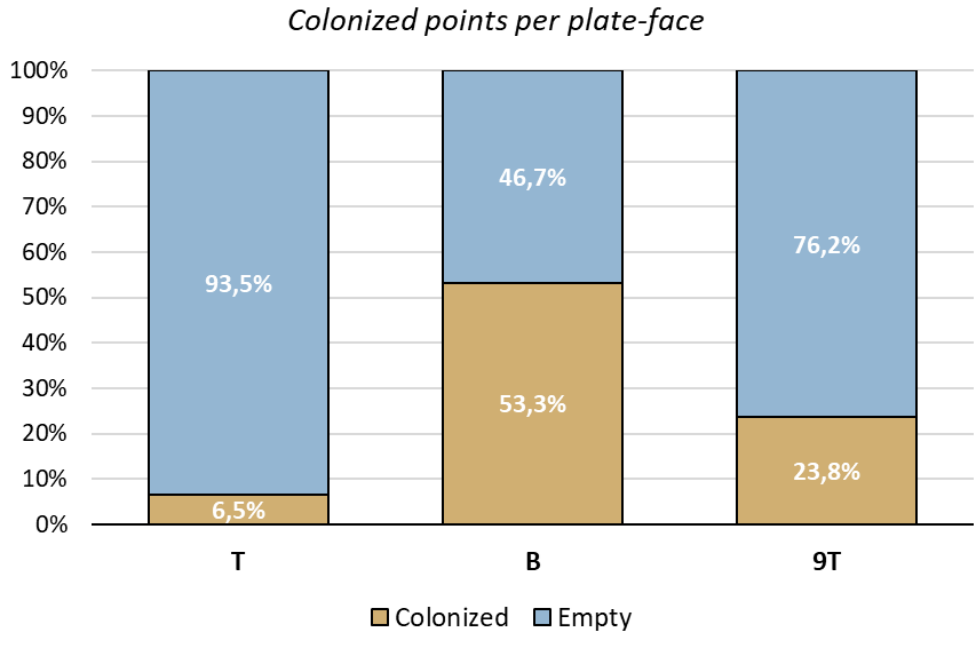

Figure 21: Stacked column charts representing colonized (sandy) and empty (blue) proportions of points on ARMS plates from the VID site, regarding their orientation (T, B, 9T). Percentage values (> 5%) are shown in white.

Column charts from **Fig. 21** clearly show that T plates express a significantly lower amount of colonized cover (6.5%), than B (53.3%) and topmost (23.8%) plates. Mann-Whitney-U pairwise test of the colonized/empty data used for **Fig. 21**, confirmed that B plates have significantly higher proportions of colonized surfaces than T (p = 3.9E-09) and 9T (p = 0.03) and that colonized proportions between T and 9T oriented plates do not differ significantly (p = 0.07).

To graphically represent the distances of the community structure on plate faces of different orientations (T, B, 9T), a 2D NMDS plot (**Fig. 22**) was constructed from all plates of the 3 ARMS units from the Buoy Vida study site. Each dot on the plot (**Fig. 22**, left) represents the community of a plate, which are labelled by colour, depending on their orientation (T = teal, B = red, 9T = sandy) . In addition to the point-only plot (**Fig. 22**, left), 95% concentration ellipses were outlined, to better visualize the overlap among T and B groups, with the absence of 9T plates (**Fig. 22**, right).

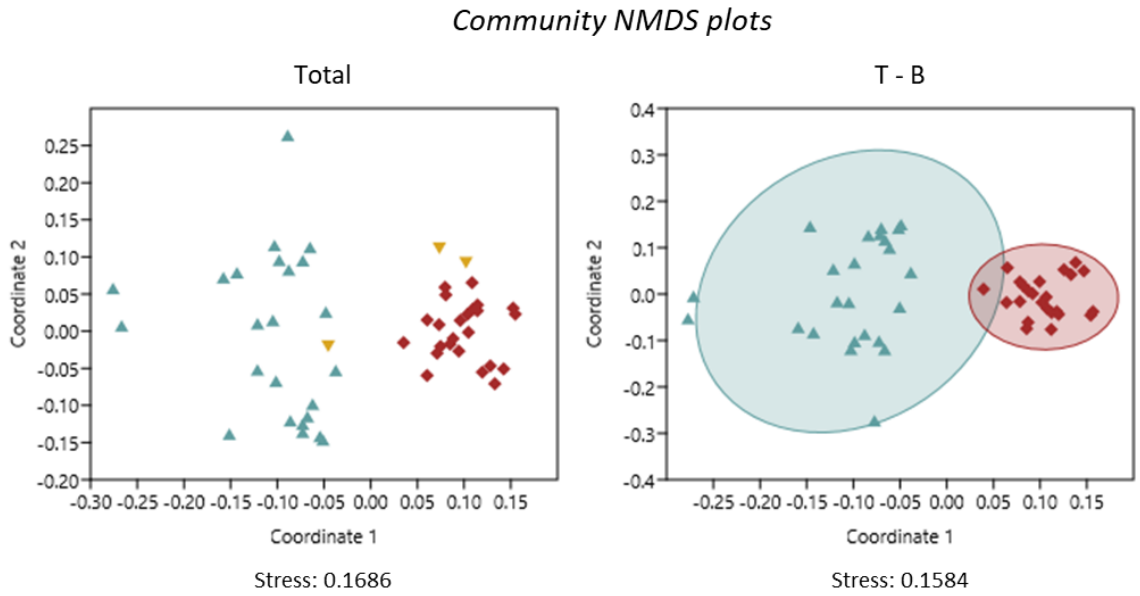

Figure 22: 2D NMDS plots based on Bray-Curtis similarity index from 300 point overlay data of the biofouling community at the VID site. Symbols are grouped by the orientation of the respected plate (T = teal, B = red, 9T = sandy).

The 2D NMDS plots (stress = 0.17 & 0.16) of **Fig. 22** (above), suggest to the clear distinction between T and B plate communities of ARMS units from the VID site. The scatter pattern of B dots appears to be much tighter, than that of T dots, hence the significantly bigger 95% ellipse of T group compared to that of B (**Fig. 22**, right). Additionally, a small overlap among the ellipses of T and B groups is present. The distribution of the 3 sandy-coloured points, belonging to topmost (9T) plates, indicates that their developed community resembles more to that on T plates for the VID_1_11M unit, whereas on VID_1_6M & VID_2_13M it resembled more to those of B plates. An additional SIMPER analysis revealed a very high overall 89.2% dissimilarity among the T, B and 9T groups, mainly contributed by the *S. triqueter* (18.1%), *Salmacina sp.* - *Filograna sp.* (15.1%) and Serpulidae *indet.* (13.6%) taxonomic categories. Dissimilarities between B - 9T (76.5%) were lower, compared to those of T - 9T (87.3%), however they still remained very high. A SIMPER analysis between T and B groups reported a very high 91.0% dissimilarity between the developed communities, mainly contributed by the *S. triqueter* (19.5%), *Salmacina sp.* - *Filograna sp.* (16.8%) and Serpulidae *indet.* (13.9%) taxonomic categories.

To illustrate how length of the deployment period influences the amount of colonized plate cover, box plots (**Fig. 23**) were made with data of colonized proportions of points from all 3 ARMS units at the Buoy Vida site.

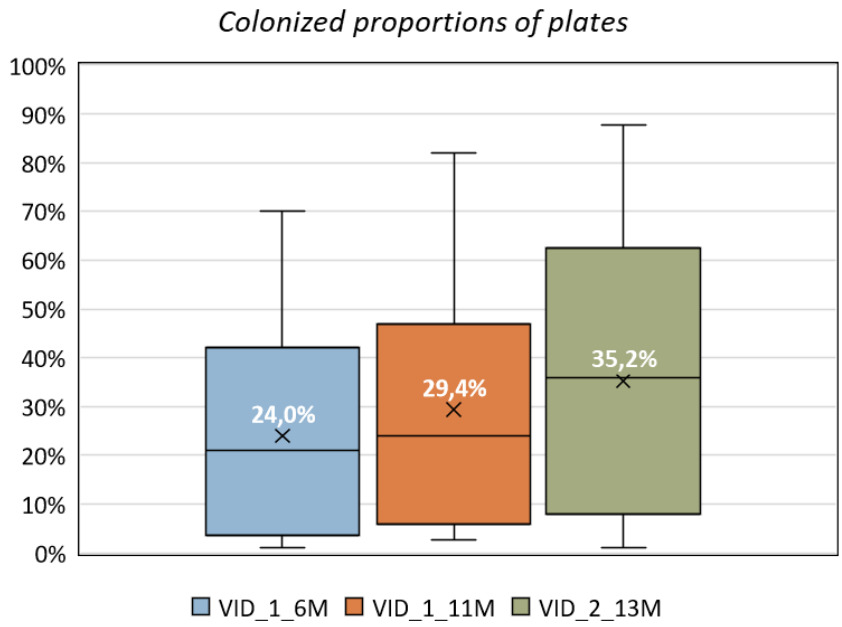

Figure 23: Box plots representing percentages of colonized points from plates for each of the 3 ARMS units, deployed at the VID site. Sample means are indicated with an X, with their values shown in white.

Results of the one-way ANOVA test (F = 0.7, p = 0.50) show that mean values of colonized proportions of points are not significantly different among all the 3 ARMS units. A pairwise Mann-Whitney-U test also confirmed (p >> 0.05) that no significant differences in colonized proportions are present among individual units. However, according to the pox plots in **Fig. 23**, plates on the VID_1_6M unit, which was deployed for the shortest period (6 months), displayed the lowest proportions of colonized cover (mean = 24.0%), whereas the VID_2_13M, that was deployed for the longest period (13 months), displayed the largest values of colonized proportions (mean = 35.2%). Plates from the VID_1_11M unit, of which deployment period was of 11 months, had colonized proportions of somewhere in between the other two units (mean = 29.4%). When looking at the median lines from the graph, the difference in colonized proportions between VID_1_11M and VID_2_13M become even more apparent, with the ones from the first deployment (VID_1) more similar. The reach (min.- max.) was overall high, but was by far the highest for the VID_2_13 unit which had the lowest surface (min. = 1.0%) and also the highest (max. = 87.7%) percentage of colonized plate surfaces.

Due to the significant influence of the plate orientation (T, B, 9T) on the amount of colonized cover, shown in **Fig. 21**, the below chart (**Fig. 24**) was constructed, in addition to the **Fig. 23** (above). Amounts of points overlying an organism from the 300 total were transformed into percentages and are shown grouped firstly by the ARMS unit and by plate orientation within.

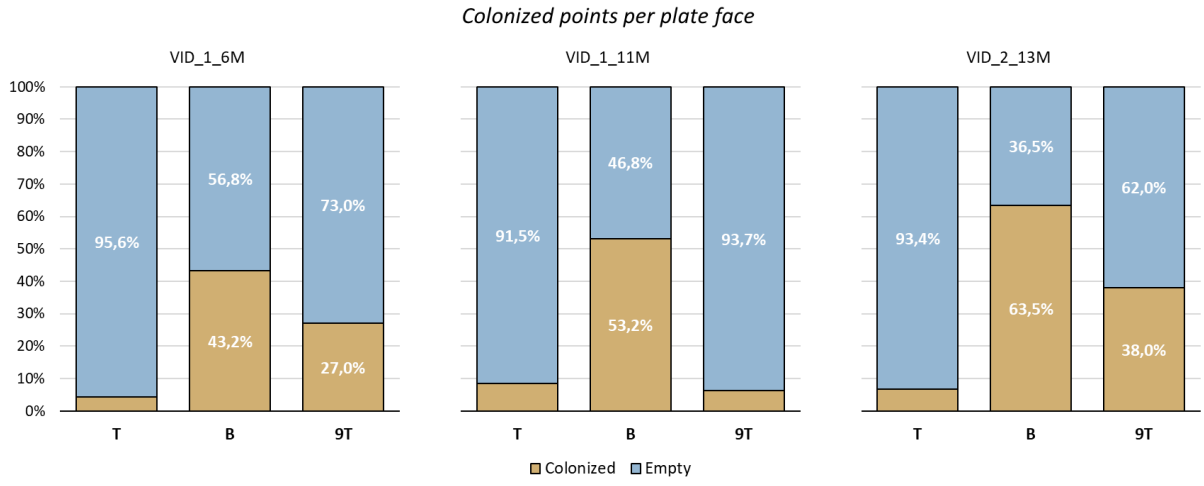

Figure 24: Stacked column charts representing colonized (sandy) and empty (blue) proportions of points on each from the 3 ARMS units from the VID site, regarding their orientation (T, B, 9T). Percentage values (> 10%) are shown in white.

Stacked column charts from **Fig. 24** clearly illustrate the apparent differences in colonized cover proportions among plates of different orientation within and among the 3 ARMS units from the VID study site. The trend of lower proportions of colonized points on T and 9T oriented plates, compared to B, can is very significant. A Mann-Whitney-U test confirmed that these differences are indeed significant among T and B plates at each of the 3 units (VID_1_6M: p = 9.4E-04, VID_1_11M: p = 9.3E-04, VID_2_13M: p = 9.3E-04). At all 3 ARMS, colonized proportions of T plates were not statistically different (Mann-Whitney-U, p > 0.05) and did not reach above 10%. Plates of B orientation were least colonized on ARMS unit with the shortest deployment period of 6 months (VID_1_6M = 43.2%), followed by that of 11 months (VID_1_11M = 53.2%) and that of the longest deployment period of 13 months (VID_2_13M = 63.5%).

The relative proportions of 6 broader taxonomic groups, that made up the sessile biofouling community, derived by the 300 point overlay method is presented in **Fig. 25** (below), for each individual ARMS unit deployed at the Buoy Vida site.

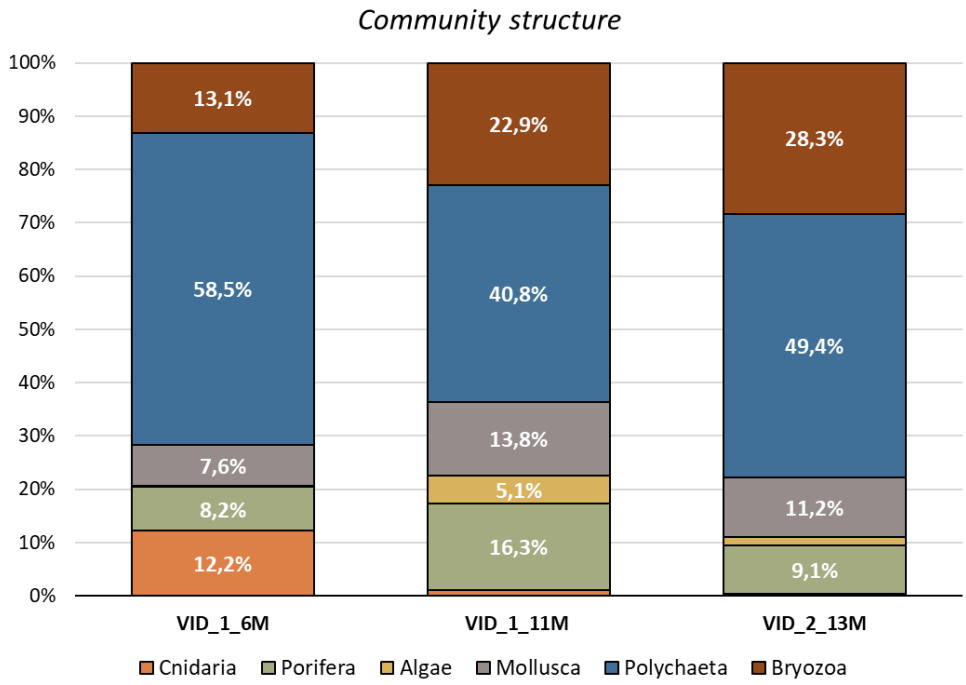

Figure 25: Stacked column charts representing the relative proportions of plate coverage of 6 broader taxonomic groups, based on 300 point overlay method from each of the 3 ARMS at the VID site. Proportion values (> 5%) are shown in white.

Relative coverage of the same taxonomic groups tend to differ slightly among different ARMS units. Polychaetes were the most dominant group on all 3 units, contributing largest proportions of 58.5% (VID_1_6M), 49.4% (VID_2_13M) and 40.8% (VID_1_11M) to the total community structure. Polychaetes were followed by bryozoan taxa which occupied around a third of annotated points on VID_2_13M (28.3%), with lower proportions on VID_1_11M (22.9%) and were least frequent on VID_1_6M (13.1%), indicating that bryozoan taxa occupied more cover on ARMS with longer deployment periods. Porifera and Molluscan taxa occupied similar proportions at each unit, with highest percentage on VID_1_11M (Porifera = 16.3%, Mollusca = 13.8%), followed by VID_2_13M (Porifera = 9.1%, Mollusca = 11.2%) and lastly VID_1_6M (Porifera = 8.2%, Mollusca = 7.6%). Cnidarian taxa occurred almost exclusively on VID_1_6M (12.2%), with a fairly apparent contribution. Algae were scarce on all units, reaching their maximum coverage on VID_1_11M unit (5.1%).

Dominant taxonomic categories, the ones which appeared under most of total annotated points, for every individual ARMS unit were *S. triqueter* (35.0%), Hydrozoa *indet.* (12.0%) and *Salmacina sp. - Filograna sp.* (11.7%) for VID_1_6M; Serpulidae *indet.* (19.6%), *S. triqueter* (17.7%), Anomidae and Porifera light brown (7.7%) for VID_1_11M; and lastly *Salmacina sp. - Filograna sp.* (34.9%), *S. sanguinea* (14.8%) and *O. edulis* (8.1%) for the VID_2_13M unit.

To display the differences in community structure based on plate orientation (T, B, 9T), each of the 3 bar charts from ARMS units from **Fig. 25** have been divided in such regard and are presented in **Fig. 26**, below.

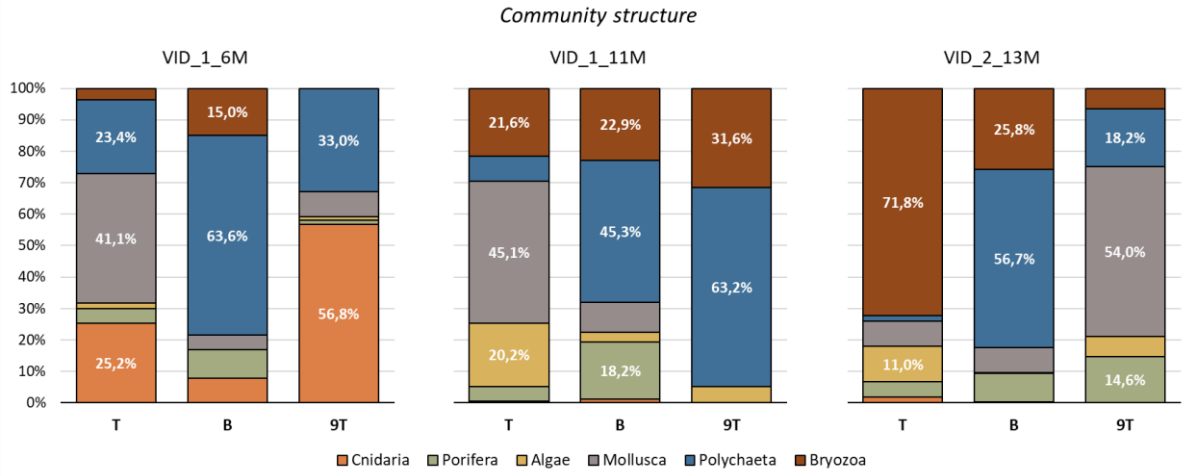

Figure 26: Stacked column charts representing the relative proportions of plate coverage of 6 broader taxonomic groups, based on 300 point overlay method from each of the 3 ARMS at

the VID site, regarding plate orientation (T, B, 9T). Proportion values (> 10%) are shown in white.

The community structure based on colonized proportions of the 6 taxonomic groups shown, seems to significantly differ in regard to the plate orientation, based on charts shown in **Fig. 26** (above). Structure of 9T plate communities is clearly very different from those of T and B within the same unit and other 9T plates of other ARMS, therefore not showing any apparent trend at all. At each 9T plate, one group clearly prevailed: cnidarians (56.8%) on VID_1_6M, polychaetes (63.2%) on VID_1_11M and molluscs (54.0%) on VID_2_13M. When comparing T and B plates from the same ARMS unit, there is a very apparent pattern of lesser coverage of Polychaetes on T plates, compared to B at every ARMS unit: VID_1_6M (T = 23.4%, B = 63.6%), VID_1_11M(T = 8.0%, B = 45.3%) and VID_2_13M (T = 1.8%, B = 56.7%). On ARMS units from the first deployment (VID_1), molluscs occupied considerably more cover on T plates, compared to B (VID_1_6M: T = 41.1%, B = 4.6% & VID_1_11M: T = 45.1%, B = 9.5%), but not on the VID_2_13M unit (T = 8.0%, B = 7.9%). Algae were most apparent on T plates from VID_1_11M (20.2%) and VID_2_13M (11.0%) but were scarcely present on B plates or on VID_1_6M unit. Taxa from the Porifera group show a slight tendency of higher coverage on B plates than those of T orientation at all 3 units, reaching their highest percentage on B plates of the VID_1_11M unit (18.2%).

Lastly, to graphically represent the distances of the biofouling community structure among units, a 2D NMDS plot (**Fig. 27**) was constructed using T and B plate coverage of the 3 ARMS units from the Buoy Vida site to illustrate the influence of deployment time, immersion period and plate orientation to the final obtained structure of the established communities. Each dot on the plot represents a community structure from one plate-face which are labelled by colour, to distinguish individual ARMS units (**Fig. 27**, left) and shade (**Fig. 27**, right), to distinguish plate-face orientation within the unit. At each plot, 95% concentration ellipses were outlined, to better visualize the overlap among groups.

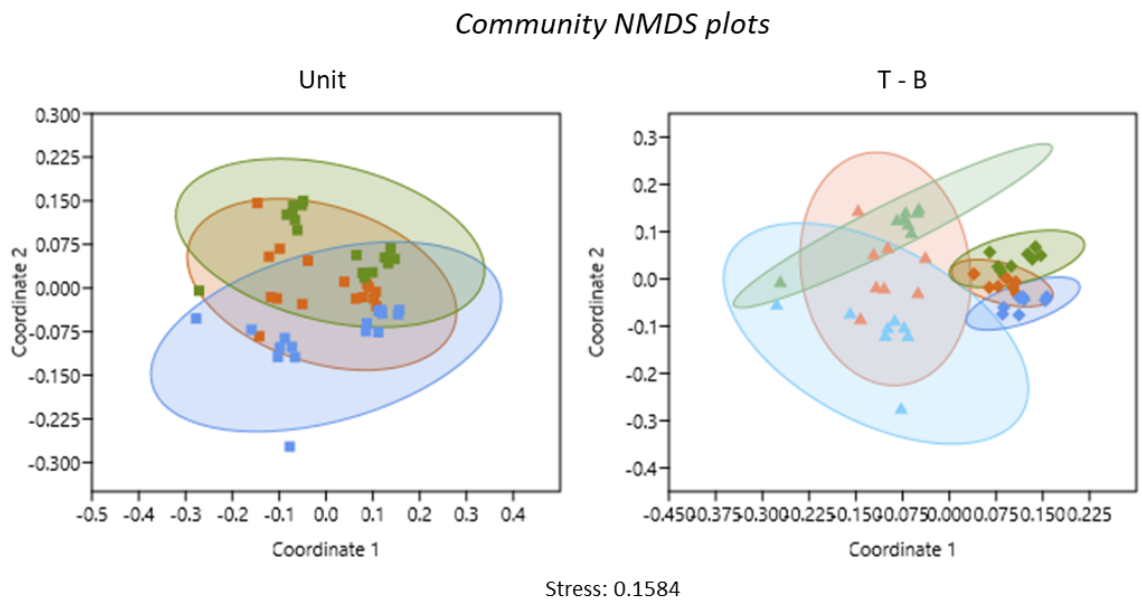

Figure 27: 2D NMDS plots based on Bray-Curtis similarity index from 300 point overlay data of the biofouling community from 3 ARMS units at the VID site from T and B oriented plates. Symbols are grouped by the ARMS unit (VID_1_6M = blue, VID_1_11M = brown, VID_2_13M = green) and plate orientation (T = light tone, B = dark tone).

The 2D NMDS scatter plot (stress = 0.16) with 95% conc. ellipses (**Fig. 27**, Left), shows a significant overlap of ellipses among all the 3 ARMS units. Units deployed the most time apart (VID_1_6M = blue & VID_2_11M = green) display the least overlap, with the remaining VID_1_11M unit (brown), of the first deployment, placed directly in between. Therefore, a significant overlap regarding the length of the deployment period (6, 11 or 13 months) is present and no significant effect of the immersion season is apparent, as units from the VID_1 were deployed in July 2019 and VID_2 in June 2020.

A SIMPER analysis between all 3 ARMS units showed a large dissimilarity of 82.6%, mainly contributed by *S. triqueter* (14.4%), *Salmacina sp. - Filograna sp.* (12.9%), *S. sanguinea* (12.6%). Differences between 3 individual ARMS units were tested with SIMPER as well. The test showed the highest dissimilarity (86.4%) of the developed community between VID_1_6M and VID_2_13M ARMS, each from a different deployment and having most contrasting deployment times of 6 and 13 months, mostly contributed by and *S. sanguinea* (17.7%), *Salmacina sp. - Filograna sp.* (17.0%) and *S. triqueter* (14.5%). SIMPER dissimilarity percentages between VID_1_6M and VID_1_11M units (80.8%), mostly contributed by: *S. triqueter* (18.7%), Serpulidae *indet.*, (13.4%) and Anomidae (8.7%), are very similar to those

between VID_1_11M and VID_2_13M (80.4%), with highest contributions from: *Salmacina sp. - Filograna sp.* (15.6%), *S. sanguinea* (13.2%) and Serpulidae *indet.* (11.3%).

Looking at the NMDS plots where plate orientations are considered (**Fig. 27**, right side), B plates (darker tone) display a significantly tighter scatter (points closer together, smaller 95% ellipses), than T (lighter tones), for all 3 ARMS units. Additionally, 95% ellipses from T plate points (lighter tone) show a big overlap with those of other units, whereas B plate ellipses of VID_1_6M and VID_2_13M are nicely separated, with the one from VID_1_11M unit symmetrically overlapping with the 2 previously mentioned ones.

According to the results of the Bray-Curtis based SIMPER test, the VID_1_6M unit, characterized by the shortest deployment period (6 months), displayed the highest dissimilarity value among T & B oriented plates (91.5%), for which *S. triqueter* (32.2%), *Salmacina sp. - Filograna sp.* (12.2%) and Serpulidae *indet.* (12.2%) were most accountable. On the contrary, plates from the VID_1_11M unit, which had the second longest deployment period (11 months), showed the lowest dissimilarity (84.2%) between differently oriented plates, contributed mostly by Serpulidae *indet.* (23.1%), *S. triqueter* (19.3%) and Encrusting bryozoan *indet.* (7.9%) categories.

8.2.3. ARMS units from the Port of Koper site

Using the 300 point overlay method on 72 (18 x 4) plate faces from 4 ARMS units deployed at the Port of Koper (PK) study site (PK_1_4M, PK_2_4M, PK_3_4M, PK_4_4M), 6516 points (30.2% of all overlaid) were annotated with 46 taxonomic categories (taxonomic categories) from 8 groups (shown in **Table 4**). From the 46 total categories, 24 were identified to the species level, 8 to the genus level (sp.) with others assigned with a less precise identification (indet.) or a morphological category. A significantly greater amount of taxonomic categories were detected on PK_1_4M and PK_4_4M units (n = 35) which were both deployed in the warmer months (June), followed by PK_3_4M (n = 24) and lastly PK_2_4M (n = 22), deployed in October and February, accordingly.

Table 4: List of 46 taxonomic categories and their 8 groups, used for the annotation of the organisms on plates of ARMS units from the Port of Koper site. Values (%) indicate the percentage of ARMS units, plates and points on which the respected taxonomic category was detected. Most frequent categories are shown in bold (> 2% of points).

Taxonomic category	Units (%)	Plates (%)	Points (%)

Cirripedia (n = 4)			
Amphibalanus amphitrite (Darwin, 1854)	25.0	2.8	0.1
Amphibalanus improvisus (Darwin, 1854)	25.0	15.3	0.6
Balanidae *indet.*	50.0	5.6	0.1
Balanus trigonus Darwin, 1854	25.0	4.2	0.1
Cnidaria (n = 2)			
Aurelia aurita (Linnaeus, 1758) polyp	50.0	9.7	0.3
Hydrozoa *indet.*	25.0	1.4	0.0
Porifera (n = 6)			
Porifera transparent	50.0	11.1	0.2
Porifera indet	50.0	11.1	0.3
Porifera light brown	50.0	22.2	1.0
Porifera yellow veins	75.0	16.7	0.4
Sycon sp.	50.0	6.9	0.1
Clathrina coriacea (Montagu, 1814)	25.0	1.4	0.0
Algae (n = 2)			
Coralligenous algae	25.0	1.4	0.0
Red macroalgae	25.0	2.8	0.0
Ascidiacea (n = 8)			
Ascidia sp.	100.0	26.4	0.9
***Ascidiella* sp.**	**75.0**	**29.2**	**3.8**
Botryllus schlosseri (Pallas, 1766)	75.0	6.9	0.1
Ciona intestinalis (Linnaeus, 1767)	75.0	9.7	1.3
Didemnidae	**100.0**	**41.7**	**4.7**
Pyura sp.	75.0	12.5	0.2
***Styela plicata* (Lesueur, 1823)**	**75.0**	**38.9**	**5.5**
Microcosmus sabatieri Roule, 1885	50.0	4.2	0.2
Mollusca (n = 8)			
Abra sp.	25.0	2.8	0.0
Anomidae	**100.0**	**76.4**	**8.0**
Bivalvia *indet.*	50.0	15.3	0.3
Hiatella arctica (Linnaeus, 1767)	50.0	12.5	0.2
Mimachlamys varia (Linnaeus, 1758)	100.0	15.3	0.3
***Mytilus galloprovincialis* Lamarck, 1819**	**75.0**	**30.6**	**6.1**
***Ostrea edulis* Linnaeus, 1758**	**75.0**	**29.2**	**4.2**
Limaria tuberculata (Olivi, 1792)	25.0	1.4	0.0
Polychaeta (n = 4)			
***Salmacina* sp. - *Filograna* sp.**	**75.0**	**52.8**	**12.5**
Serpulidae *indet.*	**100.0**	**70.8**	**8.0**
***Spirobranchus triqueter* (Linnaeus, 1758)**	**100.0**	**44.4**	**5.5**
***Spirorbis* sp.**	**100.0**	**77.8**	**4.2**
Bryozoa (n = 12)			
Aetea sp.	75.0	8.3	0.1

***Bugula neritina* (Linnaeus, 1758)**	**75.0**	**23.6**	**2.0**
Bryozoa arborescent white	**100.0**	**81.9**	**8.1**
Encrusting bryozoan *indet.*	100.0	47.2	0.9
Celleporaria brunnea (Hincks, 1884)	75.0	18.1	0.3
***Cryptosula pallasiana* (Moll, 1803)**	**100.0**	**51.4**	**2.9**
***Savignyella lafontii* (Audouin, 1826)**	**75.0**	**50.0**	**8.1**
Schizobrachiella sanguinea (Norman, 1868)	75.0	12.5	0.2
Schizoporella dunkeri (Reuss, 1848)	25.0	1.4	0.0
***Schizoporella errata* (Waters, 1878)**	**75.0**	**50.0**	**7.9**
Schizoporella unicornis (Johnston in Wood, 1844)	25.0	2.8	0.1
Watersipora arcuata Banta, 1969	50.0	5.6	0.1

Firstly, stacked column charts (**Fig. 28**) for all the 4 units combined (Total) and grouped by the orientation of the plate face (Top = T, Bottom = B, Topmost = 9T & Bottommost = 1B), were made to display the structure of the overall developed community and that of plates of different orientation with proportions of 8 taxonomic groups.

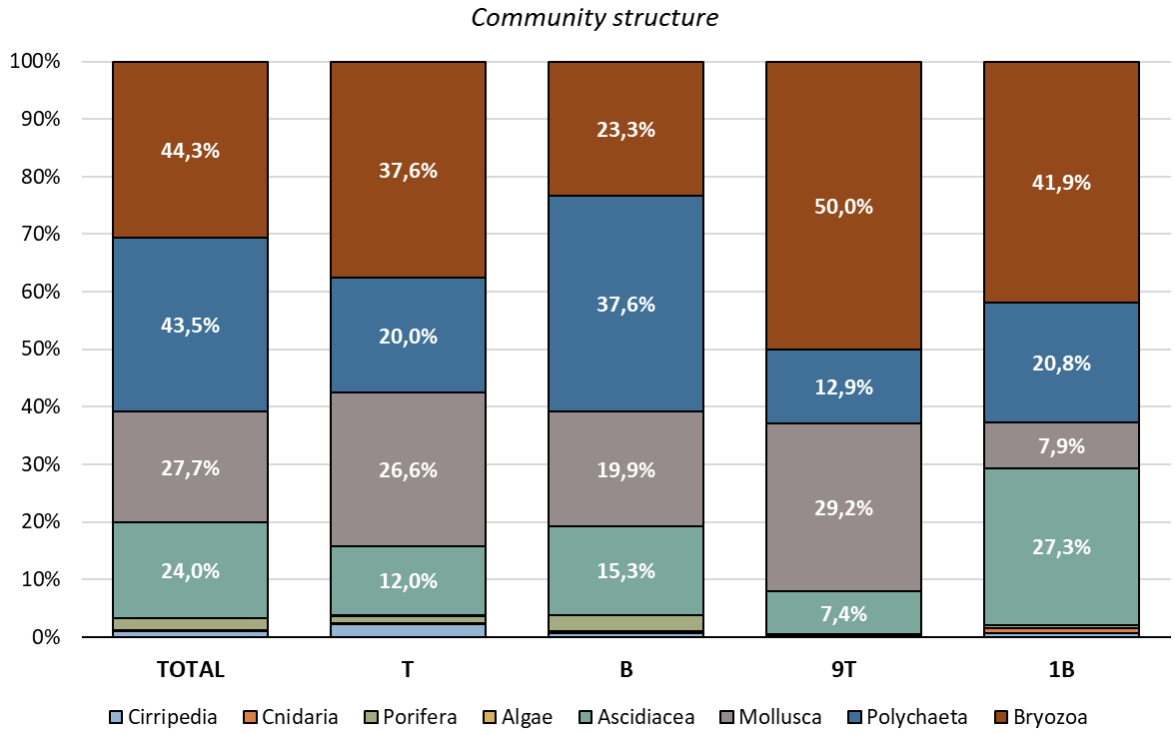

Figure 28: Stacked column chart representing the relative proportions of plate coverage of 8 broader taxonomic groups, from all the 4 ARMS at the PK site combined (Total) and based on the plate orientation (T, B, 9T, 1B). Proportion values (> 5%) are shown in white.

Concerning the community structure from all 4 units combined (**Fig. 28**, Total) taxa from Bryozoa (44.3%) and Polychaeta (43.5%) groups colonized very similar and largest proportions

of the whole community. They were followed by Mollusca (27.7%) and Ascidiacea (24.0%), which also contributed to the community with very similar proportions. Porifera (2.9%), Cirripedia (1.4%), Cnidaria (0.4%) and Algae (0.1%) groups, did not significantly contribute to the total biofouling community, as they collectively did not even reach a 5% share. The overall dominant taxonomic categories, present under the majority of annotated points were *Salmacina sp. - Filograna sp.* (12.5%), *S. lafontii* (8.1%), Bryozoa arborescent white (8.1%), Anomidae (8.0%) and Serpulidae *indet.* (8.0%).

The trend of insignificance from Porifera, Cirripedia, Cnidaria and Algae groups, seen in the Total column in **Fig. 28** (above), was also present on plates of distinct orientation (**Fig. 28**: T, B, 9T, 1B), where these 4 groups together, failed to contribute even 5% to the respected community. The 4 remaining groups (Bryozoa, Polychaeta, Bivalvia and Ascidiacea) were present in different proportions on plate faces of contrasting orientations, however they seem quite evenly distributed.

Starting at the top oriented plates (**Fig. 28**, T), the proportions were somewhat even, compared to those of other orientations, with bryozoans as the most frequent group (37.6%), followed by molluscs (26.6%), polychaetes (20.0%) and ascidians (12.0%). The most dominant categories on T plates were Anomidae (18.5% of all points annotated), *S. lafontii* (16.5%), Bryozoa arborescent white (8.2%), *S. errata* (7.2%) and bivalve *M. galloprovincialis* (7.1%).

Bottom oriented plates (**Fig. 28**, B) displayed the highest proportion of colonized space occupied by polychaetes (37.6%) from all plate-faces. Bryozoans took up 23.3% of points, which is the least amount compared to other orientations, followed by molluscs (19.9%) and ascidians (15.3%). The 5 dominant taxonomic categories of bottom oriented plates were: *Salmacina sp. - Filograna sp.* (18.0% of all points annotated), *S. triqueter* (8.4%), *S. errata* (8.1%), *M. galloprovincialis* (7.9%) and Bryozoa arborescent white (5.9%).

On plates of 9T orientation, bryozoan (50.0%) and mollusc (29.2%) taxa occupied the most coverage, compared to other plate orientations, while polychaetes (12.9%) and ascidians (7.4%) exhibited the least colonized proportions of all orientations. Concerning the dominant categories, *S. lafontii* occurred on 25.8%of all points annotated, followed by Anomidae (20.8%), Bryozoa arborescent white (15.3%), *Salmacina sp. - Filograna sp.* (6,3%) and *S. plicata* with the same percentage as *S. errata* (4,7%).

Finally, the cover of bottommost plates (**Fig. 28**, 1B), exhibited a large coverage proportion assigned to the bryozoan taxa (41.9%), followed by the ascidians (27.3%) and bivalves (7.9%),

which occupied the most and least proportions of points among differently oriented plates, accordingly. The most frequent taxonomic categories 1B plates were: Serpulidae *indet.* (17.7%), *S. plicata* (12.6%), Bryozoa arborescent white (12.5%), *S. lafontii* (9.4%) and *S. errata* (8.4%).

Using the number of points under which an organism was present (colonized) or not (empty) from the total 300 annotated, a stacked column chart (**Fig. 29**, below), was made to illustrate the amount of plate surface covered by sessile biofouling taxa, regarding the orientation of the plates (T, B, 9T and 1B) from the 4 ARMS units from the Port of Koper study site.

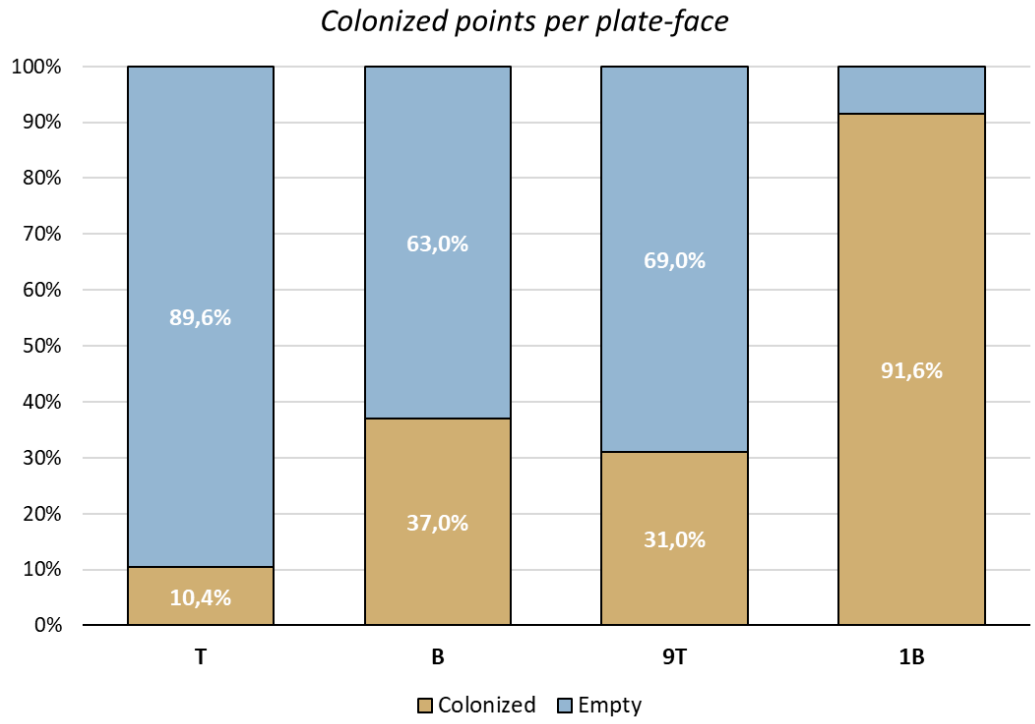

Figure 29: Stacked column charts representing colonized (sandy) and empty (blue) proportions of points on ARMS plates from the PK site, regarding their orientation (T, B, 9T). Percentage values (> 10%) are shown in white.

Column charts from **Fig. 29** show how plates of different orientations, were colonized in different proportions. The 1B oriented plates had by far the most colonized cover (91.6% of points) followed by B (37.0%), 9T (31.0%) and finally T (10.4%) plate-faces. A Mann-Whitney-U pairwise test of the colonized/empty data used for **Fig. 29**, confirmed that T plates have significantly lower proportions of colonized surfaces than B ($p = 7.3E-11$) and that colonized proportions between T - 9T ($p = 0.08$) and B - 9T ($p = 0.8$) oriented plates do not differ significantly. Despite the small number of 1B plates ($n = 4$), the Mann-Whitney-U test

confirmed, that they have significantly higher proportions of colonized coverage than T, B and 9T plates ($p < 0.05$).

The 2D NMDS plot (**Fig. 30**, below) was constructed from all plates of the 4 ARMS units from the Port of Koper site to graphically represent the distances of the biofouling community structure on plate-faces of distinct orientations (T, B, 9T, 1B). Each dot on the plot (**Fig. 30**, left) represents the community structure of a plate, which are labelled by colour, depending on their orientation (T = teal, B = red, 9T = sandy, 1B = blue) . In addition to the point-only plot (**Fig. 30**, left), 95% concentration ellipses were outlined, to better visualize the overlap among T and B groups, with 9T plates being absent (**Fig. 30**, right).

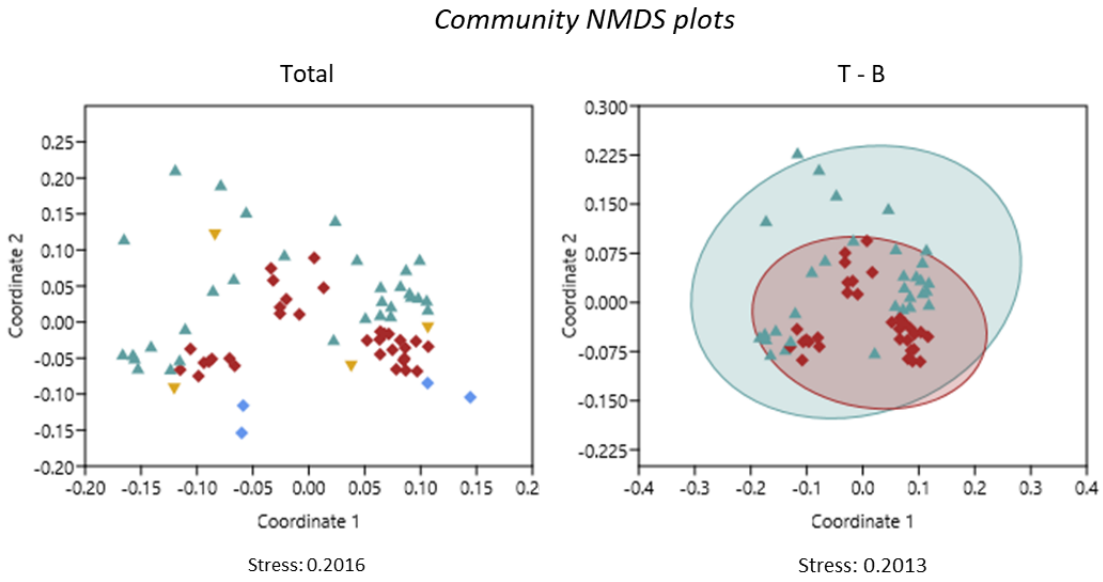

Figure 30: 2D NMDS plots based on Bray-Curtis similarity index from 300 point overlay data of the biofouling community from the PK site. Symbols are grouped by the orientation of the respected plate (T = teal, B = red, 9T = sandy, 1B = blue).

The 2D NMDS plots (stress = 0.2) of **Fig. 30** (above), suggest to a poor distinction between the communities of ARMS plates of different orientations at the PK site The distribution pattern of B dots appears to be a much more tightly scattered, than that of T dots, hence the bigger 95% ellipse of T group compared to that of B, seen on the left plot of **Fig. 30**. Additionally, the 95% ellipses display an almost total overlap among of T and B groups. Distribution of the 4 sandy-coloured points (9T), belonging to topmost (9T), does not indicate any distinct tendency to be associated to those of either T or B plates. On the contrary, points belonging to 1B plates (blue), are scattered with more tendency to the B side of the plot.

An additional SIMPER analysis revealed an overall high 83.6% dissimilarity among the T, B, 9T and 1B groups, mainly contributed by the *Salmacina sp. - Filograna sp.* (11.4%), *S. lafontii* (8.6%) and *S. triqueter* (7.8%) taxonomic categories. The highest SIMPER dissimilarity was detected between T - 1B plates (91.9%), contributed mostly by Serpulidae *indet.* (16.7%), *S. plicata* (12.9%) and Bryozoa arborescent white (10.2%) taxa, whereas 9T - B groups showed the lowest dissimilarity value of 80.7%, for which *S. lafontii* (13.9%), *Salmacina sp. - Filograna sp.* (11.6%) and Anomidae (11.1%) were most responsible. SIMPER analysis between T and B groups reported a very high 83.3% dissimilarity between the developed communities, mainly contributed by the *Salmacina sp. - Filograna sp.* (14.3%) *S. triqueter* (10.4%), Serpulidae *indet.* (16.5%) and *M. galloprovincialis* (8.9%).

To illustrate how length of the deployment period influences the plate-face colonization, box plots (**Fig. 31**) were made with data of colonized points from all 4 ARMS units, deployed at the Port of Koper study site.

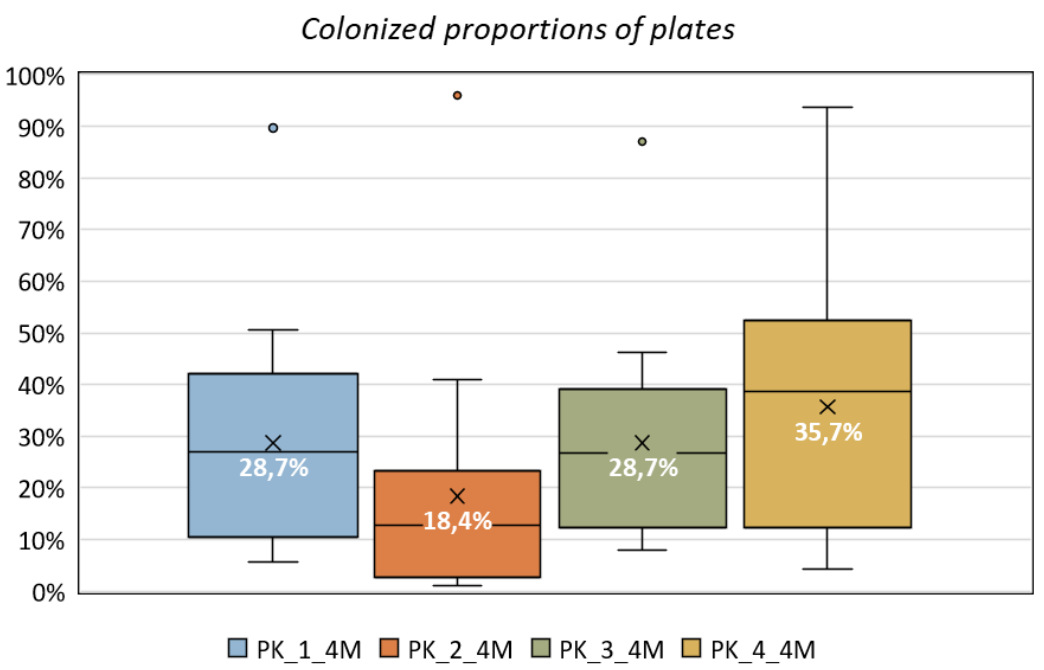

Figure 31: Box plots representing percentages of colonized points for each of the 4 ARMS units, deployed at the PK site. Sample means are indicated with an X, with their values shown in white.

Results of the one-way ANOVA test ($F = 1.8$, $p = 0.15$) show that mean values of colonized proportions of points were not significantly different among all the 4 ARMS units. However, a pairwise Mann-Whitney-U test confirmed that the plates of the least colonized unit, PK_2_4M

(mean = 18.4%), had significantly lower proportions of colonized points, than the 3 other units ($p < 0.05$). Plates of the PK_4_4M unit exhibited the highest mean colonized proportion value of 35.7%, followed by PK_1_4M and PK_3_4M which both had a similar mean value of 28.7%. When looking at the median lines from the graph, the difference in colonized proportions between 4 units become more apparent. The reach (min.- max.) was the highest for the PK_4_4M unit (min. = 4.3%, max. = 93.7%), as the 1B plate (max.) was not considered an outlier, as it was for the other 3 units.

Due to the significant influence of the plate-face orientation (T, B, 9T) on the colonized coverage, the below chart (**Fig. 32**) was constructed, in addition to the **Fig. 31** (above). Amounts of points overlying an organism from the 300 total were transformed into percentages and are shown grouped firstly by the ARMS unit and by plate orientation within.

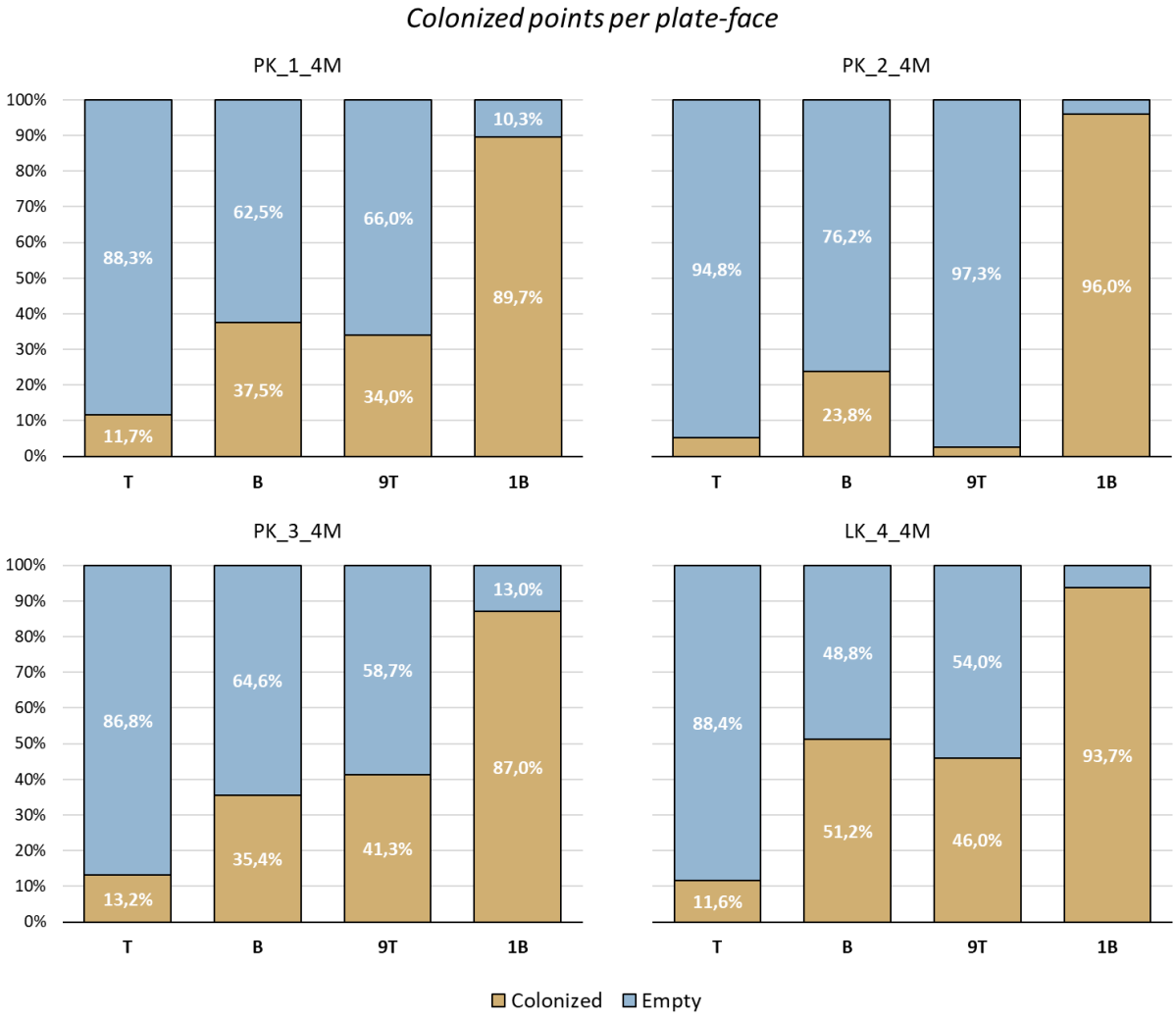

Figure 32: Stacked column charts representing colonized (sandy) and empty (blue) proportions of points on each from the 4 ARMS units from the PK site, regarding their orientation (T, B, 9T). Percentage values (> 10%) are shown in white.

Stacked column charts from **Fig. 32** show the differences in colonized coverage among plate-faces of distinct orientations within and among the 4 ARMS units from the PK study site. T plates did not even exceed a 15% proportion of colonized points (max. at PK_3_4M = 13.2%) and were very similar among all 4 units. The trend of lower colonized proportions on T oriented plates, compared to B, is evident and statistically significant (Mann-Whitney-U, $p < 0.05$) at all 4 ARMS units. PK_2_4M had the least colonized B plates (23.8%), PK_4_4M had the most colonized (51.2%), with PK_1_4M (37.5%) and PK_2_4M (35.4%) both having very similar proportions of somewhere in between. Colonized coverage of 9T plates were more or less similar, of around 40%, however it was very low on the PK_2_4M unit (2.7%). Bottommost (1B) plates were by far the most colonized at every ARMS unit deployed, and were always above 87% (PK_3_4M).

The relative proportions of coverage from 8 broader taxonomic groups, that made up the sessile biofouling community, derived by the 300 point overlay method are presented in **Fig. 33** (below), for each individual ARMS unit deployed at the Port of Koper site.

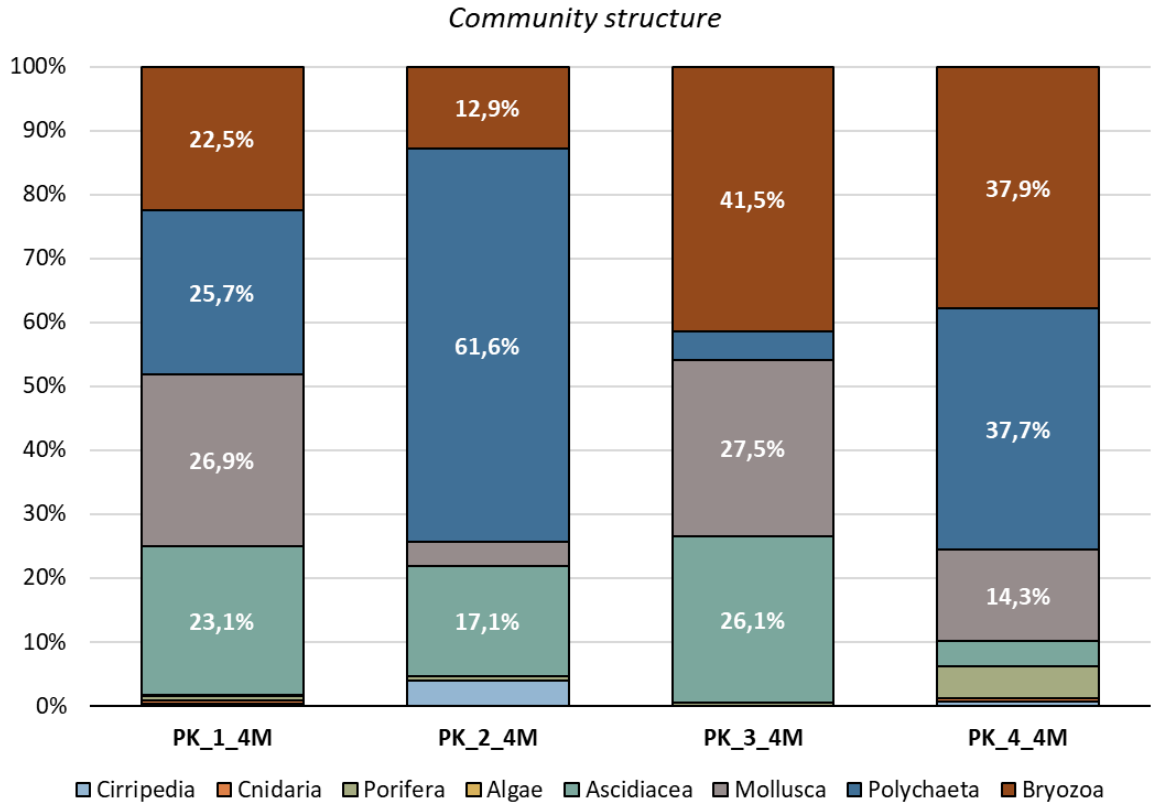

Figure 33: Stacked column charts representing the relative proportions of plate coverage of 8 broader taxonomic groups, based on 300 point overlay method from each of the 4 ARMS at the PK site. Proportion values (> 5%) are shown in white.

Relative proportions contributed by the same taxonomic groups tend to differ considerably among the 4 ARMS units deployed at the PK site. The PK_1_4M unit, had the most balanced coverage proportions of the 4 most frequent groups (Mollusca = 26.9%, Polychaeta = 25.7%, Ascidiacea = 23.1%, Bryozoa = 22.5%), each bringing about a fourth to the total community. Polychaetes were the most dominant group on the PK_2_4M unit, contributing 61.6% to the total community, with the least cover of bryozoan (12.9%) and Mollusc (3.8%) taxa at the site. Bryozoa occupied the most cover on the PK_3_4M (41.5%), followed by molluscs (27.5%) and ascidians (26.1%) which colonized similar proportions as on the PK_1_4M unit, with polychaete taxa occupying only a scarce proportion of cover (4.5%). Both bryozoan (37.9%) and polychaete (37.7%) were the most substantial groups on plates of PK_4_4M, followed by molluscs (14.3%) and the least amount of coverage from all ARMS assigned to the Ascidiacea group (4.0%). Cirripedia were almost exclusive on the PK_2_4M (4.0%) and Porifera on the PK_4_4M (4.9%) unit.

Dominant taxonomic categories, the ones which appeared under most of total overlaid points, for every individual ARMS unit were *S. plicata* (19.0%), Anomidae (13.5%) and *O. edulis* (12.7%) for PK_1_4M; *S. triqueter* (30.0%), Serpulidae *indet.* (26.2%), and *Ascidiella* sp. (7.7%) for PK_2_4M; *S. lafontii* (27.9%), *M. galloprovincialis* (24.0%) and Didemnidae (13.9%) for PK_3_4M and finally *Salmacina sp.* - *Filograna sp.* (28.0%), *S. errata* (18.0%) and Bryozoa arborescent white (15.2%) for the PK_4_4M unit.

To display the differences in community structure based on plate orientation (T, B, 9T,1B), each of the 4 bar charts from ARMS units from **Fig. 33** have been divided in such regard and are presented in **Fig. 34**, below.

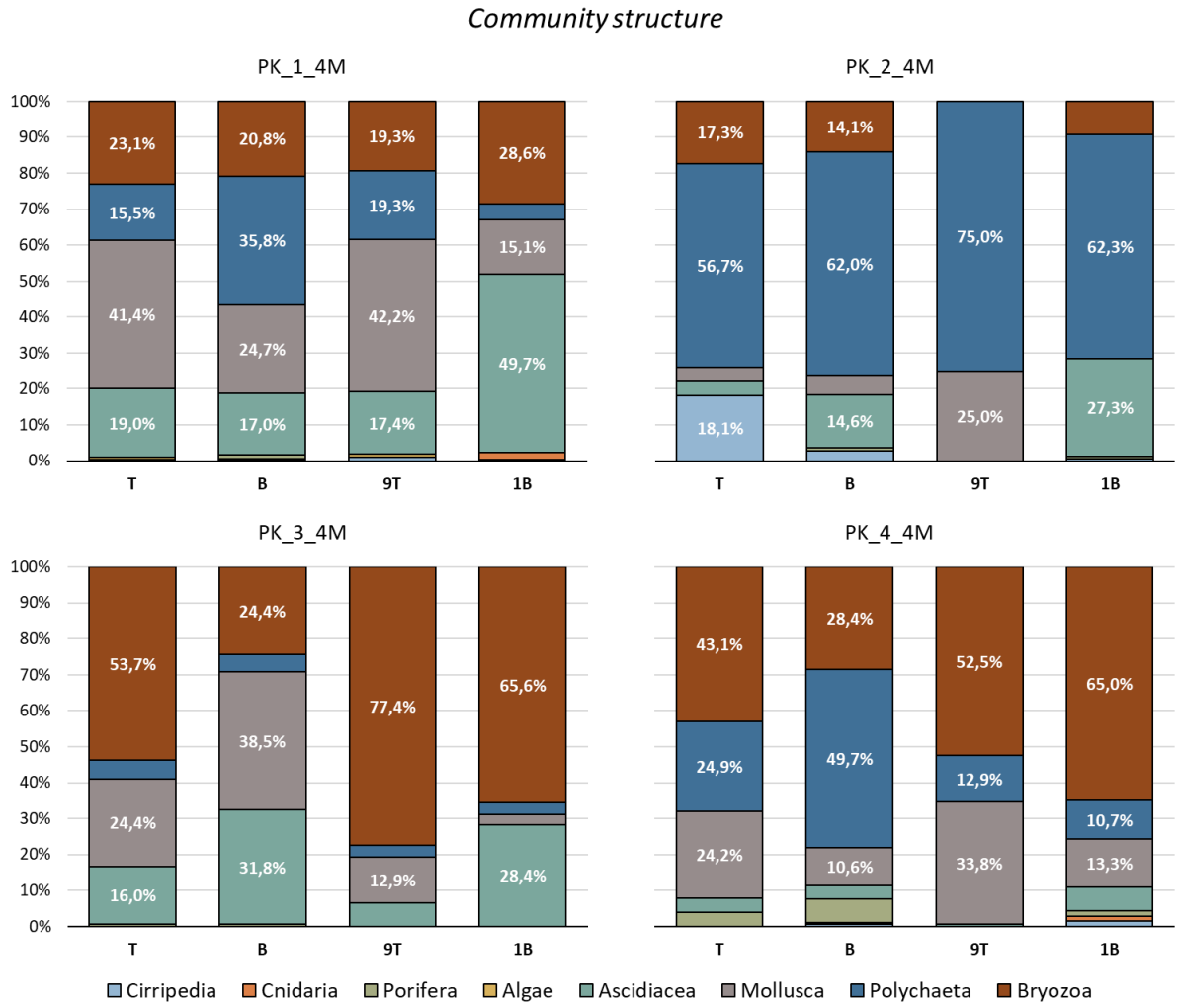

Figure 34: Stacked column charts representing the relative proportions of plate coverage of 8 broader taxonomic groups, based on 300 point overlay method from each of the 4 ARMS at the PK site, regarding plate orientation (T, B, 9T,1B). Proportion values (> 10%) are shown in white.

Seemingly, the proportional structure of the 8 taxonomic groups displayed in **Fig. 34**, differs slightly in regard to the plate orientation on individual ARMS units from the PK site. Plate-faces of distinct orientations of the same ARMS unit, displayed very similar colonized proportions, belonging to the same taxonomic group. For example, all column charts for the PK_1_4M units indicate to a very homogenous proportions of coverage distributed among the 4 most common groups. Polychaete taxa were dominant on PK_2_4M (min. = 56.7%, max. = 75.0%) and very scarce on PK_3_4M (min. = 3.2%, max. = 5.2%), compared to Bryozoa, Mollusca and Ascidiacea groups. On the PK_4_4M unit, taxonomic groups displayed a similar coverage proportion pattern, however they were not as evenly contributed as at the PK_1_4M unit.

Lastly, to graphically represent the distances of the biofouling community structure among the ARMS units, a 2D NMDS plot (**Fig. 35**) was constructed using T and B plate data of the 4 ARMS units from the Port of Koper site to illustrate the influence of deployment time, immersion period and plate-face orientation. Each dot on the plot represents a community from one of the plates which are labelled by colour, to distinguish individual ARMS units (**Fig. 35**, left) and shade (**Fig. 35**, right), to distinguish plate orientation within the unit. At each plot, 95% concentration ellipses were outlined, to better visualize the overlap among groups.

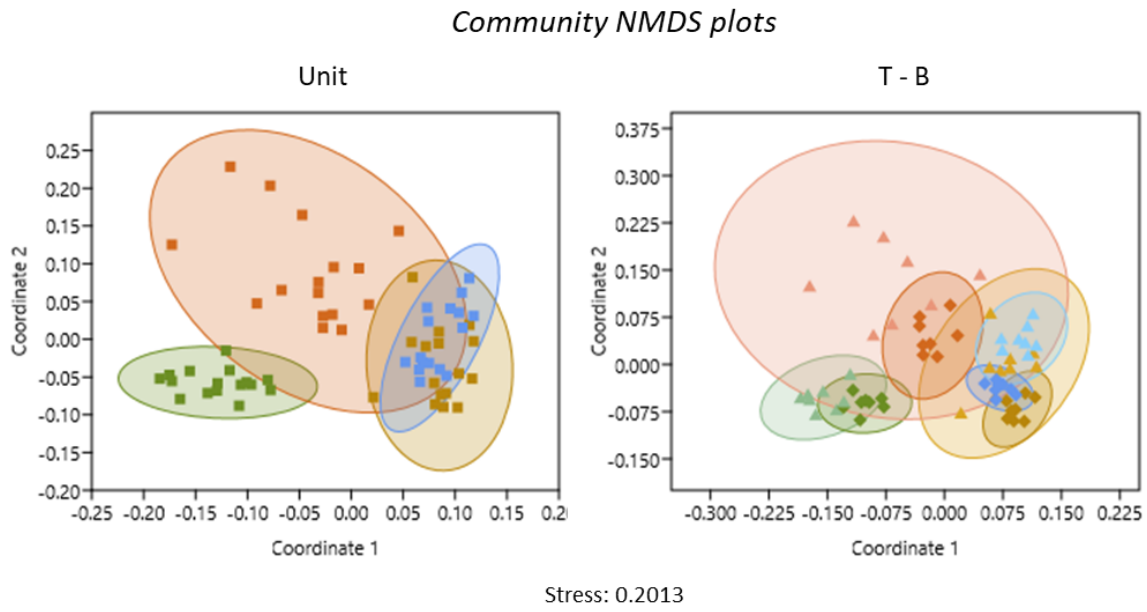

Figure 35: 2D NMDS plots with 95% conc. ellipses based on Bray-Curtis similarity index from 300 point overlay data of the biofouling community from 4 ARMS units at the PK site from T and B oriented plates. Symbols are grouped by the ARMS unit (PK_1_4M = blue, PK_2_4M = brown, PK_3_4M = green, PK_4_4M = sandy) and plate orientation (T = light tone, B = dark tone).

The 2D NMDS scatter plot (stress = 0.20) with 95% conc. ellipses (**Fig. 35**, Left), shows a considerable overlap of ellipses among the 4 ARMS units. The PK_2_4M unit (brown) has the most scatter and overlaps with all the 3 other units. On the contrary, PK_1_4M (blue) and PK_3_4M (green) both display a tight scatter and the smallest ellipses. Interestingly, the point scatter from the PK_1_4M (blue) and PK_4_4M (sandy) units, that were deployed with the most time in between (12 months), but consequently in the similar time of the year (season), revealed an almost total overlap of the 95% ellipses.

A SIMPER analysis between all 4 ARMS units showed a large dissimilarity of 85.8%, mainly contributed by *Salmacina sp. - Filograna sp.* (11.7%), *S. lafontii* (10.1%) and Anomidae (8.4%) categories. The differences between 4 individual ARMS units were tested with SIMPER as well. The test showed the highest dissimilarity (92.2%) of the developed community between PK_1_4M and PK_3_4M with highest contribution from *S. lafontii* (16.3%), *M. galloprovincialis* (13.9%) and Anomidae (9.0%) taxa. On the contrary, PK_1_4M and PK_4_4M displayed the least amount of community dissimilarities (68.1%), from *Salmacina sp. - Filograna sp.* (19.6%) *S. errata* (11.7%) and Anomidae (10.5%).

Looking at the NMDS plot where plate orientations are considered (**Fig. 35**, right side), B plates (darker tone) display a significantly tighter scatter (points closer together, smaller 95% ellipses), than T (lighter tones), at all 4 ARMS units. Additionally, 95% ellipses from T plate points (lighter tone), especially from the PK_2_4M unit, show overlap with those of other units, whereas B plate ellipses are nicely separated, except the ones from PK_1_4M and PK_4_4M.

According to the results of the Bray-Curtis based SIMPER test, the PK_2_4M unit, displayed the highest dissimilarity value among T & B oriented plates (82.3%), for which *S. triqueter* (43.5%), *Ascidiella* sp. (10.8%) and Serpulidae *indet.* (9.5%) were most accountable. On the contrary, plates from the PK_3_4M unit, showed the lowest dissimilarity (58.9%) between T and B oriented plates, contributed mostly by *M. galloprovincialis* (32.7%), *Ascidiella* sp. (13.7%) and Didemnidae (12.3%) taxonomic categories.

8.2.4. Community comparison among sites

Using the 300 point overlay method on 191 plate faces from 11 ARMS units deployed at the 3 study sites (PIR: n = 4, VID: n = 3, PK: n = 4) within the Slovenian sea, 21931 points (38.3% of all overlaid) were annotated with 62 taxonomic categories from 8 taxonomic groups. From the 62 total categories, 32 were identified to the species level, 9 to the genus level (sp.) with others assigned with a less precise identification (indet.) or a morphological category. Most taxonomic categories were detected on ARMS units deployed at the PK site (n = 46) where units were deployed in different yearly seasons, followed by VID (n = 34) and lastly PIR (n = 33), where units were deployed in more or less the warmer period of the year.

Firstly, boxplots, shown in **Fig. 36** (below), were constructed using the data from all the plates (Total, top chart) and bottom oriented only (B, bottom chart), from individual ARMS units at each of the 3 study sites to show the different amounts of biofouling categories detected on

units with different deployment periods and to compare the pattern displayed by using total and B only plates. Plates from ARMS at the PIR site, had the most taxonomic categories per plate-face when all units were combined (PIR overall mean = 11.3, not shown), followed by PK (overall mean = 10.6, not shown) and VID (overall mean = 9.6, not shown). On the other hand, when only B plate-faces were considered, ARMS at the VID site, had the most taxonomic categories present when all units were combined (overall mean = 14.7, not shown), followed by PK (overall mean = 14.4, not shown) and PIR (overall mean = 13.9, not shown).

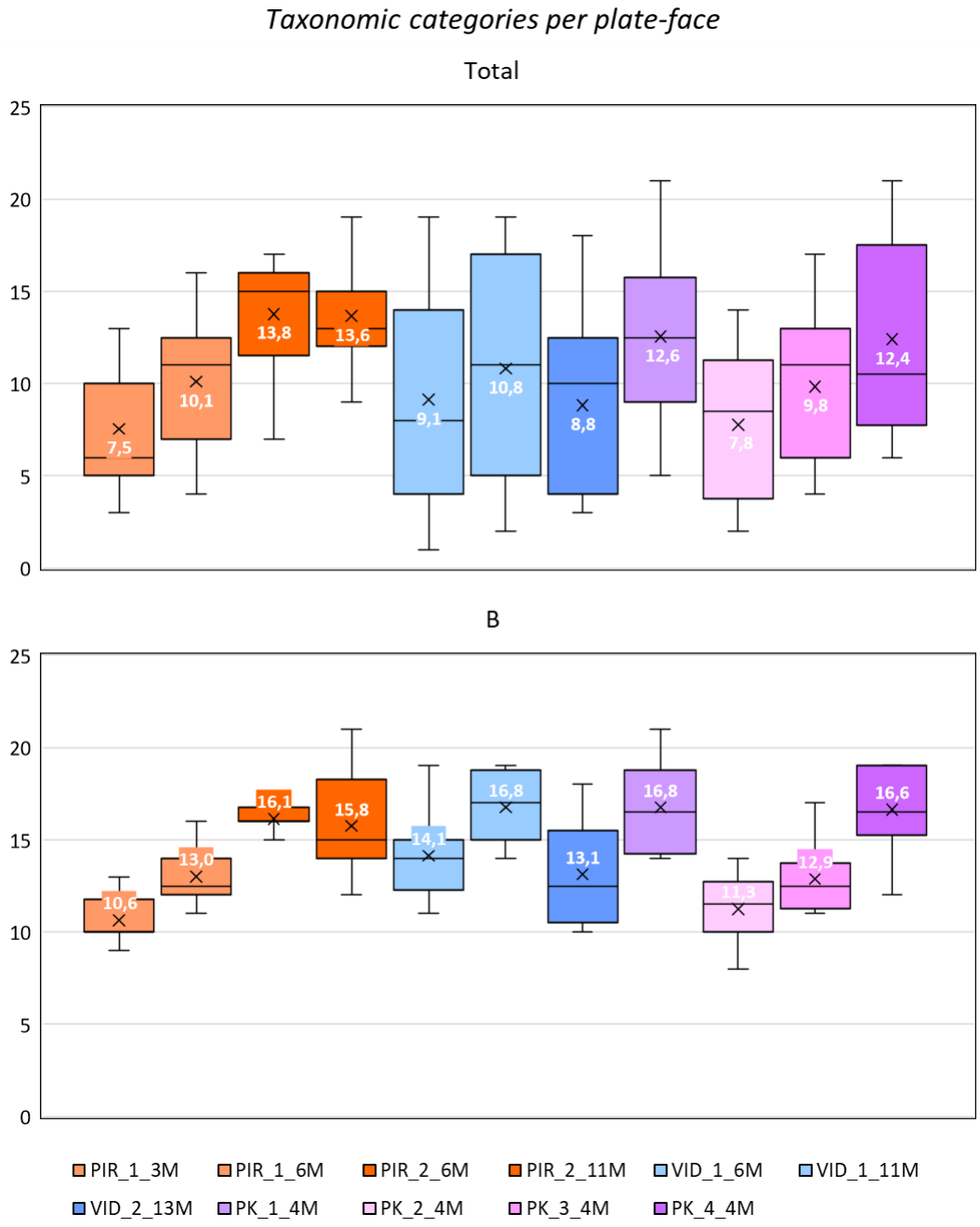

Figure 36: Box plots representing the number of taxonomic categories, detected per plate on each of the 11 ARMS units, grouped by location (PIR = orange, VID = blue, PK = violet)

using plates of all orientations (Total) and bottom only (B). Units from different deployments at the same site (PIR_1 and PIR_2, etc.) are distinguished by the shade (lighter- darker) of their respected colour. Mean values are indicated with an X, with their values shown in white.

Looking at the Total section of **Fig. 36** (above), ARMS units from the second deployment at the PIR site (PIR_2), which had deployment periods of 6 and 11 months, both displayed the highest amount of detected taxonomic categories per plate-face (PIR_2_6M = 13.8, PIR_2_11M = 13.6) of all the 11 units. Both units from PIR_2 had significantly (Mann-Whitney-U, $p < 0.05$) more taxonomic categories per plate as ARMS units with the same deployment periods from the same location but different deployment (PIR_1_6M mean = 10.1) and those with similar deployment periods from the VID study site (VID_1_6M mean = 9.1, VID_2_13M mean = 8.8). Numbers of taxonomic cat per plate-face on ARMS at the PK site, which were all deployed for 4 months at different times were higher than on plates deployed for 3 months at the PIR site (PIR_1_3M) and similar to those of 6 (PIR_1_6M, VID_1_6M) or even 11-13 months (VID_1_11, VID_2_13). A Mann-Whitney-U test ($p > 0.05$) also showed that numbers of taxonomic categories on PK_1_4M (mean = 12.6) and PK_4_4M (mean = 12.4) plates are not significantly different from those on PIR_2_6M and PIR_2_11M, despite having a much longer deployment period of 6-11 month, compared to 4 months at the PK site.

Comparing the boxplots produced by all plate orientations (**Fig. 36**, Total) to those of bottom oriented plates (**Fig. 36**, B), the latter (B) display much shorter ranges (min. – max.) and have higher mean values at all 11 ARMS units considered. Additionally, the boxplots from B plate-faces, displayed a very similar order between ARMS units within the same location, whereas the differences in numbers of taxonomic categories per plate among locations became more equal and in a different order. The highest mean number of taxonomic categories per plate were present at the same units as before, but in a different array: VID_1_11M & PK_1_4M (mean =16.8), PK_4_4M (mean = 16.6), PIR_2_6M (mean =16.1) and PIR_2_11M (mean =15.8). The lowest mean value was again at the PIR_1_3M unit (mean = 10.6), with other ARMS units in between those previously mentioned. The trend of higher amounts of taxonomic cat with increasing deployment periods is present for only the PIR site and shift considerably at the VID and PK sites.

To show the different amounts colonized coverage proportions of ARMS plates of units from different sites with particular deployment periods and to compare the pattern displayed by using all (Total) and B only plates, boxplots in **Fig. 37** (below), were constructed using the data from

all the plates (Total) and bottom oriented (B), from individual ARMS units at each of the 3 study sites. Plate-faces from ARMS at the PIR site, had the highest colonized proportions when all units were combined (PIR overall mean = 42.5%, not shown), followed by VID (overall mean = 29.5%, not shown) and PK (overall mean = 27.9%, not shown). On the other hand, when only B plate-faces into were considered, ARMS at the PIR site, had the most plate proportions colonized when all units were combined (overall mean = 61.9%, not shown), followed by VID (overall mean = 53.3%, not shown) and PIR (overall mean = 37.0%, not shown), when only taking.

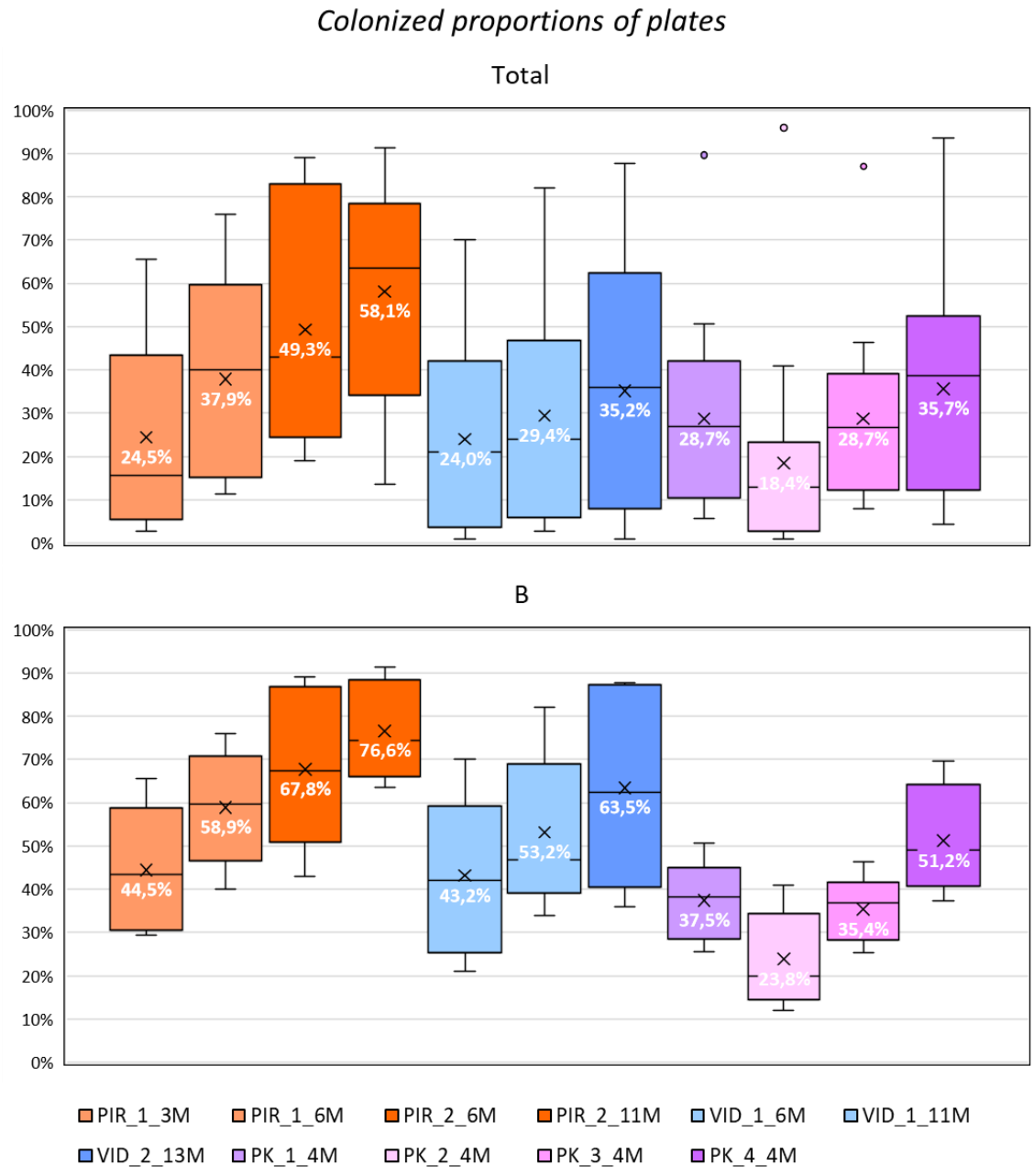

Figure 37: Box plots representing the colonized plate coverage proportions of on each of the 11 ARMS units, grouped by location (PIR = orange, VID = blue, PK = violet) using plates of all orientations (Total) and bottom only (B). Units from different deployments at the same site (PIR_1 – PIR_2, etc.) distinguished by the shade (lighter- darker) of their respected colour. Mean values are indicated with an X, with their values shown in white.

Looking at the Total section of **Fig. 37** (above), ARMS units from the second deployment at the PIR site (PIR_2), which had deployment periods of 6 and 11 months, both displayed the highest mean values of colonized proportions (PIR_2_11M = 58.1%, PIR_2_6M = 49.3%) of all the 11 units. Plates of PIR_2 units had much larger colonized proportions as ARMS units with the same deployment periods from the same location (PIR_1_6M mean = 37.9%) and those with similar deployment periods from the VID study site (VID_1_6M mean = 24.0%, VID_1_11M mean = 29,4%, VID_2_13M mean = 35.2%). Colonized proportions on ARMS plates at the PK site, which were all deployed for 4 months at different times (deployments) were higher than on plates deployed for 3 months at the PIR site (PIR_1_3M mean = 24.5%) and similar to those of 6 (VID_1_6M) or even 11-13 months (VID_1_11, VID_2_13). A Mann-Whitney-U test ($p > 0.05$) also showed that colonized proportions on all 4 ARMS from PK site are not significantly different from all 3 at the VID site and PIR_1_6M, despite them having a much longer deployment period of 6-13 month, compared to 4 at the PK.

Comparing the boxplots produced by all plate orientations (**Fig. 37**, Total) to those of bottom oriented plates (**Fig. 37**, B), the latter (B) display fairly shorter ranges (min.- max.) and have significantly higher proportions at all 11 ARMS units. Additionally, the boxplots considering only B plates, displayed a very similar order between ARMS units within the same location and made differences of colonized proportions among the 3 locations even more evident, specially at the PK site. Therefore, the boxplots representing ARMS of the PK site (4 months deployment) have colonized proportions similar, or smaller, to those of the PIR_1 deployment (3-6 months). The highest colonized proportions were present in the similar, but higher array as before: PIR_2_11M (mean = 76.6%), PIR_2_6M (mean = 67.8%) and VID_2_13M (mean = 63.5%) The lowest mean value was at the PK_2_4M unit (mean = 23.8%), with other ARMS units in between the previously mentioned ones. The trend of higher colonized proportions with increasing deployment periods is present at both total and B plots for the PIR and VID site, however at the PK site it shifts at each unit, as they were deployed at different times of the year.

To illustrate and compare the biofouling community structure that developed on ARMS units at the 3 study sites, stacked column charts (**Fig. 38**) from all (Total) and bottom only (B) plates with coverage proportions of 8 taxonomic groups.

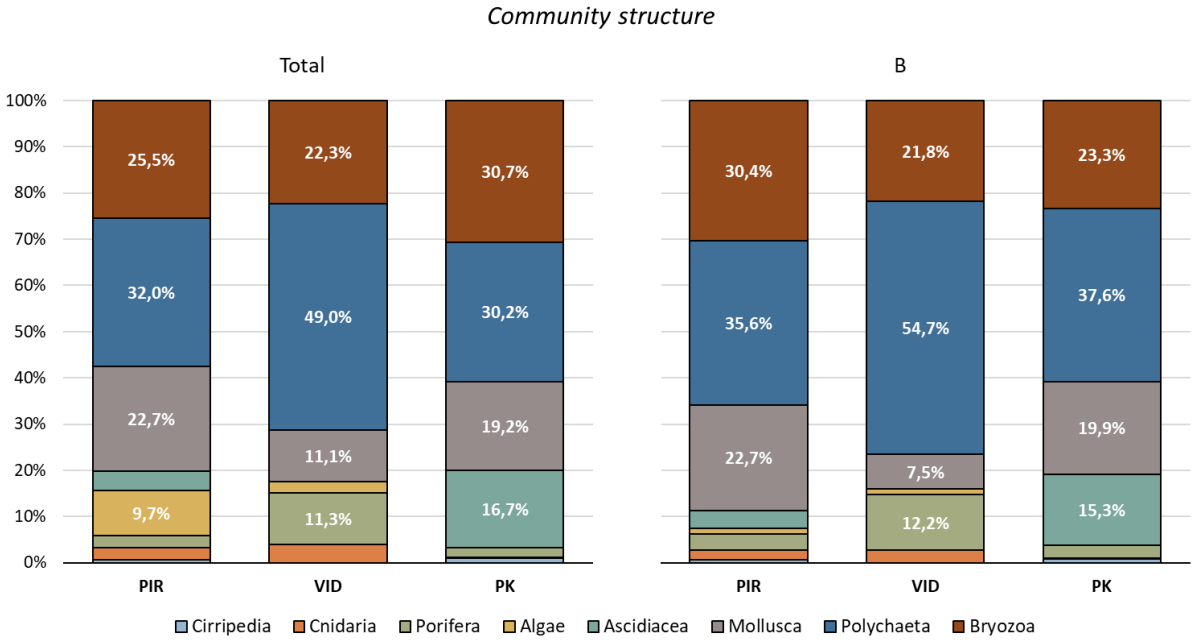

Figure 38: Stacked column charts representing the relative proportions of 8 broader taxonomic groups on ARMS units from 3 study sites (PIR, VID, PK), from all plates (Total) and bottom only (B). Proportion values (> 5%) are shown in white.

Column charts from **Fig. 38** (Total) indicate that proportions contributed by the 3 most frequent groups (Polychaeta, Bryozoa and Mollusca) are quite similar among the sampling sites, especially PIR and PK. Polychaetes were the most dominant on ARMS plates at the VID site (49.0% of points), and were present in similar proportions on PIR (32.0%) and PK (30.2%) units, along with bryozoan (PIR = 25.5%, PK = 30.7%) and molluscan taxa (PIR = 22.7%, PK = 19.2%). Ascidian taxa expressed significant coverage only on plates at the PK location (16.7%) and occurred on only 4.2% of overlaid points at the PIR site. Porifera colonized most cover on ARMS at the VID site (11.3%), followed by very modest proportions on PIR (2.6%) and PK (2.0%) units. Algae occurred mostly on plates at the PIR site (9.7%), and in much lower share at the VID site (2.4%). Cnidarian taxa were overall scarce, with their highest proportions at the VID (3.9%) and PIR (2.9%) sites. Cirripedia had the least percentage cover of all the groups, as they did not obtain even 1% of cover at any location (max. at PK = 0.9%).

The column charts, for which only B oriented plates were considered (**Fig. 38**, B), displayed very similar proportions for each of the 7 taxonomic groups at all 3 sites, when compared to

those generated with all plates (**Fig. 38,** Total). The only evident difference is that proportion of Algae coverage at the PIR site is lower (Total = 9.7%, B = 1.3%).

Lastly, as a graphical comparison of the distances among and within the biofouling community structure of 11 ARMS units at 3 study sites, 2D NMDS plots (**Fig. 39**, below) were constructed according to Jaccard-Dice (**Fig. 39**, left) and Bray-Curtis (**Fig. 39**, right) similarity indexes, using data from B plate-faces, to illustrate the influence of location (surrounding habitat), deployment period and immersion season on the community structure. Each dot on the **Fig. 39** represents a community from one B plate-face, which are labelled by colour according to their location (PIR = orange, VID = blue, PK = violet), shade to distinguish immersion seasons (same deployment, PIR_1, etc.) and symbols regarding the different deployment periods (3-13 months). On the bottom plots, 95% concentration ellipses were outlined, to better visualize the overlap among groups.

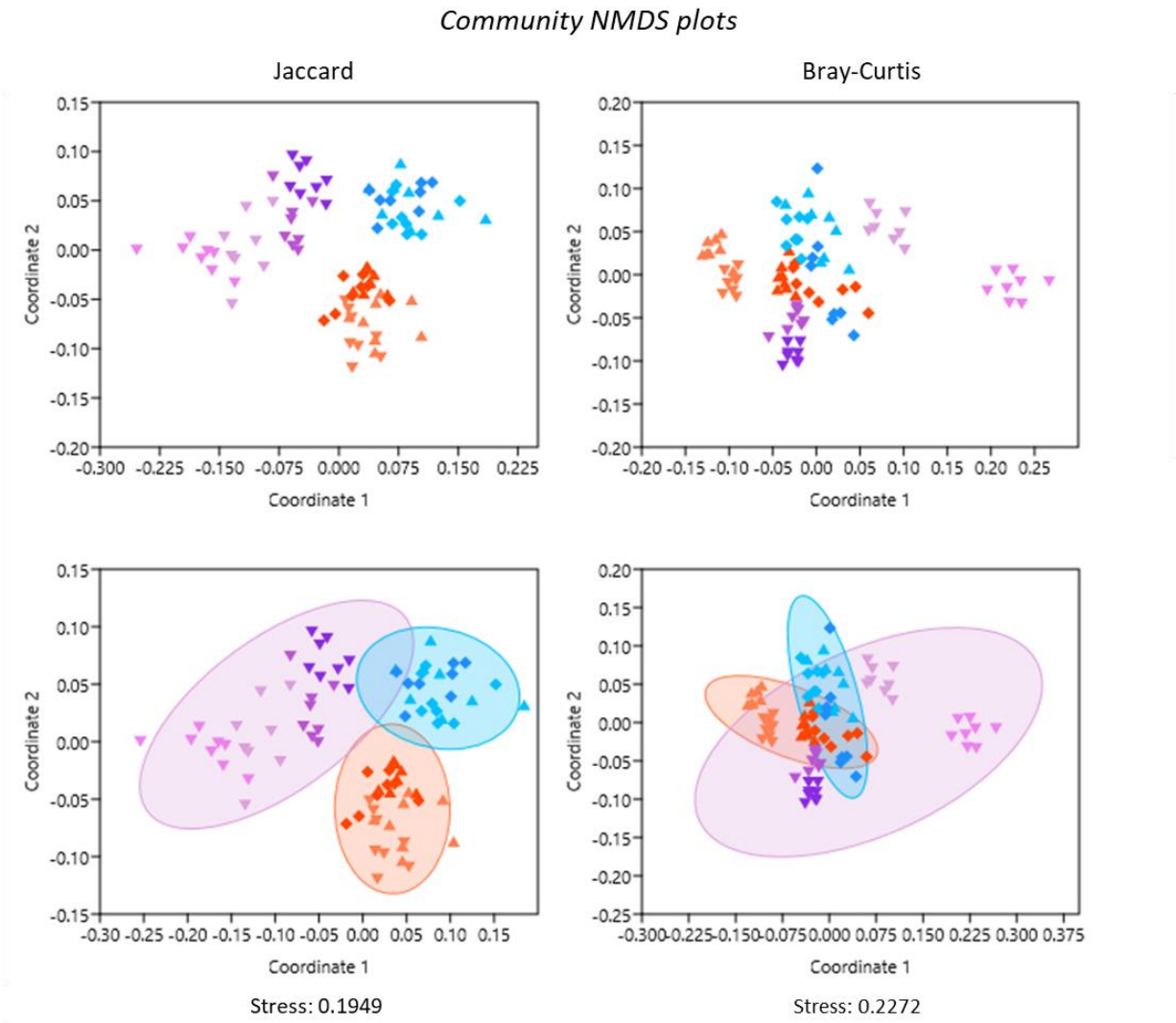

Figure 39: 2D NMDS plots based on Jaccard (left) and Bray-Curtis (right) similarity indexes from 300 point overlay data of the biofouling community from B plates of all 11 ARMS units Points are grouped by the study site (PIR = orange, VID = blue, PK = violet), and have different colour tone according to the immersion season (deployment) and symbols, according to the deployment period.

The 2D NMDS scatter (stress = 0.2), produced by Jaccard (-Dice) similarity index (**Fig. 39**, left), which mainly considers presence and absence data of different taxonomic categories, clearly distinguished the biofouling communities from the B plates of the 3 study sites (PIR, VID, PK). According to the shade of the points, those from ARMS units from different sites with higher colonized proportions are closer together (as in **Fig. 36** & **37**). Considering the 95% ellipses, the points from PK site display the loosest scatter and have most overlap with the ellipse from the VID site, however still very small.

On the contrary, the 2D NMDS plot (stress = 0.2), produced by the Bray-Curtis similarity index (**Fig. 39**, right), which mainly considers the abundance data of different taxonomic categories, depicts a very different scatter than that of Jaccard similarity (**Fig. 39**, left). The scatter displays a centered group of points coming from ARMS of different sites and deployment periods, but have a similar immersion season, within June or July, at different years (PIR_2 = July 2019, VID_1 = July 2019, VID_2 = June 2020, PK_1 = June 2020, PK_4 = June 2021). Within this group, points from VID (VID_1, VID_2) and PK (PK_1, PK_4) locations have the biggest distance between, with those from PIR situated in the middle. Points from the PIR_1 deployment (PIR_1_3M, PIR_1_6M), which were immersed in August 2019, were very close together but did not overlap with the previously mentioned group. Additionally, the scatters of PK_2 (immersion season = October 2020) and PK_3 (immersion season = February 2021) were not connected with the scatter of the main group and had fair distances in between them, with the PK (Feb. 2021) being most distant to other ARMS units. Consequently, the 95% conc. ellipse for the PK site was much bigger than those of PIR and VID, with all 3 having significant overlaps with one another.

A Bray-Curtis SIMPER test using data from B plates, revealed a large 78.2% dissimilarity among the biofouling communities of all 3 study sites, contributed mostly by *Salmacina sp.* - *Filograna sp.* (11.1%), *O. edulis* (10.5%), Serpulidae *indet.* (10.4%), *S. triqueter* (9.7%) and *T. complanata* (9.1%). The same test showed that ARMS units from the VID site had the lowest dissimilarity (61.2%) within the site, contributed by Salmacina sp. - Filograna sp. (23.4%), S. triqueter (16.4%) and Serpulidae indet. (8.2%), followed by PIR (65.7% dissimilarity), with

highest contributions from *O. edulis* (19.6%), *T. complanata* (18.1%) and Serpulidae *indet.* (12.2%), with ARMS from the PK site having the highest dissimilarity among units (79.5%), for which *Salmacina sp. - Filograna sp.* (17.5%), *M. galloprovincialis* and *S. triqueter* (both 10.6%) taxa were the most revealing. Dissimilarities of the communities among sites were the highest between PIR - PK (80.5%), contributed by *T. complanata* (13.4%), Serpulidae *indet.* and *O. edulis* (13.2%) followed by VID - PK (80.0%), which had highest contributions from *Salmacina sp. - Filograna sp.* (12.4%), *S. triqueter* (14.2%) and Serpulidae *indet.* (7.7%) and were least dissimilar between PIR - VID (73.3%), for which *O. edulis* (12.7%), *T. complanata* (12.6%) and *Salmacina sp. - Filograna sp.* (10.1%) were most accountable.

9. DISCUSSION

As mentioned in the introduction, this thesis consisted of evaluating the sessile biofouling community on 11 ARMS units deployed in 3 distinct locations (PIR, VID, PK) within the Slovenian sea through the years 2018-2020 by the use of 3 different photo-analysis methods (100 point, 300 point and 5x5 grid), to detect the influences of immersion season, deployment period and the surrounding habitat to the final community structure . As the main focus was on developing and evaluating the optimal methodological protocols of ARMS sampling, the obtained results and observations produced important findings, which are of great importance when establishing ARMS-based observatory sites for both long-term biodiversity monitoring and NIS survey purposes.

9.1. Methodological sampling approach

The simple and robust design of ARMS units made their assembly at the day of deployment very convenient and could be even done on the go (aboard the research vessel Sagitta), without consuming too much valuable fieldwork time, with spare parts always at hand. The fact that a new ARMS unit could be deployed at the same time the old one is being retrieved, as was done at VID and PK sites, made such sampling very convenient and time-efficient. For this to be achieved, only 2 experienced SCUBA divers were required, with one of them even photographing the surrounding habitat and the ARMS unit in between tasks. Of all the 11 ARMS units used, of which 7 were secured on the seabed (PIR & VID) and 4 within the water column underneath the pier, by the aid of plastic ropes (**Fig. 2, 3, 4**), none was severely damaged or lost during the months of deployment or at the retrieval. The plastic crate used for the unit's retrieval should be made of very firm plastic, to minimize disturbances to the fragile community while it is put on the boat and transported to the laboratory.

In most cases, the wet-laboratory part of the retrieval process, consisting of the ARMS disassembly, plate-face photo-documentation, visual inspection of plates and morphological sample collection of organisms could be done in the same day as retrieval or the following day, which is the best option, as the organism disturbances are kept at a minimum. In addition to the sessile fauna of interest, some representatives of vagile macroscopic fauna were detected during the disassembly as well. These were organism from the taxonomic groups Nudibranchia, Echinoidea, Turbellaria, Actiniaria, Brachyura, Gastropoda and vagile polychaetes.

Morphological organism identification for the use in photo-analysis was very challenging, even for more experienced assisting personnel. This was namely by the fact that their morphological features were hardly distinguishable among individuals (*Ascidiella* sp., *Ascidia* sp.), not yet fully developed (juvenile individuals) due to short deployment periods (e.g. Porifera, Anomidae), visually unnoticeable (Serpulid operculum) or were small in size (e.g. bryozoan colonies etc.). This resulted in certain taxa being grouped into broader (less precise) taxonomic (*indet.*) and morphological (e.g., coralligenous algae) categories for the analysis, a common case for studies of such sort (Danovaro et al. 2016; David et al. 2019). Photographs of the significant representatives of flora and fauna in the vicinity of the ARMS units could be somewhat advantageous, especially for slower growing taxa like porifera and colonial ascidians (Fava et al., 2016), serving as a starting point for their identification. However, the usage of very precise organism identifications for photo-analysis could be very hard and susceptible to errors, as identification features are hardly or even impossible to see on a photograph. In this regard, we stress the importance of obtaining high-resolution photo records of organisms, as they serve as partial enlargements of the fouling taxa on plate-faces, enabling a more precise organism identification.

A full examination of plate-faces under a stereomicroscope, such as in the study of Fortič et al. 2021, would surely contribute to the identification precision of taxa, but would significantly increase the time and effort, which is not preferable for routine monitoring methods of such sorts (Moore et al., 2019; Drummond & Connell, 2005).

When comparing the established taxonomic categories used in a similar photo-analysis on 3 ARMS, that were also deployed in the northern Adriatic (no. of taxonomic categories = 36) by David et al. (2019), our photo-analysis approach provided a somewhat larger taxa list (no. of taxonomic categories = 62), with surprisingly similar identification precision. Similar taxa were identified to the species (*S. triqueter*, *O. edulis*, etc.) or genus level (*Filograna* sp.) and even morphological categories (coralligenous algae), which illustrates the photo-analysis method advantage concerning the comparisons of biofouling communities from different study sites.

9.2. Photo-analysis method comparison

A side by side comparison of data from the three different photo-analysis methods, showed that the 5x5 grid method, which estimates the taxa coverage based on their presence/absence at each of the 25 cells surveyed, provides the highest taxonomic richness values (per plate), compared to 300 and 100 point methods (**Fig. 6** & **7**). This is to be expected, and was already stressed by

Moore et al. (2019), as the method inspects the total surface of the AMRS plates, whereas the point overlay methods only sample a part of the surface that lies under the points. However, the 5x5 grid method tends to have a major drawback of down-weighting the most abundant ground covering taxa (e.g., bryozoan colonies, larger bivalves, etc.) and up-weight the small bodied widely-scattered taxa (e.g., serpulid polychaetes, spirorbids, etc.) compared to point overlay methods (Moore et al., 2019). Our results, shown in **Fig. 8**, suggest the same tendency, as the coverage proportions derived by the 5x5 grid survey of the larger surface covering taxa (Polychaeta and Mollusca) were smaller, with those of small-bodied taxa (Polychaeta and Cirripedia) being larger, compared to both point overlay methods.

The special feature of the 5x5 grid survey method is that it provides information about the amount of taxonomic categories present at each of the 25 individual squares, which was used to create graphical representations of ARMS plates, proving that edges have higher taxonomic dens. than central parts of the plates (**Fig. 9** & **10**). However, it is important to note that this is not true organism density, rather just the density of taxonomic categories, which does not directly mean that plate edges are more colonized. On the contrary, the point overlay methods provide information about the number of points which were colonized by biofouling taxa or were empty, providing an insight in the succession-colonization pattern of the community. Such information is of great importance in studies which focus on temporal changes, succession patterns and long-term biodiversity monitoring, which are the main topics and subjects of interest addressed in numerous studies of such invertebrate communities (Fortič et al., 2021; Nerlović et al. 2018, Sokołowski et al., 2016; Fava et al., 2016; etc.).

The 2 point-overlay methods, which proved to be an efficient and accurate method for estimating the coverage of sessile organisms on artificial surfaces (Drummond & Connell, 2005), producing data that seemed to represent actual abundances or coverage of taxa, when compared to grid survey methods (Moore et al., 2019), delivered very similar contributions of broader taxonomic groups to the whole community regardless of the treatment used (100 point & 300 point overlay, **Fig. 8**). This corresponds to the conclusions of the study by Drummond & Connell (2005), where it was observed that increasing the intensity of sampling (higher number of overlaid points) did not have substantial effects on percentage cover of broader taxonomic groups.

As the main drawback of the point overlay method regards the capacity to detect (precision) small-bodied taxa (*Spirorbis* sp., *Patinella radiata*, etc.), especially when they are present in low abundances (Moore et al., 2019), increasing the intensity of sampling should reduce this

error to at least some degree and, at the same time, reduce the sample variation and potential under- or over-estimation of their cover (Drummond & Connell, 2005). The findings of this thesis did in fact confirm this, as more taxonomic categories were detected by the use of 300, rather than 100 point overlay method on the same plates and on the individual ARMS units as well (**Fig. 6** & **7**), with significant differences between samples (no. of points overlaid by 100 & 300 methods) of less abundant taxa. This aspect is crucial for studies, where NIS detection and their coverage estimations are of great importance (Danovaro et al. 2016). In this regard, point-overlay based photo-analysis methods should only be used for estimating coverage of taxa (Drummond & Connell, 2005), and not organism detection itself.

Additionally, the comparisons of the NMDS plots produced by each method, confirmed the increased precision (less scatter) and capability to differentiate communities (less ellipse overlap) of the 300 point method, compared to the 100 point overlay. The displayed patterns of both 5x5 grid and 300 point overlay methods were more similar, resulting in a more resembling coverage estimations of the community. Therefore, the 300 point method seems to be more capable in distinguishing different community between sites and also time-series, which is especially useful in long-term monitoring activities where detection of slight changes may be crucial (Danovaro et al., 2016; Obst et al., 2020; Moore et al., 2019).

Another important consideration of plate photo-analysis for repeated monitoring practice is the amount of time and effort used, as it has large effects on the overall-efficiency (Moore et al., 2019). In this study the 5x5 grid method was by far the most demanding, with the annotation usually taking around 20-30 minutes per plate-face, depending on the amount of taxa present, with longest brakes in between. It was very advisable (almost necessary) to use 2 computer screens, one for enlarging the plate surface of the current surveyed cell and the other for displaying the large excel spreadsheet where taxonomic categories presence data were manually inputted for each of the 25 total cells. As such annotation required a lot of focus and concentration at each cell of the 4 ARMS units (total of 68 plate-faces) and was done plate by plate all in a few days, my eyes were not at ease at the end. This made the 5x5 grid survey method more prone to human errors, due to manual data input and loss of focus/concentration, which was illustrated by the fact that on the PIR_1_3M unit, 300 point method detected 2 more taxonomic categories than the 5x5 grid method, both coming from taxa that were fairly small and rare (*Anadara transversa* & coralligenous algae).

On the contrary, the automatization provided by the CPCe programme, made annotations by point overlay methods very straightforward and rapid, lasting at most 5-10 minutes per plate

for 100 point method and 10-15 minutes at most for 300 point overlay method. The fact that data input into the programme is direct and that the total dataset can be exported into excel automatically, makes the ratio between increased sampling intensity (100 vs 300 points) and time used in the favour of the 300 point overlay method. The method seems to be less prone to human error as only one point is annotated at a time making it very easy to focus with the additional option to review the whole point overlay at any given time. Due to the patchy heterogenous colonization patterns that were observed on ARMS plates, the 300 point overlay did in fact noticeably increase the sampling intensity, when visually compared to the 100 point overlay (illustrated in **Fig. 40**, below).

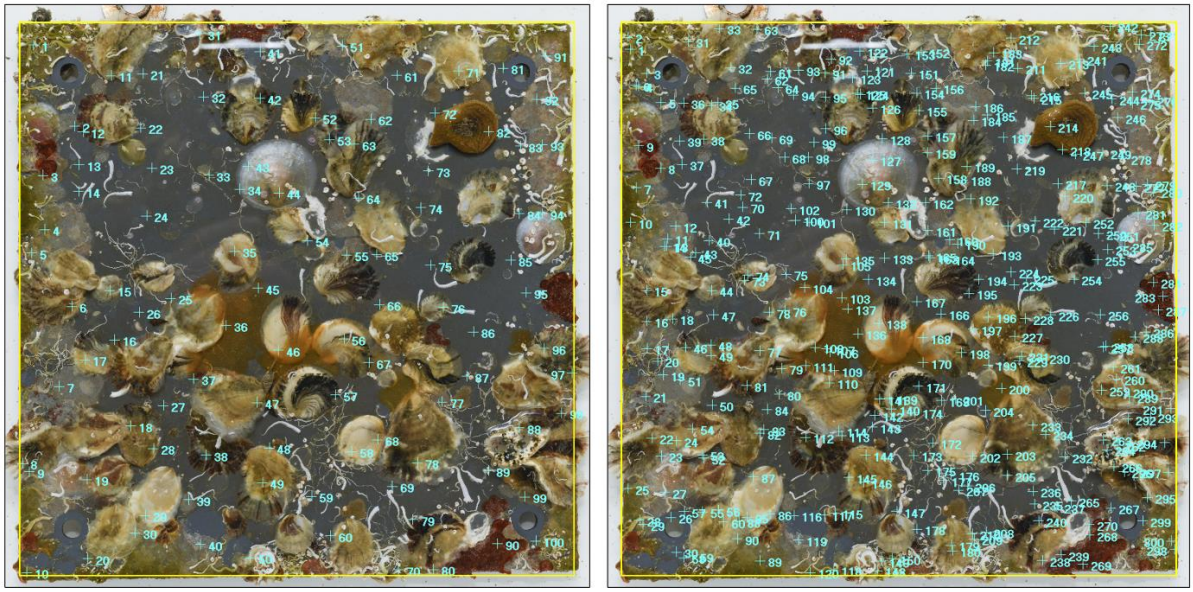

Figure 40: Visual comparison among the 100 (left) and 300 (right) point overlays (light blue) in the CPCe programme, to better signify the increased sampling intensity between the two methods. Plate photos are from ARMS at the PIR site.

According to the evidence of the method comparisons, which are explained in detail, above, we determined the 300 stratified random point overlay as the best option for estimating percentage cover of biofouling taxa, due to its rapidly obtained, accurate and statistically robust results, which can be easily re-done for repeated monitoring practices and compared with results from other ARMS plates at a different study site. We stress the importance of making a species list of all taxa present by manual inspection on plate-faces, and then using the respected species list for estimating organism cover trough point-overlay photo-analysis method. In this way, no organism would be overlooked, the only thing lacking may be cover estimates of the very small and rare organism.

9.3. Colonization patterns on ARMS plates

The results of the study, derived by the 300 point overlay method, depict significant differences in colonization patterns among ARMS plates of distinct orientations (T, B ,9T, 1B), deployment sites (PIR, VID, PK) and deployment periods (3 – 13 months).

At all 3 study sites, ARMS plates of bottom faced orientation (1B & B) displayed significantly greater colonized coverage than top oriented (9T & T) faces (illustrated in **Fig. 13, 21** and **29**), as was also observed on ARMS units deployed within the Adriatic Sea in the similar study of David et al. (2019). Although only present at PK site, 1B plates were by far the richest in epifauna and were considered as outliers (**Fig. 31**) by the amount of colonized coverage. This successional dominance of 1B plates might be a consequence of the plate-surface not being confined by other plates, which drastically reduces the colonizable space and waterflow (David et al., 2019). As a consequence of this higher exposure of the 1B plates to the water column, more larvae were available for settlement, with more space for biofouling taxa to grow and increased food availability for the established filter-feeding taxa. This theory goes in concordance with the observed increased colonization at plate edges, pictured by lateral encroachment of some taxa (bryozoan colonies, Porifera, Didemnidae and coralligenous algae) and presence of larger bodied-taxa (bivalves, tunicates, arborescent bryozoans) on the edges of ARMS plates (**Fig. 2, 3, 4**), which was to some degree illustrated by the graphical diagrams of taxonomic density (**Fig. 9** & **10**). This initial colonization on the edges then leads to an even greater restriction of water flow to the central plate surfaces.

As a consequence of greater exposure to the water column, the biofouling community that formed on the 1B plates was of higher resemblance to the epifauna, observed on surrounding pillars (larger tunicates and bivalves, arborescent bryozoans, etc.). On the contrary, the confined B plates seemed to represent the endofaunal community, with higher amounts of larger vagile organisms than the more exposed counterparts. This makes sense, as ARMS were initially developed for sampling cryptic endofauna of the coral reef habitats (David et al., 2019; Danovaro et al., 2016) . In regard to these important observations, we recommend a deployment of an additional ARMS unit with fairly larger spacers between the plates, beside the regular one, to test this hypothesis. If significant differences would be detected, such ARMS units with larger spacers would more representatively sample the epifaunal communities, while retaining the high comparability and other advantages of the original ARMS units.

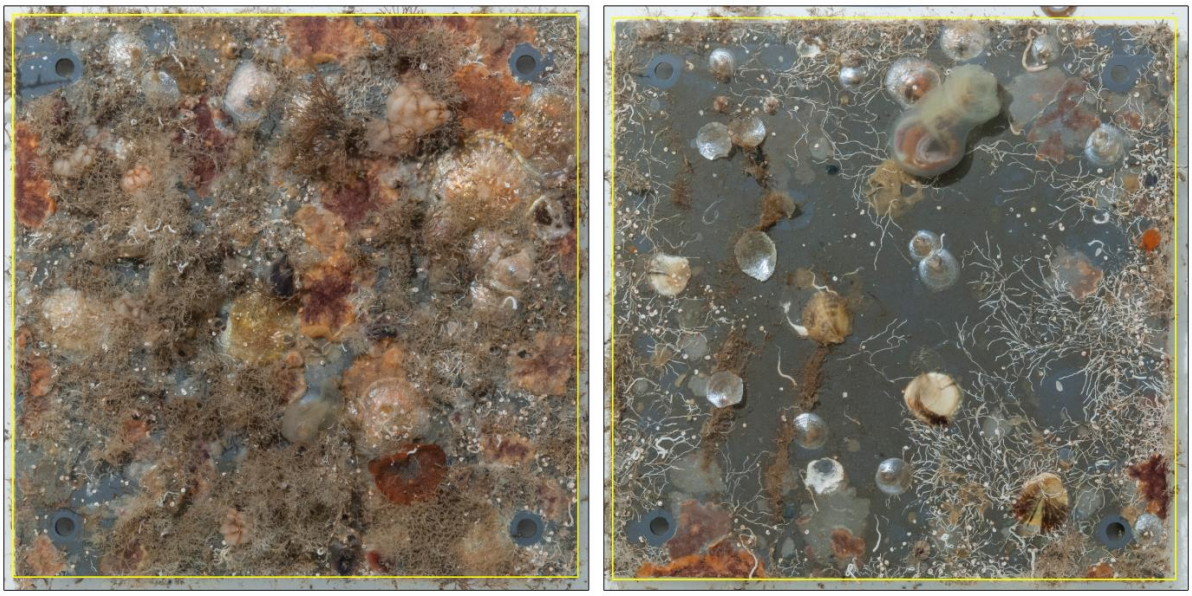

Figure 41: Visual comparison among the cover of 1B (left) and B (right) plate-faces from the PK site, to better represent the increased colonized cover regarding the distinct orientations. Note the uniform colonization of 1B and edge colonization (bryozoan colonies, polychaetes) on B plate-faces.

The inferior colonization of top oriented plate-faces (9T & T) especially T, compared to bottom oriented (B), seem to be a consequence of increased sedimentation of particles on the plate surface, which were observed when units were visually inspected (illustrated in **Fig. 35**, below). This observation goes in concordance to the findings of the study by Maughan (2001), where sedimentation and light exposure were linked to higher diversity and occupied cover of encrusting biofouling taxa, as they negatively affect larvae settlement (negative phototaxis) and increase the susceptibility of sediment clogging the filter-feeding organisms (Maldonado & Young, 1996). These environmental factors therefore seem very depicting, as the whole study area is characterized by high sedimentation rates (Ogorelec et al., 1991) and the fact that this trend was mostly evident on ARMS units from the VID (**Fig. 18**) and PK (**Fig. 26**) sites, where the adjacent habitat is full of detritus and has high sedimentation and resuspension due to currents, wave dynamics and ship manoeuvres. Despite the fact that bottommost (1B) plate-faces have the same exposure to the water column as the topmost (9T) plates, the latter were severely less colonized on the same ARMS units at the PK site (**Fig. 28**), additionally indicating to the effect of particle sedimentation. Another obvious characteristic of top oriented plate-faces (T & 9T) was the presence of algal taxa, which were responsible for the differentiation of communities, especially significant for 9T plates. This is a very similar conclusion as in papers of David et al., 2019 and Pennesi & Danovaro, 2017.

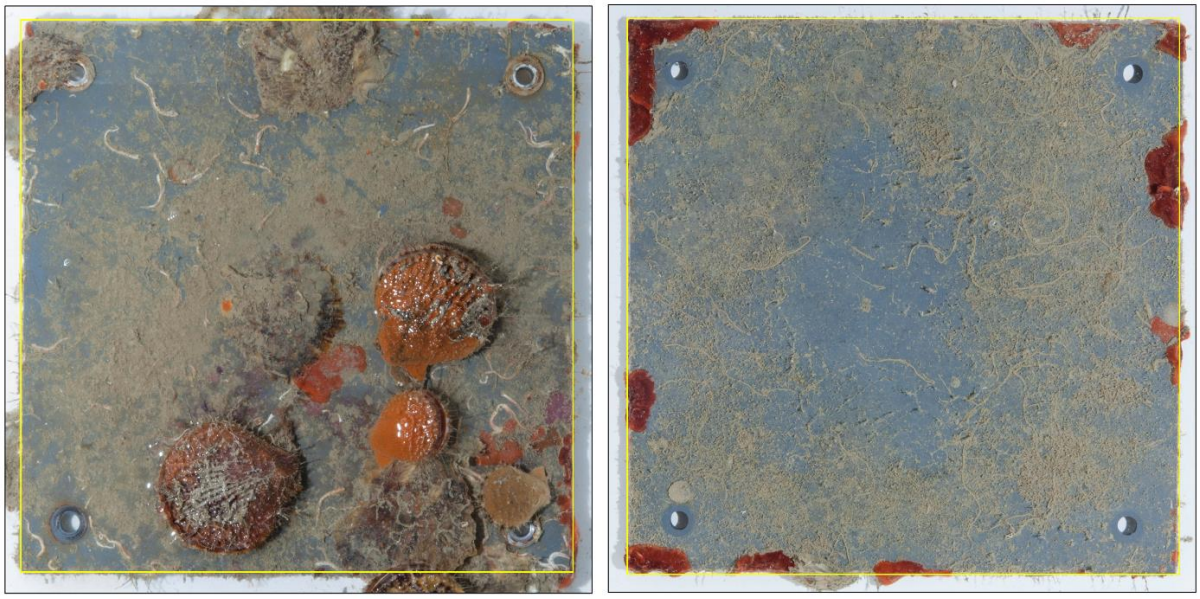

Figure 42: Visual comparison among the cover of 9T (left) and T (right) plate-faces from the VID site. Note the significant amount of sediment on both plate-faces and very low colonization (lateral encroachment of bryozoan colonies) on T plate-faces.

The differences among colonized cover of ARMS plates with similar deployment periods between the three sites, particularly PIR and VID, could again be related to differences in sedimentation rates and light availability (depth), as they might be the cause of the lower colonization observed at the VID site (**Fig. 37**). Further, the positive corelation between the length of deployment period and colonized cover observed at PIR and VID sites, was not surprising as time allows the settled organism to grow in size and morphological complexity, allows new settlements of biofouling taxa and enables the progress of other succession dynamics (Sutherland & Karlson, 1977).

In connection to the methodological characteristics of the point overlay sampling trough photo-analysis, and the results of such method produced by this thesis, discussed in detail in the previous chapter (**9.2**), it is reasonable to consider only B plate-faces for cover estimation analysis. We based this assumption on the significant colonization of biofouling taxa on B plates at the 3 studied sites, which provides a bigger and more representative sample of the community, as more overlaid points are underlined by a fouling organism (colonized). The results were therefore more accurate (less variability), observed by a lesser NMDS scatter (**Fig. 14, 22 & 30**) and statistically robust, due to higher amounts of informative data (colonized points), when compared to those on T & 9T oriented plate-faces, which were highly variable. This is an important addition to the findings of David et al., (2019), who requested a similar

study to evaluate all 17 plate-faces and try to establish an appropriate subset of plates for photo-analysis methods.

9.4. Biofouling community on ARMS plates

9.4.1. Community structure

The results of this thesis demonstrate that PVC plate-faces and sandwich-like sampling design of the ARMS units, serves as a suitable colonization area, capable of developing a rich biofouling community even at shorter deployment periods (e.g., 4 months). The developed sessile biofouling community on ARMS was observed to be mostly represented by polychaetes, bryozoans and molluscs in the respected order and site specific occurrence of algal (at PIR site), poriferan (at VID site) and ascidian (at PK site) taxa, which signified their importance in the distinct biofouling community of the sampled habitats. The same 3 dominant groups of fouling taxa were identified on ARMS plates within the study of David et al. (2019) and terra-cotta tiles by Fortič et al., (2021), which adds to their role as predominant earlier colonizers of different hard substrata in the northern Adriatic Sea. Coverage from cnidarian and cirripedian taxa was very low, as was noted within the previously mentioned studies as well. Polychaetes, especially *S. triqueter*, which were also the most dominant fouling group in the study of Fava et al., (2016), are known as a fast-growing pioneer colonizing species in the Mediterranean (Fava et al., 2016, Cotter et al., 2003; Gravina et al., 1989). These traits may be the cause of their large coverage contributions to the communities of PIR_1_3M unit which had the shortest deployment period of all (3 months). Encrusting bryozoan colonies also appeared as an important part of the established community, due to the fact that their ability of overgrowth by asexual reproduction, which was observed as a considerable advantage over other solitary taxa, especially encrusting serpulid worms and similar (Nandakumar et al., 1993; Greene et al., 1985). Surfaces of solitary bivalve taxa, especially *O. edulis*, which represented secondary hard surfaces, were observed to be colonized by polychaetes and encrusting bryozoans, with *M. varia* shells associated with cover of poriferan taxa. Anomidae, another important colonizer in the northern Adriatic (Fava et al., 2016; Fortič et al., 2021) were significant on T oriented plate-faces at all 3 sites, which may be due to the fact that they are less susceptible to the factor of particle sedimentation (Maughan et al., 2001). The PIR_2_11M unit, when compared to 3 other units at the site, nicely portrayed the overgrowth pattern of a colonial ascidian from the Didemnidae family and encrusting porifera taxa, which are both considered slower colonizers, due to their main colonization mode by lateral encroachment (Fava et al., 2016). On the contrary, ARMS

deployed for shorter periods (4 months) at the Port of Koper, all had significant cover occupied by solitary ascidians.

The community structure of the broader biofouling taxonomic groups demonstrated that the same taxonomic groups contributed to the final established community structure on ARMS plates in different proportions, depending on plate-face orientation from the same unit (T v B), among units deployed at the same site at a different season (PK) for different periods (PIR & VID) and also between study sites, regardless of the season or period (**Fig. 38**). These differences significantly increased, when total community structure was considered, portrayed by high dissimilarity indexes in multivariate comparisons among community structure (NMDS, SIMPER), where percentage cover estimates (amount of points overlaid) of each taxonomic categories were considered (**Fig. 19, 27** & **35**). In this regard, the usage of finer taxonomic categories would increase the power do detect smaller changes in species structure within and among different study sites/habitats (David et al., 2019). The large dissimilarity values of community structures, even at plate-face level of a single ARMS unit, demonstrate the usefulness of ARMS sampling. The distinct plate-face orientations are exposed different environmental factors of light exposure, sedimentation and water flow, that significantly influence the development of epifaunal communities (David et al., 2019; Fava et al., 2016, Maughan, 2001).

The results of the study clearly showed the influence of the surrounding habitat (location), immersion season and deployment period to the final community structure , even if only plates of B orientation were considered (**Fig. 38** & **39**). Of these three factors, which were hypothesized to influence the developed community structure, immersion season appeared as the most significant. This was demonstrated by the NMDS scatter pattern of **Fig. 39**, where points of ARMS that were deployed in June or July months, congregated a tight and overlapping group, excluding those that were deployed at different months (August, October and February), regardless of the deployment year (2018-2021), period (3-13 months) or location (PIR, VID, PK). Even within the congregated group, the units deployed in June were more distant to those of July. Additionally, units deployed in August or October of which immersion seasons were closer to those within the congregated group, displayed a lesser distances in community structure to that of February. Further, the community structure of ARMS at the PK site (**Fig. 35**), where units were deployed for the same period in a consequent manner, showed an almost total overlap from the two units, deployed in the same month of a different year. These observations go in concordance with the findings of many studies, which showed the

significance of placement season to the developed sessile benthic community, especially in temperate coastal seas (Dziubińska & Janas, 2007; Qiu et al., 2003; Lezzi et al., 2017; Qvarfordt et al., 2006), where the environmental variation is the most pronounced. A recent study by Fortič et al., (2021) signified this importance of placement season on the development of fouling communities in the Slovenian sea, where two distinct groups of communities developed, based on the factor of plate immersion season in winter and summer months. In this regard, the presence of larvae and propagules in the water column at the time of ARMS deployment, governed by temperature and the reproductive cycles of the fouling species is crucial, as they are readily-available to settle and begin the plate-face colonization process very rapidly (Khalaman, 2010; Sutherland, 1981).

The effect of the surrounding habitat and environmental conditions to the final community structure was mostly observed by presence of distinct taxonomic categories and amounts of their colonized proportion of cover, which were the main reason for the evident separation of the study site groups in **Fig. 39** (left). For example, some taxa like *T. complanata, S. lafontii*, *Ascidiella* sp., *Mytilus* sp., Bryozoa arborescent white, etc. that were exclusive for a study site, also contributed a great amount of coverage to the final developed community. Additionally, the previously mentioned taxonomic groups which contributed significant proportions to the final community structure at each study site (Algae at PIR, Porifera at VID and Ascidiacea at PK), further signify this effect of the monitored habitat and indicate that colonized cover is more influenced by the available larval-pool in the habitat and not by their incapability to colonize PVC plate-faces.

Based on our results, the influence of the deployment period length could not be directly linked to the taxonomic richness (no. of taxonomic categories) of ARMS units or plate faces. However, units with shorter deployment period, particularly PIR_1_3M, were characterized by lesser colonized cover, organism overgrowth and lesser developed biofouling organisms (smaller bryozoan colonies, juvenile bivalves, etc.). Some slower growing taxa like porifera and colonial ascidians (Fava et al., 2016), that were observed as important components of the surrounding habitats, were more noticeable on ARMS units with deployment periods of more than 6 months. There was no apparent pattern of any die-off or significant overgrowth of fouling taxa present, which could lower the relevance-applicability of ARMS units with longer deployment periods (Obst et al., 2020), as they would not effectively represent the community or make annotation by photo-analysis very hard to carry out.

In connection from the findings of colonization patterns from the previous chapter (**9.3**) and the characteristics of the biofouling community, discussed in detail above, we propose that ARMS units meant for long-term biodiversity monitoring should be deployed for a period of around 12 months or similar.

9.4.2. Non-indigenous and cryptogenic species

NIS and cryptogenic species were observed on ARMS from all 3 sites. Altogether 9 NIS and cryptogenic species were found in this study. Most such species were present at the Port of Koper (PK) site (n = 8), which had short deployment times with frequent re-deployments by a new AMRS unit (4 months), to facilitate new colonization from the larval-pool in different yearly seasons, followed by PIR (n = 2) and VID (n = 1). *S. plicata* and *B. neritina* were very abundant on the plates at the PK site, with the taxonomic category Bryozoa arborescent white illustrating the importance of precise taxonomic identification to species or at least genus level, for such purposes, as individuals may be from the non-native *Tricellaria inopinata* (d'Hondt & Occhipinti Ambrogi, 1985) species. This elevated amount of NIS on PK ARMS was to be expected, as the Port of Koper serves as an important introduction hotspot for such species in the area (Spagnolo et al., 2017), introduced trough ship ballast waters and hull-surfaces (Lipej et al., 2012; Fortič et al., 2019) and the distinctive hydrographic and morphological features, which aid the settlement and proliferation of NIS (Spagnolo et al., 2017).

Analysis of ARMS could provide important observations of interactions between NIS and native taxa as they are aprioristically competing for colonized space on plate surfaces. For example, overcrowding of 1B plates from *S. plicata* ascidian and *B. neritina* was present at the PK site, indicating that important succession patterns like overgrowth or overcrowding could be derived from visual or even photo-analysis examinations of ARMS plates.

However, presence of NIS should not be derived solely from the point overlay photo-analysis methods, as they can be very small or cryptic (*Watersipora* sp., *A. transversa*, etc.), which could lead to them being overlooked, as only a small portion of the surface is sampled by such surveys (Moore et al., 2019). The method should therefore only be used for estimating the coverage of NIS and not their presence or absence (Drummond & Connell, 2005). This signifies the importance of previously suggested species lists to be made by visual inspections of the ARMS plates, to minimize the chance of overlooking an organism. Additionally, we stress the importance of other sampling methods concerning NIS research, like scuba-diver and other

surveys (Orlando-Bonaca et al., 2019; Lipej et al., 2020), to be used in tandem with ARMS in a jointly effort for detection and assessment purposes of such invasive species.

10. CONCLUSIONS

As many observations and significant patterns of the community structure could be interpreted from the results of 300 point-overlay based photo-analysis of ARMS plates, even if only B plate-faces were considered, such methodology could be a useful, simple and effective complementary method of sampling and detecting changes of the biofouling community for studies addressing long-term biodiversity monitoring, effects of seasonality and NIS detection in different habitats of the northern Adriatic Sea and broader. This thesis contributes important information to the existing knowledge on the research theme in evaluating the usefulness of software supported photo-analysis methods (Moore et al., 2019), analysis of all 17 plate-faces and consideration of a subset of plates for community assessments, while at the same time acquiring important information of the current biofouling communities at 3 new ARMS-based observatory sites in the Slovenian Sea.

The 300 point-overlay proved to be the most appropriate of all 3 photo-analysis methods, as it provided the most statistically robust dataset with accurate and precise coverage estimates of taxa in a reasonably short time, due to the benefits of the CPCe annotation software. However, we acknowledge that for cover estimates of broader taxonomic groups, the 100 point-overlay method could be sufficient as well. Usage of specialized annotation software like CPCe was proven very useful, as it significantly reduced the time and effort of the photo-analysis procedures, which is crucial when numerous plates are analysed in a consequent and repeated manner.

A different fouling community structure had developed on ARMS units at each individual study site. As such pattern was acquired solely by the 300 point-overlay method, this verified the assumption of David et al. (2019), that photo-analysis could be used tool to detect changes in the community structure in distinct benthic habitats at very small spatial scales, as close as 2 km. However, it is critical to notice that such analysis methods only reveal a superficial part of the local biodiversity, therefore not accurately representing the full diversity of such highly complex habitats.

Concerning the length of the deployment periods, ARMS units designated for long-term biodiversity monitoring should be deployed for 12 months or similar, as the developed biofouling community on such units was characterized by greater colonized proportions, more developed organisms (larger individuals and colonies, less juveniles, etc.) and presence of some

slower colonizing taxa (porifera, colonial ascidians), which altogether help to illustrate a more representative community of the surrounding flora and fauna.

On the other hand, the deployment of ARMS units for shorter 4 month periods in consequent times of the year, determined for NIS sampling, proved very useful for detecting seasonal changes in the established fouling communities. Distinct larval-propagule pools present in the water column at the individual immersion season were observed to develop different biofouling communities. A newly deployed ARMS unit provides new surfaces suitable for larval settlement and thus increases the chance of NIS propagules to colonize empty plate surfaces.

Plate-face orientation was also proven as a key factor influencing the structure of the biofouling community. The communities, present on bottom (B) oriented plate-faces were richer, more developed and occupied larger proportions of plate cover, on all 11 ARMS units deployed. This pattern seemed most probably a consequence of the lack of sedimentation on downward-faced ARMS plate surfaces. Additionally, the increased cover of Algal taxa on top (T) oriented plate-faces indicated the significant influence of light availability/exposure to the established organisms. The results of the quite distinct community developed on the bottommost downward-faced surfaces (1B) shows that available space between the plates also influences the community development. This higher exposure enables more water circulation, increases light availability and available space for organism growth and thus a different community, which is more epifaunal when compared with the more endofaunal community that developed within the small spacing of the inner plates.

The PVC plates of ARMS units were observed as an appropriate surface for colonization of biofouling taxa and by developing a rich community at only 6 months of submersion proven as an efficient sampling tool for endofauna and flora of distinct benthic habitats in the northern Adriatic Sea. Our observations suggest, that by the use of larger spacers, which would enable more exposure to the water column, a richer epifaunal community would develop in even shorter deployment periods of 4 months or similar. We recommend that a future study compares the fouling communities on such modified ARMS to the regular units, as they might be a better option for research based solely on larger sessile epifauna.

Based on the above mentioned observations and trends, we recommend the following photo-analysis based protocol to be followed for future ARMS deployments in the Slovenian sea:

- ARMS units for long-term biodiversity monitoring should be deployed in the summer season, preferably in June for a period of around 12 months.

- ARMS units for NIS detection should be deployed for 4 months in a consequent manner, to detect the seasonal variability of the biofouling community and maximize the colonization from non-native taxa.
- A list of all present taxa, identified to the lowest level possible, trough manual inspections of all individual plate-faces of ARMS units at the time of the retrieval, should be generated to minimize the chance of overlooking an organism. This should be supported by close-up photos of the less evident taxa, to increase the potential for proper organism identification.
- Only B oriented plate-faces can be annotated with a 300 point-overlay based photo-analysis by the CPCe software, to obtain percentage cover of different taxonomic categories, which serve as precise and accurate estimates of the community structure .

In conclusion, this work established a photographic based method of biofouling community assessments to be used in the Slovenian Sea, for long-term biodiversity monitoring and NIS detection purposes. We hope that this thesis will facilitate the establishments of similar ARMS observatory sites in the region and fill the missing gap of research interest for these fundamental communities of marine organisms in the region.

11. REFERENCES

Adey, W. H., & Loveland, K. (2007). Dynamic aquaria: B and Restoring Living Ecosystems. Elsevier.

Andrew, N. L., & Mapstone, B.D. (1987). Sampling and the description of spatial pattern in marine ecology. Oceanographic Marine Biology Annual Review 25, 39–90.

Barausse, A., Duci, A., Mazzoldi, C., Artioli, Y. & Palmeri, L. (2009). Trophic network model of the Northern Adriatic Sea: analysis of an exploited and eutrophic ecosystem. Estuarine, Coastal and Shelf Science 83, 577–590. doi: 10.1016/j.ecss.2009.05.003

Barausse, A., Michieli, A., Riginella, E., Palmeri, L., & Mazzoldi, C. (2011). Long-term changes in community composition and life-history traits in a highly exploited basin (northern Adriatic Sea): the role of environment and anthropogenic pressures. Journal of Fish Biology, 79(6), 1453–1486. doi:10.1111/j.1095-8649.2011.03139.x

Barnosky, A. D., Matzke, N., Tomiya, S., Wogan, G. O. U., Swartz, B., Quental, T. B., … Ferrer, E. A. (2011). Has the Earth's sixth mass extinction already arrived? Nature, 471(7336), 51–57. doi:10.1038/nature09678

Barrio Froján , C. R. S., Cooper, K. M., & Bolam, S. G. (2016). Towards an integrated approach to marine benthic monitoring. Marine Pollution Bulletin, 104(1-2), 20–28. doi:10.1016/j.marpolbul.2016.01.054

Beisiegel, K., Darr, A., Gogina, M., & Zettler, M. L. (2017). Benefits and shortcomings of non-destructive benthic imagery for monitoring hard-bottom habitats. Marine Pollution Bulletin, 121(1-2), 5–15. doi:10.1016/j.marpolbul.2017.04.009

Beyan, C., & Browman, H. I. (2020). Setting the stage for the machine intelligence era in marine science. ICES Journal of Marine Science. doi:10.1093/icesjms/fsaa084

Bicknell, A. W., Godley, B. J., Sheehan, E. V., Votier, S. C., & Witt, M. J. (2016). Camera technology for monitoring marine biodiversity and human impact. Frontiers in Ecology and the Environment, 14(8), 424–432. doi:10.1002/fee.1322

Boicourt, W. C., Kuzmić, M., & Hopkins, T. S. (1999). The Inland Sea: Circulation of Chesapeake Bay and the. Ecosystems at the Land-Sea Margin: Drainage Basin to Coastal Sea, 55, 81-129.

Borja, A. (2014). Grand challenges in marine ecosystems ecology. Frontiers in Marine Science, 1. doi:10.3389/fmars.2014.00001

Borja, A., & Elliott, M. (2013). Marine monitoring during an economic crisis: The cure is worse than the disease. Marine Pollution Bulletin, 68(1-2), 1–3. doi: 10.1016/j.marpolbul.2013.01.041

Borja, A., Elliott, M., Andersen, J. H., Berg, T., Carstensen, J., Halpern, B. S., et al. (2016). Overview of integrative assessment of marine systems: The ecosystem approach in practice. Front. Mar. Sci. 3 doi:10.3389/fmars.2016.00020

Borja, A., Marín, S.L., Muxika, I., Pino, L., Rodríguez, J.G., (2015). Is there a possibility of ranking benthic quality assessment indices to select the most responsive to different human pressures? Mar. Pollut. Bull. 97,

Bowden, D.A., Clarke, A., Peck, L.S., Barnes, D.K., (2006). Antarctic sessile marine benthos: colonisation and growth on artificial substrata over three years. Mar. Ecol. Prog. Ser. 316, 1–16.

Broderick, A. C. (2015). Grand challenges in marine conservation and sustainable use. Frontiers in Marine Science, 2. doi:10.3389/fmars.2015.00011

Caldwell, M. M., Heldmaier, G., Jackson, R. B., Lange, O. L., Mooney, H. A., Schulze, E. D., & Sommer, U. (2009). Marine hard bottom communities. M. Wahl (Ed.). Springer.

Cardinale, B. J., Duffy, J. E., Gonzalez, A., Hooper, D. U., Perrings, C., Venail, P., … Naeem, S. (2012). Biodiversity loss and its impact on humanity. Nature, 486(7401), 59–67. doi:10.1038/nature11148

Carugati, L., Corinaldesi, C., Dell'Anno, A., & Danovaro, R. (2015). Metagenetic tools for the census of marine meiofaunal biodiversity: An overview. Marine Genomics, 24, 11–20. doi:10.1016/j.margen.2015.04.010

Carvalho, S., Aylagas, E., Villalobos, R., Kattan, Y., Berumen, M., & Pearman, J. K. (2019). Beyond the visual: using metabarcoding to characterize the hidden reef cryptobiome. Proceedings of the Royal Society B: Biological Sciences, 286(1896), 20182697. doi:10.1098/rspb.2018.2697

Cochrane, S. K., Andersen, J. H., Berg, T., Blanchet, H., Borja, A., Carstensen, J., ... & Renaud, P. E. (2016). What is marine biodiversity? Towards common concepts and their implications for assessing biodiversity status. Frontiers in Marine Science, 3, 248. https://doi.org/10.3389/fmars.2016.00248

Cotter, E., O'Riordan, R.M., Myers, A.A., (2003). A histological study of reproduction in the serpulids Pomatoceros triqueter and Pomatoceros lamarckii (Annelida: Polychaeta). Mar. Biol. 142, 905–914. http://dx.doi.org/10.1007/s00227-002-0987-2

Cozzi, S., Cabrini, M., Kralj, M., De Vittor, C., Celio, M., & Giani, M. (2020). Climatic and Anthropogenic Impacts on Environmental Conditions and Phytoplankton Community in the Gulf of Trieste (Northern Adriatic Sea). Water, 12(9), 2652. doi:10.3390/w12092652

Crocetta, F. (2011). Marine alien Mollusca in the Gulf of Trieste and neighbouring areas: a critical review and state of knowledge (updated in 2011). Acta Adriatica, 52 (2), 247-259

Danovaro, R., Carugati, L., Berzano, M., Cahill, A. E., Carvalho, S., Chenuil, A., … Borja, A. (2016). Implementing and Innovating Marine Monitoring Approaches for Assessing Marine Environmental Status. Frontiers in Marine Science, 3. doi:10.3389/fmars.2016.00213

Drummond, S. & Connell, S. (2005). Quantifying percentage cover of subtidal organisms on rocky coasts: A comparison of the costs and benefits of standard methods. Marine and Freshwater Research - Mar Freshwater Res. 56. 10.1071/MF04270.

Durden, Jennifer & Bett, B. & Schoening, Timm & Morris, Kirsty & Nattkemper, Tim & Ruhl, Henry. (2016). Comparison of image annotation data generated by multiple investigators for benthic ecology. Marine Ecology Progress Series. 552. 61-70. 10.3354/meps11775.

Dziubińska, A., & Janas, U. (2007). Submerged objects - a nice place to live and develop. Succession of fouling communities in the Gulf of Gdańsk, Southern Baltic. Oceanological and Hydrobiological Studies, 36(4). doi:10.2478/v10009-007-0026-1

Fava, F., Ponti, M., & Abbiati, M. (2016). Role of Recruitment Processes in Structuring Coralligenous Benthic Assemblages in the Northern Adriatic Continental Shelf. PLOS ONE, 11(10), e0163494. doi:10.1371/journal.pone.0163494

Fortič, A., Mavrič, B., Pitacco, V., & Lipej, L. (2021). Temporal changes of a fouling community: Colonization patterns of the benthic epifauna in the shallow northern Adriatic Sea. Regional Studies in Marine Science, 101818.

Fortič, A., Mavrič, B., Pitacco, V., & Lipej, L. (2021). Temporal changes of a fouling community: Colonization patterns of the benthic epifauna in the shallow northern Adriatic Sea. Regional Studies in Marine Science, 45, 101818. doi:10.1016/j.rsma.2021.101818

Fortič, A., Trkov, D., Mavrič, B., Lipej, L. (2019). Assessment of Bryozoan Xenodiversity in the Slovenian Coastal Sea. 29. 173-186. 10.19233/ASHN.2019.17.

France, J., & Mozetič, P. (2006). Ecological characterization of toxic phytoplankton species (Dinophysis spp., Dinophyceae) in Slovenian mariculture areas (Gulf of Trieste, Adriatic Sea) and the implications for monitoring. Marine pollution bulletin, 52(11), 1504-1516.

Giani, M., Djakovac, T., Degobbis, D., Cozzi, S., Solidoro, C., & Umani, S. F. (2012). Recent changes in the marine ecosystems of the northern Adriatic Sea. Estuarine, Coastal and Shelf Science, 115, 1–13. doi:10.1016/j.ecss.2012.08.023

Glasby T (1999) Interactive effects of shading and proximity to the seafloor on the development of subtidal epibiotic assemblages. Marine Ecological Progress Series 190: 113–124, https://doi.org/ 10.3354/meps190113

Glasby T (2001) Development of sessile marine assemblages on fixed versus moving substrata. Marine Ecological Progress Series 215: 37–47, https://doi.org/10.3354/meps215037

Gofas, S., & Zenetos, A. (2003). Exotic molluscs in the Mediterranean basin: Current status and perspectives. Oceanography and Marine Biology, 41, 237-277.

Gravina, M.F., Ardizzone, G., Belluscio, A., (1989). Polychaetes of an artificial reef in the central mediterranean sea. Estua. Coast. Shelf Sci. 28 (2), 161–172. http://dx.doi.org/10.1016/0272-7714(89)90063-2

Greene, C., Schoener, A., Corets, E., (1983). Succession on marine hard substrata: the adaptive significance of solitary and colonial strategies in temperate fouling communities. Mar. Ecol. Prog. Ser. 13 (2–3), 121–129. http://dx.doi.org/10.3354/meps013121.

Halpern, B. S., Walbridge, S., Selkoe, K. A., Kappel, C. V., Micheli, F., D'Agrosa, C., … Watson, R. (2008). A Global Map of Human Impact on Marine Ecosystems. Science, 319(5865), 948–952. doi:10.1126/science.1149345

Hammer, Ø., Harper, D.A.T., Ryan, P.D. (2001). PAST: Paleontological statistics software package for education and data analysis. Palaeontologia Electronica 4(1): 9pp.

Hustache, Julie & Fagundes, Luisa & Sumi, Mariana & Ferrari Legorreta, Renata & Ayroza, Camila. (2015). Finding the Right Tool for Benthic Image Analysis. Reef Encounters: International Society for Reef Studies, 30, 34.

Khalaman, V.V., (2010). Life strategies of marine sessile organisms as an approach for exploration of structure and succession of fouling communities. In: Chan, J., Wong, S. (Eds.), Biofouling: Types, Impact and Anti-Fouling. Nova Science Publishers, Inc., pp. 1–33.

Kohler, K. E., & Gill, S. M. (2006). Coral Point Count with Excel extensions (CPCe): A Visual Basic program for the determination of coral and substrate coverage using random point count methodology. Computers & Geosciences, 32(9), 1259–1269. doi:10.1016/j.cageo.2005.11.009

Leray, M., & Knowlton, N., (2015). DNA barcoding and metabarcoding of standardized samples reveal patterns of marine benthic diversity. Proc. Natl. Acad. Sci. 112, 2076–2081.

Lezzi, M., Del Pasqua, M., Pierri, C., Giangrande, A., (2017). Seasonal nonindigenous species succession in a marine macrofouling invertebrate community. Biol. Invasions 20, 937–961. http://dx.doi.org/10.1007/s10530-017-1601-3.

Lindeyer, F. & Gittenberger, A. (2011). Ascidians in the succession of marine fouling communities. Aquatic Invasions. 6. 421-434. 10.3391/ai.2011.6.4.07.

Lipej, L., A. Fortič, B. Mavrič, M. Orlando-Bonaca, D. Trkov (2020): Pregled stanja morske biodiverzitete v akvatoriju Luke Koper. Poročila Morske biološke postaje 189, 61 str.

Lipej, L., Mavric, B., Orlando-Bonaca, M., & Malej, A. (2012). State of the art of the marine non-indigenous flora and fauna in Slovenia. Mediterranean Marine Science, 13(2), 243-249.

Lipej, L., Orlando-Bonaca, M., & Mavric, B. (2016). Biogenic formations in the Slovenian sea. Marine Biology Station, Piran: National Institute of Biology

Lotze, H. K. (2006). Depletion, Degradation, and Recovery Potential of Estuaries and Coastal Seas. Science, 312(5781), 1806–1809. doi:10.1126/science.1128035

MacMahon JA (1979) Ecosystems over time: succession and other types of change. In: Waring RH (ed) Forests: Fresh perspectives from ecosystem analysis. Oregon State University Press, Corvalis, pp 27–58

MacMahon, JA (1979) Ecosystems over time: succession and other types of change. In: Waring RH (ed) Forests: Fresh perspectives from ecosystem analysis. Oregon State University Press, Corvalis, pp 27–58

Maldonado, M. & Young, C.M., (1996). Effects of physical factors on larval behaviour, settlement and recruitment of four tropical demosponges. Mar. Ecol. Prog. Ser. 138, 169–180.

Mancinelli, G., Fazi, S., & Rossi, L. (1998). Sediment structural properties mediating dominant feeding types patterns in soft-bottom macrobenthos of the Northern Adriatic Sea. Hydrobiologia, 367(1-3), 211-222.

Marbà, N., Krause-Jensen, D., Alcoverro, T., Birk, S., Pedersen, A., Neto, J. M., … Duarte, C. M. (2012). Diversity of European seagrass indicators: patterns within and across regions. Hydrobiologia, 704(1), 265–278. doi:10.1007/s10750-012-1403-7

Marraffini, M.L., Ashton, G.V., Brown, C.W., Chang, A.L., Ruiz, G.M., (2017). Settlement plates as monitoring devices for non-indigenous species in marine fouling communities. Management 8, 559–566.

Mather, J. (2013). Marine invertebrates: communities at risk. Biology, 2(2), 832-840. doi:10.3390/biology2020832

Maughan, B.C., (2001) The effects of sedimentation and light on recruitment and development of a temperate, subtidal, epifaunal community. J Exp Mar Biol Ecol 256: 59–71. doi: https://doi.org/10.1016/S0022-0981(00)00304-X

McElwain, J. C., & Punyasena, S. W. (2007). Mass extinction events and the plant fossil record. Trends in Ecology & Evolution, 22(10), 548–557. doi:10.1016/j.tree.2007.09.003

Moore, J., van Rein, H., Benson, A., Sotheran, I., Mercer, T. & Ferguson, M. (2019). Optimisation of Benthic Image Analysis Approaches, JNCC Report, No. 641, JNCC, Peterborough, ISSN 0963-8091.

Mozetič, P., Fonda Umani, S., Cataletto, B., Malej, A., (1998). Seasonal and inter-annual plankton variability in the Gulf of Trieste (northern Adriatic). ICES Journal of Marine Science, 55, 711-722.

Mozetič, P., Malačič, V., & Turk, V. (2008). A case study of sewage discharge in the shallow coastal area of the Northern Adriatic Sea (Gulf of Trieste). Marine Ecology, 29(4), 483-494.

Mozetič, P., Solidoro, C., Cossarini, G., Socal, G., Precali, R., Francé, J., ... & Umani, S. F. (2010). Recent trends towards oligotrophication of the northern Adriatic: evidence from chlorophyll a time series. Estuaries and coasts, 33(2), 362-375.

Nandakumar, K., Tanaka, M., Kikuchi, T., (1993). Interspecific competition among fouling organisms in Tomioka Bay. Japan. Mar. Ecol. Prog. Ser. 94, 43–50. http://dx.doi.org/10.3354/meps094043.

Neeman, N., Servis, J. A., & Naro-Maciel, E. (2015). Conservation Issues: Oceanic Ecosystems. Reference Module in Earth Systems and Environmental Sciences. doi:10.1016/b978-0-12-409548-9.09198-3

Nerlović, V., Perić, L., Slišković, M., & Mrčelić, G. J. (2018). The invasive Anadara transversa (Say, 1822)(Mollusca: Bivalvia) in the biofouling community of northern Adriatic mariculture areas. Management of Biological Invasions, 9(3), 239.

Nicholls, R. J., & Small, C. (2002). Improved estimates of coastal population and exposure to hazards released. Eos, Transactions American Geophysical Union, 83(28), 301. doi:10.1029/2002eo000216

Obst, M., Exter, K., Allcock, A. L., Arvanitidis, C., Axberg, A., Bustamante, M., ... & Pavloudi, C. (2020). A marine biodiversity observation network for genetic monitoring of hard-bottom communities (ARMS-MBON). Frontiers in Marine Science, 7. doi: 10.3389/fmars.2020.572680

Occhipinti-Ambrogi, A., Marchini, A., Cantone, G., Castelli, A., Chimenz, C., Cormaci, M., Froglia, C., Furnari, G., Gambi, M.C., Giaccone, G., Giangrande, A., Gravili, C., Mastrototaro, F., Mazziotti, C., Orsi-Relini, L., Piraino, S., (2011). Alien species along the Italian coasts: an overview. Biol. Invasions 13, 215–237.

Officer, C.G., T.J. Smayda & R. Mann (1982): Benthic filter feeding: A natural eutrophication control. Mar.Ecol.Prog.Ser., 9, 203-210.

Ogorelec, B., Mišič, M., Faganeli, J., (1991). Marine geology of the Gulf of Trieste (Northern Adriatic): Sedimentodological aspects. Marine Geology, 99, 79-92.

Orlando-Bonaca, M., A. Fortič, J. Francé, L. Lipej, B. Mavrič, P. Mozetič, P. Slavinec, V. Pitacco, D. Trkov, I. Vascotto in L. Zamuda (2020): Spremljanje vrstne pestrosti in abundance tujerodnih vrst v slovenskem morju. Drugo fazno poročilo, junij 2020. Poročila 192. Morska Biološka Postaja, Nacionalni Inštitut za Biologijo, Piran, 60 str.

Orlando-Bonaca, M., A. Fortič, J. Francé, L. Lipej, B. Mavrič, P. Mozetič, P. Slavinec, D. Trkov in L. Zamuda (2019): Spremljanje vrstne pestrosti in abundance tujerodnih vrst v slovenskem morju. Prvo fazno poročilo, junij 2019. Poročila 181. Morska Biološka Postaja, Nacionalni Inštitut za Biologijo, Piran, 98 str.

Orlando-Bonaca, M., Mavrič, B., & Urbanič, G. (2012). Development of a new index for the assessment of hydromorphological alterations of the Mediterranean rocky shore. Ecological Indicators, 12(1), 26–36. doi:10.1016/j.ecolind.2011.05.010

Pearman, J. K., Anlauf, H., Irigoien, X., & Carvalho, S. (2016). Please mind the gap – Visual census and cryptic biodiversity assessment at central Red Sea coral reefs. Marine Environmental Research, 118, 20–30. doi:10.1016/j.marenvres.2016.04.011

Pearman, J. K., Chust, G., Aylagas, E., Villarino, E., Watson, J. R., Chenuil, A., … Carvalho, S. (2020). Pan-regional marine benthic cryptobiome biodiversity patterns revealed by metabarcoding Autonomous Reef Monitoring Structures. Molecular Ecology. doi:10.1111/mec.15692

Pearman, J., Aylagas, E., Voolstra, C. R., Anlauf, H., Villalobos, R., & Carvalho, S. (2019). Disentangling the complex microbial community of coral reefs using standardized Autonomous Reef Monitoring Structures (ARMS). Molecular Ecology. doi:10.1111/mec.15167

Pearman, J.K., Leray, M., Villalobos, R., Machida, R.J., Berumen, M.L., Knowlton, N., Carvalho, S., (2018). Cross-shelf investigation of coral reef cryptic benthic organisms reveals diversity patterns of the hidden majority. Sci. Rep. 8. https://doi.org/10.1038/s41598-018-26332-5.

Peck, L. S., Clark, M. S., Power, D., Reis, J., Batista, F. M., & Harper, E. M. (2015). Acidification effects on biofouling communities: winners and losers. Global Change Biology, 21(5), 1907–1913. doi:10.1111/gcb.12841

Pennesi, C., & Danovaro, R. (2017). Assessing marine environmental status through microphytobenthos assemblages colonizing the Autonomous Reef Monitoring Structures (ARMS) and their potential in coastal marine restoration. Marine Pollution Bulletin, 125(1-2), 56–65. doi:10.1016/j.marpolbul.2017.08.001

Petchey OL. & Gaston KJ. (2006) Functional diversity: back to basics and looking forward . Ecol Lett 9 : 741 – 758

Pitacco, V., Orlando-Bonaca, M., Mavrič, B., Popović, A., & Lipej, L. (2014). Mollusc fauna associated with the Cystoseira algal associations in the Gulf of Trieste (Northern Adriatic Sea). Mediterranean Marine Science, 15(2), 225-238.

Qiu, J.W., Thiyagarajan, V., Leung, A.W., Qian, P.Y., (2003). Development of a marine subtidal epibiotic community in Hong Kong: implications for deployment of artificial reefs. Biofouling 19 (1), 37–46. http://dx.doi.org/10.1080/0892701021000060851.

Qvarfordt, S., Kautsky, H., & Malm, T. (2006). Development of fouling communities on vertical structures in the Baltic Sea. Estuarine, Coastal and Shelf Science, 67(4), 618–628. doi:10.1016/j.ecss.2006.01.004

Ransome, E., Geller, J.B., Timmers, M., Leray, M., Mahardini, A., Sembiring, A., Collins, A.G., Meyer, C.P., (2017). The importance of standardization for biodiversity comparisons: a case study using autonomous reef monitoring structures (ARMS) and metabarcoding to measure cryptic diversity on Mo'orea coral reefs, French Polynesia. PLoS One 12, e0175066. https://doi.org/10.1371/journal.pone.0175066.

Rees, H.L. & Bergman, M.J.N. & Birchenough, Silvana & Borja, A. & Boois, I. (2009). Guidelines for the study of the epibenthos of subtidal environments. ICES Techniques in Marine Environmental Sciences. 42. 88 p.

Reiss, H., Birchenough, S., Borja, A., Buhl-Mortensen, L., Craeymeersch, J., Dannheim, J., … Degraer, S. (2014). Benthos distribution modelling and its relevance for marine ecosystem management. ICES Journal of Marine Science, 72(2), 297–315. doi: 10.1093/icesjms/fsu107

Rockstrom, J., Steffen, W., Noone, K., Persson, A., Chapin, F. S., Lambin, E. F., et al. (2009). A safe operating space for humanity. Nature, 461(7263), 472-475. doi:10.1038/461472a

She, J., Allen, I., Buch, E., Crise, A., Johannessen, J. A., Le Traon, P. Y., … Wehde, H. (2016). Developing European operational oceanography for Blue Growth, climate change adaptation and mitigation and ecosystem-based management. Ocean Science Discussions, 1–59. doi:10.5194/os-2015-103

Sheehan, E. V., Cousens, S. L., Nancollas, S. J., Stauss, C., Royle, J., & Attrill, M. J. (2013). Drawing lines at the sand: Evidence for functional vs. visual reef boundaries in temperate Marine Protected Areas. Marine Pollution Bulletin, 76(1-2), 194–202. doi:10.1016/j.marpolbul.2013.09.004

Sini, M., Kipson, S., Linares, C., Koutsoubas, D., Garrabou, J., (2015). The Yellow Gorgonian Eunicella cavolini: demography and disturbance levels across the Mediterranean Sea. PLoS One 10, e0126253.

Sokołowski, A., Ziółkowska, M., Balazy, P., Kuklinski, P., Plichta, I., (2016). Seasonal and multi-annual patterns of colonisation and growth of sessile benthic fauna on artificial substrates in the brackish low-diversity system of the baltic sea. Hydrobiologia 790, 183–200. doi: http://dx.doi.org/10.1007/s10750-016-3043-9.

Spagnolo, A., Auriemma, R., Bacci, T., Balković, I., Bertasi, F., Bolognini, L., … Žuljević, A. (2017). Non-indigenous macrozoobenthic species on hard substrata of selected harbours in the adriatic sea. Marine Pollution Bulletin. doi:10.1016/j.marpolbul.2017.12.031

Spalding, M. D., Fox, H. E., Allen, G. R., Davidson, N., Ferdaña, Z. A., Finlayson, M. A. X., ... & Robertson, J. (2007). Marine ecoregions of the world: a bioregionalization of coastal and shelf areas. BioScience, 57(7), 573-583.

Sutherland, J. P., & Karlson, R. H. (1977). Development and Stability of the Fouling Community at Beaufort, North Carolina. Ecological Monographs, 47(4), 425–446. doi:10.2307/1942176

Sutherland, J.P., (1981). The fouling community at Beaufort, North Carolina: A study in stability. Amer. Nature 118 (4), http://dx.doi.org/10.1086/283844.

Vrišer, B., (1978). Raziskovanja biološke obrasti v Piranskem zalivu. Biološki vestnik 26 (1), 47–59.

Vrišer, B., (1986). Biološka obrast na apnenčastem substratu, zaščitenem pred morskim ježem Paracentrotus lividus (L.). Biološki vestnik 34 (1), 101–114.

Waddington, K. I., Piek, B. W., Payne, A. D., Grove, S. L., Harvey, E. S., Kendrick, G. A., … Meeuwig, J. J. (2010). Description of a Remote Still Photography System for Collection of Benthic Photo-Quadrats. Marine Technology Society Journal, 44(2), 56–63. doi:10.4031/mtsj.44.2.1

Worm, B., Barbier, E. B., Beaumont, N., Duffy, J. E., Folke, C., Halpern, B. S., … Watson, R. (2006). Impacts of Biodiversity Loss on Ocean Ecosystem Services. Science, 314(5800), 787–790. doi:10.1126/science.1132294